universität wien

DISSERTATION | DOCTORAL THESIS

Titel | Title

Highdimensional Quantum Information Theory

verfasst von | submitted by

Paul Appel B.Sc. M.Sc.

angestrebter akademischer Grad | in partial fulfilment of the requirements for the degree of

Doktor der Naturwissenschaften (Dr.rer.nat.)

Wien | Vienna, 2025

Studienkennzahl lt. Studienblatt | Degree programme code as it appears on the student record sheet:	UA 796 605 411
Dissertationsgebiet lt. Studienblatt | Field of study as it appears on the student record sheet:	Physik
Betreut von | Supervisor:	Mag. Dr. Marcus Huber Privatdoz.

Zusammenfassung

Die Quanteninformationstheorie hat sich traditionell auf Zweiniveausysteme (Qubits) konzentriert, obwohl zahlreiche experimentelle Plattformen – darunter photonische Modi, gefangene Ionen und supraleitende Schaltkreise – von Natur aus höherdimensionale Qudits realisieren. Diese Arbeit entwickelt drei komplementäre Ansätze zu einer dimensionsbewussten Erweiterung der Quanteninformationstheorie, die den operativen Kern bewahrt und zugleich die strukturelle Komplexität von Systemen mit höherer lokaler Dimension berücksichtigt.

Im ersten Teil werden dimensionsabhängige Quasi-Monogamie-Relationen für Korrelationsmaße in der Bloch Darstellung hergeleitet. Parallel dazu werden neue Tsallis-2-Entropie-Ungleichungen mit explizit dimensionsabhängingen Parametern formuliert, darunter eine verallgemeinerte Form der strikten Subadditivität. Diese Ergebnisse verdeutlichen, wie sich Geometrie und Entropie quantenmechanischer Korrelationen mit wachsender Dimension verändern, und bieten eine Verallgemeinerung qubitspezifischer Relationen wie der Coffman–Kundu–Wootters-Ungleichung.

Der zweite Teil führt Finite-Function-Encoding (FFE)-Zustände ein, welche die phasenkodierte logische Struktur von Qubit-Hypergraph-Zuständen auf beliebige d-stufige Systeme verallgemeinern. Innerhalb dieses Rahmens wird die polynomiale Unterklasse über Tensor-Kanten-Hypergraphen beschrieben, und für allgemeine FFE-Zustände wird ein Stabilisatorformalismus entwickelt. Die Analyse der lokalen Äquivalenz unter unitären und endlichen Funktions-Pauli-Transformationen führt zu einer vollständigen Klassifikation bipartiter FFE-Zustände für lokale Dimensionen drei und vier und zeigt strukturelle Verbindungen zur Klassifikation komplexer Hadamard-Matrizen auf.

Im dritten Teil wird ein zweistufiges Verfahren zur quditbasierten Schaltkreiskompression vorgestellt. In der ersten Stufe werden mehrere Qubits mittels schnittminimierender Graphpartitionierung zu Qudits zusammengefasst; in der zweiten Stufe werden eingebettete Zwei-qubit-Gatter durch native Zwei-qudit-Operationen ersetzt. Es werden obere und untere Schranken für die erreichbare Reduktion des nichtlokalen Gatteraufwands hergeleitet und Fälle identifiziert, in denen diese Schranken saturiert werden. Insgesamt entsteht so ein kohärenter Rahmen zur Übertragung qubitbasierter Paradigmen auf höherdimensionale Architekturen, der sowohl theoretische Einsichten als auch praktische Vorteile für Quantenhardware mit kohärenter Mehrniveausteuerung bietet.

Abstract

Quantum information theory has traditionally centered on two-level systems—qubits—even though many experimental platforms, such as photonic modes, trapped ions, and superconducting circuits, naturally implement higher-dimensional qudits. This thesis presents three complementary approaches toward a dimension-aware extension of quantum information theory that retains its operational foundations while adapting to the structural complexity of systems with higher local dimension.

First, the work derives dimension-dependent quasi-monogamy relations for correlation measures expressed within the Bloch and correlation-tensor formalisms. In parallel, it establishes new Tsallis-2 entropy inequalities that include explicit dimensional parameters, among them a generalized form of strong subadditivity. Together, these results show how the geometry and entropy of quantum correlations evolve with increasing local dimension and provide a systematic generalization of qubit-specific relations, such as the Coffman–Kundu–Wootters inequality.

Second, the thesis introduces finite-function-encoding (FFE) quantum states, which extend the phase-encoded logical structure of qubit hypergraph states to general d-level systems. Within this framework, the polynomial subclass is characterized through tensor-edge hypergraphs, and a stabilizer formalism for arbitrary FFE states is developed. The analysis of local equivalence under both unitary and finite-function-Pauli transformations yields a complete classification of bipartite FFE states for local dimensions three and four, and furthermore demonstrating a structural link to the classification of complex Hadamard matrices.

Third, a two-stage qudit-based circuit compression method is proposed. The first stage groups multiple qubits into composite qudits via cut-minimizing graph partitioning, while the second replaces embedded two-qubit operations with native two-qudit gates. The study proves upper and lower bounds on the achievable reduction in nonlocal gate cost and presents cases in which these bounds are saturated. Collectively, these developments establish a coherent framework for extending qubit-based paradigms to higher-dimensional architectures, demonstrating both theoretical insight and practical advantages for quantum hardware supporting coherent multilevel control.

Contents

1 Introduction

Quantum information theory has largely been developed around two-level systems, or qubits, whose mathematical simplicity and geometric representations have driven early breakthroughs in communication [1, 2], computation [3, 4], and cryptography [5, 6]. At the same time, many physical platforms—photonic modes [7, 8], trapped-ion manifolds [9], and superconducting circuits [10]—naturally realize higher-dimensional (qudit) systems.

Recent results further highlight clear advantages of qudits: high-dimensional quantum key distribution achieves higher key rates and operates robustly under noise compared to qubit schemes [11, 12]; photons entangled in large Hilbert spaces certify stronger violations of Bell inequalities [13, 14]; qudit encodings reduce circuit complexity by replacing inter-qubit entangling operations with local multilevel operations [15, 16]; error-correcting codes over higher dimensions raise thresholds or lower overheads in fault-tolerant architectures [17, 18]; prime-d magic-state distillation exhibits improved performance [19]; and qudit architectures natively support richer coherence and entanglement structures that can be harnessed for more efficient quantum information processing [20, 21]. Together, the natural prevalence of qudit systems and these demonstrated benefits motivate an in-depth study of qudit quantum information frameworks.

In this thesis, three approaches to qudit generalization are pursued. The first approach in Section 3 develops dimension-dependent corrections and relaxations that extend monogamy relations and entropy inequalities beyond their qubit-specific forms, establishing quasi-monogamy bounds and clarifying where qudit behavior departs from two-level intuitions. The second approach in Section 4 identifies operationally useful subfamilies of the qudit state space—finite-function-encoding states—and shows how focusing on these tailored structures preserves critical qubit-like properties while sidestepping complete dimensional complexity. The third approach in Section 5 demonstrates direct performance gains by embedding qubit registers into higher-dimensional qudits and exploiting genuinely multilevel operations to reduce resource costs in concrete protocols. Together, these approaches show when dimension-sensitive extensions suffice, when specialized subfamilies provide a practical alternative, and when entirely new mathematical tools are required.

2 Generalization in Quantum Information Theory

In this section, we examine selected concepts from quantum information theory and their generalization to higher-dimensional systems. The aim is not to provide a comprehensive review, but to highlight representative examples that are relevant for the subsequent discussions and our results in [22, 23, 24].

It is well known that the description and solution of many problems can become more tractable when embedded in a more general theoretical framework. For example, the need to describe mixed quantum states can be circumvented by considering a larger Hilbert space in which these mixed states are viewed as reduced pure states after tracing out an environment. This point of view is often referred to as the "Church of the Larger Hilbert Space," a term attributed to Smolin [25]. Such an extension can simplify the mathematical structure of the problem and provide access to more powerful solution techniques; it can also yield operational advantages, although these are independent aspects of generalization that need not coincide.

This perspective is naturally relevant in quantum information theory. Historically, many foundational developments were based on the implicit or explicit assumption that binary logic suffices, leading to a focus on two-level systems—qubits—and a well-developed toolbox for communication, computation, and cryptography. The restriction to qubits is not fundamental, yet generalizing known results to arbitrary dimensions is nontrivial: qubit systems benefit from compact representations and geometric intuitions that do not extend easily, and naïve lifts can obscure the operational content.

It is tempting to demand that familiar qubit formulas survive intact in higher dimensions, but that expectation is more aesthetic than principled. What should be preserved is the conceptual invariant—the operational content and the symmetries—not necessarily the functional form of its expression. When the underlying structure is stable, form often carries over verbatim; when geometry, extremal structure, or information measures change with dimension, the qubit formulas become misleading. Allowing the functional form to change is therefore a diagnostic that reveals the organizing structure rather than a concession. The preference of a physicist for a familiar formula is not without value, but it should not be treated as an obligation (cf. Wigner's reflection on the fit between mathematics and physics [26]).

To anchor the discussion, we point to five examples drawn from the definitions that follow. The Schmidt decomposition (Section 2.3) carries over verbatim to arbitrary local dimension and retains its role in characterizing bipartite pure-state entanglement . The Bloch representation (Section 2.4) appears to generalize in form, yet its consequences differ: beyond qubits the $su(d)$-based coordinates no longer parametrize a full sphere of physical states and positivity imposes nontrivial manifold constraints . Monogamy relations (Section 2.5) preserve the physical idea that entanglement cannot be freely shared, while the qubit-style inequalities

typically fail and require relaxed, dimension-dependent statements. Hypergraph states (Section 2.6) show that a change in expression can reveal the right organizing feature: moving from qubit edge-phase rules to d-ary phase functions brings polynomiality to the foreground as the criterion for when a qudit state admits a graph description. Finally, the circuit model (Section 2.7) preserves the concept of computation as local composition on a tensor-product register, while the form of the primitive library and hardware-relevant costs can change with local dimension; asymptotically, there is no generic advantage in finding algorithms, but on multilevel hardware genuine qudit gates can reduce nonlocal depth when coherence and fidelities permit.

Finally, a word on motivation. Generalization serves different purposes: sometimes the aim is to translate a useful physical notion to higher local dimension without loss of operational meaning—as with the Schmidt decomposition and appropriately relaxed monogamy statements (Section 2.3, Section 2.5); sometimes the aim is structural insight—allowing the functional expression to change exposes the invariant that actually organizes the theory, such as higher-order positivity constraints in the Bloch picture and polynomiality in the passage from qubit hypergraphs to qudit FFE states (Section 2.4, Section 2.6); and sometimes the aim is operational advantage—on platforms with coherent multilevel control, genuine qudit gates can reduce nonlocal depth or resource overhead in concrete protocols (Section 2.7, Section 5).

With these observations in place, we first fix the notation and basic definitions, then return to the five examples—Schmidt decomposition Section 2.3, Bloch representation Section 2.4, monogamy of entanglement Section 2.5, hypergraph states Section 2.6, and the circuit model Section 2.7. The detailed investigations of generalization that motivate this thesis are developed later: finite-function-encoding and its relation to hypergraphs Section 4, quasi-monogamy and entropy inequalities Section 3, and circuit-level compression in multilevel architectures Section 5.

2.1 General Definitions

In quantum mechanics, we make extensive use of bounded linear operators acting on a Hilbert space $\mathcal{H}$. Note that we focus on finite-dimensional spaces, since most of quantum information theory is based on finite-dimensional quantum mechanics. With that being said, let us introduce some useful concepts. We follow [27] for notation and the operator-algebraic formulation.

In quantum theory, a finite-dimensional physical system is modeled by a complex Hilbert space $\mathcal{H} = \mathbb{C}^d$, where $d \in \mathbb{N}$ is the Hilbert space dimension. The dual space $\mathcal{H}^*$ consists of all linear functionals acting on $\mathcal{H}$.

The space of linear operators on $\mathcal{H}$ is denoted $\mathcal{B}(\mathcal{H})$. It forms an algebra over $\mathbb{C}$ under addition, scalar multiplication, and operator composition. This space becomes a Hilbert space when equipped with the Hilbert–Schmidt inner product:

$$\langle A, B\rangle_{\mathsf{HS}} := \mathrm{Tr}(A^\dagger B), \quad A, B \in \mathcal{B}(\mathcal{H}).$$

The associated norm is

$$\|A\|_{\mathsf{HS}} := \sqrt{\mathrm{Tr}(A^\dagger A)}.$$

This inner product induces an identification between $\mathcal{B}(\mathcal{H})$ and its dual space $\mathcal{B}(\mathcal{H})^*$. Specifically, every linear functional $A' \in \mathcal{B}(\mathcal{H})^*$ can be uniquely represented by an operator $A \in \mathcal{B}(\mathcal{H})$ such that

$$A'(B) = \mathrm{Tr}(AB).$$

We will use this identification to simplify notation by treating linear functionals and their representing operators interchangeably under the trace pairing.

Finally, there exists a canonical vector space isomorphism

$$\mathcal{B}(\mathcal{H}) \cong \mathcal{H} \otimes \mathcal{H}^*,$$

under which a rank-one operator $|\psi\rangle\langle\phi| \in \mathcal{B}(\mathcal{H})$ corresponds to the simple tensor $|\psi\rangle \otimes \langle\phi| \in \mathcal{H} \otimes \mathcal{H}^*$. This identification is useful, for example, when representing operators in terms of tensor products of state vectors and dual vectors.

In finite dimensions, we also have the concrete identifications $\mathcal{H} \cong \mathbb{C}^d$ and $\mathcal{B}(\mathcal{H}) \cong M_d(\mathbb{C})$, the space of $d \times d$ complex matrices. This allows every operator to be represented by a matrix and every state $|\psi\rangle \in \mathcal{H}$ to be written as a column vector.

2.2 Quantum Mechanics in Finite Dimensions

In quantum theory, a finite-dimensional physical system is modeled on a Hilbert space $\mathcal{H}$ with observables given by the algebra $\mathcal{B}(\mathcal{H})$ of linear operators.

A *quantum state* is represented by a density operator $\rho \in \mathcal{B}(\mathcal{H})$ with $\rho \geq 0$ and $\operatorname{Tr} \rho = 1$, giving expectation values via $\rho(A) = \operatorname{Tr}(\rho A)$ for $A \in \mathcal{B}(\mathcal{H})$.

A *measurement* is specified by a positive operator-valued measure (POVM), i.e., a family of effects $\{E_i\} \subset \mathcal{B}(\mathcal{H})$ with $E_i \geq 0$ and $\sum_i E_i = \mathbb{1}$. For a state ρ, the probability $\Pr$ of outcome i is given by:

$$\Pr(i \,|\, \rho) = \operatorname{Tr}(\rho E_i),$$
$$\sum_i E_i = \mathbb{1}.$$

Projective measurements arise from the spectral decomposition of a Hermitian observable $A = A^\dagger$,

$$A = \sum_i a_i P_i,$$

with outcomes a_i and projectors P_i.

The state space $\mathcal{D}(\mathcal{H}) = \{\rho \in \mathcal{B}(\mathcal{H}) : \rho \geq 0,\ \operatorname{Tr} \rho = 1\}$ is convex, and its extremal points are the pure states (rank-one projectors). Likewise, the set of POVMs is convex, with projective measurements as extremal elements. Classical randomization of preparations or measurements corresponds to convex mixing at the operator level.

Physical evolutions and noise are modeled by completely positive trace-preserving (CPTP) linear maps $\Phi : \mathcal{B}(\mathcal{H}) \to \mathcal{B}(\mathcal{H}')$. They satisfy complete positivity and trace preservation:

$$\Phi \otimes \mathrm{id}_k \text{ is positive for all } k \geq 1, \qquad \operatorname{Tr}[\Phi(\rho)] = \operatorname{Tr} \rho.$$

Where $\mathrm{id}_k : \mathcal{B}(\mathbb{C}^k) \to \mathcal{B}(\mathbb{C}^k)$ denotes the identity channel on a k-dimensional ancillary system, i.e., $\mathrm{id}_k(Y) = Y$ for all $Y \in \mathcal{B}(\mathbb{C}^k)$.
Standard examples include unitary conjugation and partial trace:

$$\rho \mapsto U \rho U^\dagger, \qquad \rho_A \,=\, \operatorname{Tr}_B(\rho).$$

Composite systems are modeled on tensor products $\mathcal{H} = \mathcal{H}_1 \otimes \cdots \otimes \mathcal{H}_n$ with $\mathcal{H}_k \cong \mathbb{C}^{d_k}$. A state is *product* if it factorizes as $\rho = \rho_1 \otimes \cdots \otimes \rho_n$ and *entangled* otherwise. Reduced states are obtained by the partial trace; for $\rho \in \mathcal{D}(\mathcal{H}_A \otimes \mathcal{H}_B)$ the marginal on A is

$$\rho_A = \operatorname{Tr}_B(\rho).$$

We now turn to standard representations of qubits and qudits. For a qubit with $\mathcal{H} \cong \mathbb{C}^2$, pure states have the form

$$|\psi\rangle = \alpha \,|0\rangle + \beta \,|1\rangle\,, \qquad |\alpha|^2 + |\beta|^2 = 1,$$

and measurements are POVMs $\{E_i\}$ with $0 \leq E_i \leq \mathbb{1}$ and $\sum_i E_i = \mathbb{1}$. For a qudit with $\mathcal{H} \cong \mathbb{C}^d$, pure states are

$$|\psi\rangle = \sum_{j=0}^{d-1} \alpha_j \,|j\rangle\,, \qquad \sum_{j=0}^{d-1} |\alpha_j|^2 = 1,$$

and the same formalism for effects, POVMs, and channels applies unchanged.

2.3 Schmidt Decomposition

Any pure bipartite state $|\psi\rangle \in \mathcal{H}_A \otimes \mathcal{H}_B$ admits a Schmidt decomposition [28, 29].

$$|\psi\rangle = \sum_{i=1}^{r} \lambda_i \,|a_i\rangle \otimes |b_i\rangle\,,$$
$$\lambda_i \geq 0, \qquad \sum_{i=1}^{r} \lambda_i^2 = 1, \qquad r \leq \min(d_A, d_B),$$

where $\{|a_i\rangle\} \subset \mathcal{H}_A$ and $\{|b_i\rangle\} \subset \mathcal{H}_B$ are orthonormal sets and r is the Schmidt rank.

The reduced states share the same nonzero spectra.

$$\rho_A = \mathrm{Tr}_B\big(\,|\psi\rangle\,\langle\psi|\,\big) = \sum_{i=1}^{r} \lambda_i^2\,|a_i\rangle\,\langle a_i|\,,$$
$$\rho_B = \mathrm{Tr}_A\big(\,|\psi\rangle\,\langle\psi|\,\big) = \sum_{i=1}^{r} \lambda_i^2\,|b_i\rangle\,\langle b_i|\,.$$

A pure state is separable if and only if $r = 1$. The Schmidt coefficients $\{\lambda_i\}$ are unique up to degeneracies, and the decomposition follows from the singular value decomposition of the coefficient matrix of $|\psi\rangle$ [30].

This construction generalizes verbatim to arbitrary finite local dimensions, i.e., no qubit-specific structure is required and only the admissible range of r changes with d_A and d_B. Its operational content is dimension-agnostic: bipartite pure-state entanglement is completely determined by $\{\lambda_i^2\}$. In contrast, there exists no analogous single parameter factorization for generic multipartite pure states or for mixed states [31, 32].

2.4 Bloch Representation

Since $\mathcal{B}(\mathcal{H})$ is a Hilbert space with respect to the Hilbert–Schmidt inner product, one can fix an orthonormal basis of Hermitian operators $\{\lambda_\mu\}_{\mu=0}^{d^2-1} \subset \mathcal{B}_{\mathrm{Herm}}(\mathcal{H})$ with [33, 34]

$$\lambda_0 = \mathbb{1}_d, \qquad \mathrm{Tr}(\lambda_\mu\lambda_\nu) = d\delta_{\mu\nu}, \qquad \mathrm{Tr}\,\lambda_k = 0 \quad (k \geq 1).$$

Every density operator $\rho \in \mathcal{D}(\mathcal{H})$ admits the expansion

$$\rho = \frac{1}{d}\left(\mathbb{1}_d + \sum_{k=1}^{d^2-1} \langle\lambda_k\rangle\ \lambda_k\right), \qquad \langle\lambda_k\rangle := \mathrm{Tr}(\rho\,\lambda_k),$$

which we refer to as the generalized Bloch decomposition [33, 34].
Purity is quadratic in the Bloch coordinates:

$$\mathrm{Tr}(\rho^2) = \frac{1}{d}\left(1 + \sum_{k=1}^{d^2-1} \langle\lambda_k\rangle^{\,2}\right).$$

Geometrically, the quantum state space $\mathcal{D}(\mathcal{H})$ is a compact convex set whose extreme points are pure states [29]. In multipartite settings, the tensor-product of local Bloch bases induces correlation tensors whose norms we will use below [34, 35].
For $d = 2$, choose $\{\lambda_0, \lambda_k\} = \{\mathbb{1}_2, \sigma_k\}_{k=1}^3$ with Pauli matrices $\{\sigma_k\}$. Note that we normalize as $\mathrm{Tr}(\lambda_k\lambda_j) = 2\delta_{kj}$ Then

$$\rho = \frac{1}{2}\left(\mathbb{1}_2 + \sum_{k=1}^{3} \langle\sigma_k\rangle\ \sigma_k\right), \qquad \langle\sigma_k\rangle := \mathrm{Tr}(\rho\,\sigma_k),$$

and the physical Bloch vectors fill the unit ball $\{\vec{r} \in \mathbb{R}^3 : \|\vec{r}\| \leq 1\}$ with pure states on the sphere $\|\vec{r}\| = 1$ [29]. Moving beyond $d = 2$, the same construction yields a qudit Bloch representation, but several geometric features change in essential ways.

For general local dimension $d \geq 2$, fix any orthonormal traceless basis $\{\lambda_k\}_{k=1}^{d^2-1}$ (e.g., generalized Gell–Mann or Heisenberg–Weyl) [36, 37]. The trace and purity formulas above imply that the affine image of $\mathcal{D}(\mathcal{H})$ lies on a hypersphere centered at the maximally mixed state, but positivity $\rho \geq 0$ imposes additional nonlinear constraints on the coordinates $\{\langle\lambda_k\rangle\}$ [33, 34]. In terms of quantum states this means that pure state lie on the sphere $\|\vec{r}\| = \sqrt{d-1}$, but for $d > 2$ not every point of that sphere is physical; in fact pure states lie within convex sub-manifolds on the surface of the sphere. Thus, while the *form* of the decomposition generalizes, several *consequences* specific to $d = 2$ do not: the "Bloch ball" intuition breaks down, and positivity is captured by higher-order polynomial constraints rather than a single Euclidean norm bound [33, 34, 29].

2.5 Entanglement and Monogamy Relations

Entanglement is a defining feature of quantum mechanics and a fundamental resource in quantum information theory [30]. To quantify it, one uses *entanglement measures* $\mu : \mathcal{D}(\mathcal{H}_{AB}) \to [0, \infty)$ with the following standard properties: (i) *faithfulness on separable states*, $\mu(\rho) = 0$ if ρ is separable; (ii) *LOCC monotonicity*,

$\mu(\Lambda_{\mathrm{LOCC}}(\rho)) \leq \mu(\rho)$ for every LOCC map Λ_{LOCC}; (iii) *convexity*, $\mu(p\rho_1+(1-p)\rho_2) \leq p\,\mu(\rho_1)+(1-p)\,\mu(\rho_2)$ for $p \in [0,1]$ [38, 30]. Here Λ_{LOCC} denotes a channel implementable by sequences of local CPTP maps coordinated by two-way classical communication between the parties, i.e., LOCC operations, which cannot increase entanglement on average [30]. Examples include concurrence and entanglement of formation [39, 40], and negativity and squashed entanglement [41, 42].

Monogamy relations constrain how bipartite entanglement can be distributed within a multipartite system [43]. For a tripartite state ρ_{ABC} and a measure μ, a strict monogamy is defined as

$$\mu_{A:BC}(\rho_{ABC}) \;\geq\; \mu_{A:B}(\rho_{AB}) \;+\; \mu_{A:C}(\rho_{AC})\,.$$

In the qubit case, the Coffman–Kundu–Wootters (CKW) inequality establishes monogamy for the squared concurrence (the *tangle*) [44]. Writing $C(\cdot)$ for concurrence,

$$C^2_{A:BC} \;\geq\; C^2_{A:B} \;+\; C^2_{A:C}\,.$$

This result extends to n-qubit systems for the tangle [45] and connects to trade-off relations relevant for cryptographic settings [46]. Beyond qubits, the *concept* of monogamy survives but the *formal* qubit inequality typically fails. For higher local dimensions, many popular measures (including concurrence and entanglement of formation) are not strictly monogamous; valid statements often require either (a) switching to measures known to be monogamous in all dimensions (notably squashed entanglement [42]), or (b) adopting *dimension-aware relaxations*. We will return to these points in Section 3, where we develop quasi-monogamy bounds and entropy-inequality extensions that make the dimension dependence explicit.

2.6 Hypergraph States and Generalizations

Hypergraph states form a structured yet expressive subset of multipartite entangled states: specified by simple combinatorial data, they capture genuinely multipartite correlations, exhibit strong nonlocality, and in suitable families serve as universal resources for measurement-based quantum computation [47, 48, 49].

A (finite) hypergraph is a pair $H = (V, E)$ with vertices $V = \{1, \ldots, n\}$ and hyperedges $E \subseteq 2^V$. To each hyperedge e one associates a multi-controlled phase gate U_e that multiplies computational-basis states by a phase conditioned on all sites in e. Applying all such phases to the uniform superposition $|+\rangle^{\otimes n}$, with $|+\rangle = (|0\rangle + |1\rangle)/\sqrt{2}$, defines the (qubit) hypergraph state $|H\rangle := \big(\prod_{e\in E} U_e\big)\,|+\rangle^{\otimes n}$ [50]. Equivalently, writing $f(x) = \sum_{e\in E}\prod_{i\in e} x_i$ as a square-free polynomial over $\mathbb{F}_2$, one has

$$|H\rangle = \frac{1}{\sqrt{2^n}} \sum_{x\in\mathbb{F}_2^n} (-1)^{\,f(x)}\,|x\rangle\ ,$$

so monomials label hyperedges and degree equals edge size [50].

For higher local dimension it is convenient to adopt a phase-encoding view that subsumes the qubit case and its extensions. Let $d \geq 2$ and $\omega := e^{2\pi i/d}$, and consider states of the form

$$|\Psi_f\rangle = \frac{1}{\sqrt{d^n}} \sum_{x} \omega^{\,f(x)}\,|x\rangle\ ,$$

with $f : S^n \to S$ chosen to match the finite set S that labels the local computational basis of each site (e.g., $S = \mathbb{F}_q$ or $S = \mathbb{Z}_d$). This isolates the operational *concept* (function→phase) and lets the concrete *form* be dictated by the underlying finite set and its arithmetic (field versus ring), such as $\mathbb{F}_q$ or $\mathbb{Z}_d$. In [51] the qudit hypergraph is constructed with the local label set as a finite field $\mathbb{F}_q$ with $q = p^m$ a prime power, and $f : \mathbb{F}_q^{\,n} \to \mathbb{F}_q$ is *multilinear* (linear in each variable); generalized controlled-phase gates then implement the corresponding monomials, preserving the graphical form of the qubit construction [51]. These (qubit and qudit) hypergraph states support genuine multipartite entanglement, admit efficient certification via commuting symmetries, and, in suitable families, serve as universal MBQC resources [47, 48, 49].

The phase-encoding perspective also reveals where the graphical model stops. Over finite fields every function $g : \mathbb{F}_q^{\,n} \to \mathbb{F}_q$ has a polynomial representative of bounded degree, but graphical hypergraph rules require (square-free) *multilinear* structure; over rings like $\mathbb{Z}_d$ with composite d not every function $h : \mathbb{Z}_d^{\,n} \to \mathbb{Z}_d$ is polynomial at all [52, 53]. Finite-function-encoding (FFE) states retain the function→phase concept and drop the multilinearity restriction, thereby extending the construction to all functions on the chosen label set; as developed in Section 4, polynomiality then becomes the criterion linking functional encodings back to (hyper)graph descriptions, while stabilizer-like control persists in the broader non-graphical class. Read in the context of our generalization program, the hypergraph route preserves the *form* of the qubit construction when arithmetic permits, whereas the FFE route preserves the *concept* while allowing the form to change, making explicit that it is the underlying algebra (field versus ring) and not qubit convenience that determines the appropriate higher-dimensional expression.

2.7 The Circuit Model of Quantum Computation

We recall the circuit model in finite dimensions, fix conventions for registers, gates, depth and cost, and then indicate how the qudit lift fits our generalization perspective. A finite register is modeled on a tensor-product Hilbert space

$$\mathcal{H} = \bigotimes_{i=1}^{n} \mathcal{H}_i, \qquad \mathcal{H}_i \cong \mathbb{C}^{d_i}.$$

A *gate* acts as a unitary on a small subset $S \subseteq \{1, \ldots, n\}$ and as the identity elsewhere. A *layer* is a product of gates with disjoint supports; a (depth-L) *circuit* is an ordered product of layers $C = L_L \cdots L_2 L_1$ constrained by the hardware coupling graph.

Given a fixed primitive gate library and coupling graph, the *depth* is the minimal number L of layers; the *gate count* is the total number of primitive gates; a hardware-aware cost counts *nonlocal* (e.g., two-site) gates. For qubits, universal libraries exist—e.g., all one-site gates together with any entangling two-site gate [54, 55]. For qudits, a general characterization ("all one-qudit gates plus almost any entangling two-qudit gate") is provided by Brylinski–Brylinski [56], and constructive exact-universal libraries follow from Muthukrishnan–Stroud and from Brennen–Bullock–O'Leary [57, 16].

Local unitaries admit ϵ-approximations whose length scales polylogarithmically in $1/\epsilon$ (Solovay–Kitaev), uniformly for fixed d [58]. Many exact/minimal synthesis tasks are intractable in the worst case; search and meet-in-the-middle methods remain exponential in the relevant parameters [59]. For qudit libraries, practical universality criteria mirror the qubit case via algebraic and t-design conditions [60, 61].

The *concept*—computation as composition of local transformations on a tensor-product register—survives unchanged when passing from qubits to qudits. What may change is the *form* of the primitive library and the *resource accounting* on real hardware. Asymptotically, merely increasing d does not provide a generic advantage in *finding* optimal circuits. Practically, multilevel devices enable (i) *register compression* (fewer sites, same logical unitary) and (ii) *native d-ary synthesis* (genuinely multilevel gates), which can reduce nonlocal depth when coherence and fidelity of qudit operations are competitive. We quantify such depth and nonlocal-cost reductions in Section 5.

3 Monogamy of Correlations and Entropy Inequalities in the Bloch Picture

3.1 Summary

Monogamy relations are central to the security of quantum communication protocols, where the assumption that correlations cannot be freely shared guarantees secrecy. Although monogamy constraints are fundamental to extending security proofs to arbitrary-dimensional protocols, only a limited set of such constraints has been established beyond qubits. This scarcity is expected: strict monogamy can hold only for entanglement measures, and most familiar measures cannot simultaneously satisfy geometric faithfulness and strict monogamy; moreover, many "dimension-free" statements in the qubit literature carry implicit dependencies on local dimension that must be made explicit in $d > 2$.

We build on [62] by introducing explicit dimension factors and deriving *quasi-monogamy* relations for a correlation quantity defined in the Bloch/correlation-tensor picture. Rather than adhering to the qubit-specific formalism of monogamy, we emphasize its operational core: strong correlation between two subsystems necessarily limits the correlation either can share with a third. To expose the role of local dimension and low-rank support, we develop a *split Bloch basis* that replaces the global identity by subspace identities, yielding a block-sparse operator basis in which low-rank states embed transparently into higher-dimensional Hilbert spaces and purity/correlation sums display their dimensional prefactors.

Within matched subspaces, we define a correlation monotone and prove quasi-monogamy bounds that carry explicit dimension dependence. The monotone is convex and invariant under local isometries, enabling fair comparison across embeddings and subspace reductions. For qubits, our bounds recover the familiar CKW-type form (up to normalization), while for higher local dimensions the dimensional prefactors are necessary and unavoidable. Moreover, *in our framework*, any meaningful entanglement measure is *monotonic* in the underlying correlations, so the above correlation bounds translate directly into *dimension-dependent entanglement bounds* across the same partition.

On the entropic side, we obtain new *Tsallis-2* inequalities that make dimension explicit, including a dimension-dependent analogue of strong subadditivity and a nonlinear generalized pseudo-additivity inequality. The generalized pseudo-additivity bound is independent of subadditivity and can be strictly tighter for *asymmetric* local dimensions, whereas for *equal* local dimensions standard subadditivity remains stronger.

Overall, the split-Bloch formalism clarifies how local dimension structures correlations, and it yields practical, dimension-sensitive quasi-monogamy and Tsallis-2 entropy bounds for multipartite states beyond qubits.

3.2 Own Contribution

This paper builds on research done in my master thesis. Each author contributed equally to the conception, development, and writing of the manuscript. The underlying concept was initially proposed by my PhD supervisor, Marcus Huber. Claude Klöckl, who was a postdoctoral researcher in Marcus Huber's group at the time, primarily focused on the quadratic entropy inequality. While contributing to the overall development of the manuscript, I mainly focused on the proof of Theorem 2 and contributed substantially to the definition and construction of the split Bloch basis.

Monogamy of correlations and entropy inequalities in the Bloch picture

Paul Appel,[1,*] Marcus Huber,[1,†] and Claude Klöckl[1,2,‡]

[1] *Institute for Quantum Optics and Quantum Information - IQOQI Vienna, Austrian Academy of Sciences, Boltzmanngasse 3, 1090 Vienna, Austria*

[2] *Institute of Computer Science, Masaryk University, Botanická 68a, 60200 Brno, Czech Republic*

(Dated: October 25, 2021)

We investigate monogamy of correlations and entropy inequalities in the Bloch representation. Here, both can be understood as direct relations between different correlation tensor elements and thus appear intimately related. To that end we introduce the *split Bloch basis*, that is particularly useful for representing quantum states with low dimensional support and thus amenable to purification arguments. Furthermore, we find dimension dependent entropy inequalities for the Tsallis 2-entropy. In particular, we present an analogue of the strong subadditivity and a quadratic entropy inequality. These relations are shown to be stronger than subadditivity for finite dimensional cases.

I. INTRODUCTION

This articles covers two important themes of quantum information: *entropy inequalities* and *monogamy relations*. The first focus of our article are entropy inequalities. Entropy has been described by many differing mathematical definitions, but essentially the entropy of a quantum state always describes the lack of knowledge about the respective system. Entropy inequalities govern the way information about some constituents of the system determines our knowledge about the remainder of the system. They could be broadly equated to the "natural laws" of information. Typically entropy can be either formulated in a classical or quantum version. Throughout this article, we will be discussing the quantum case. How well these laws are understood varies greatly depending on the exact mathematical formulation of entropy. The standard formulation of the Shannon entropy [1] as well as its quantum analogue the von Neumann entropy have been thoroughly classified [2, 3]. Many further parametrized families of entropies are known. The two most well-known single-parameter examples are the Rényi α-entropy [4] and the Tsallis q-entropy [5]. Recently, important progress was made on the family of the Rényi α-entropies [6, 7]. This almost completed the description of the better-known entropies. For the Tsallis q-entropy there are, to the best of our knowledge, no complete classification results known. Even though the whole family of q-entropies (sometimes also referred to as q-logarithms) is well studied [8], of relevance for the field of complex systems [9–11] and in case of the Tsallis 2-entropy frequently employed in quantum mechanics under the name *linear entropy*.

Note that a number of powerful no-go results are known, specifically regarding the impossibility of linear inequalities for Rényi entropies for $\alpha \neq 0, 1$ [6] and the unachievability of strong subadditivity for Tsallis q-entropies with $q \neq 1$ [12]. The Tsallis q-entropies directly translate to Rényi α-entropies, but the impossibility of linear inequalities for the Rényi 2-entropy does not imply the same for the Tsallis 2-entropy. Indeed, the Tsallis 2-entropy is subadditive [13]. Nonetheless we are able to circumvent these no-go results in the form of dimension-dependent analogues to strong subadditivity and pseudo-additivity for the linear entropy. These analogues hold where their dimension-independent counterparts do not. We can hence trade dimension dependency for a broader range of applicability. In particular we introduce a linear and another non-linear entropy inequality for the Tsallis 2-entropy.

The second focus of this article concerns correlations. In quantum physics some correlations exhibit a property commonly referred to as monogamy [14]. Monogamy intuitively means that whenever two parties share a sufficient amount of monogamous correlations it prohibits a third party from also being correlated in a non-trivial way to the former. In other words we could see them as a "natural law" limiting correlated information in analogy to the way we introduced entropy inequalities before. This simple idea is not only of interest when trying to understand the fundamental structure of quantum correlations, but it is also the base for the security proofs of quantum key distribution (see the security proof of either Lo-Chau's protocol [15] or the security proof [16] of the BB84 protocol [17]). Therefore monogamy of entanglement is an essential tool for one of the most mature practical applications from the field of quantum information. Formalizing the intuitive idea of monogamy has been the subject of a long-standing debate within the quantum information community [18–21].

Let us review a few well-known facts about monogamy and motivate the introduction of dimension-dependent factors. It is noteworthy that the *strict* classical definition of monogamy, e.g. $\mu_{AB|C}(\rho_{ABC}) \geq \mu_{A|C}(\rho_{AC}) + \mu_{B|C}(\rho_{BC})$

* paul.jonas.appel@gmail.com
† entangledanarchist@gmail.com
‡ claudio.kloeckl@reflex.at

where μ is an entanglement measure in arbitrary dimension, is intimately connected to the notion of entanglement: It has been shown, that *only* entanglement measures, in contrast to measures of other correlations, can be *strictly* monogamous in arbitrary dimension [22]. On the other hand, even though many relations have been found to fulfill this definition for *qubits*, e.g. the Coffman-Kundu-Wootters (CKW) inequality [18], and even though a generalization for n-qubit case [19] is available, there exists only one known entanglement measure which fulfills this strict notion of monogamy in *arbitrary dimension*: Squashed entanglement [21]. Unfortunately squashed entanglement is hardly computable; even numerically. Many other entanglement measures can not be readily generalized to arbitrary dimension, e.g. the CKW inequality [23, 24]. Even though common monogamy inequalities do not explicitly feature dimension dependent factors, they are indeed implicitly dimension dependent, i.e. assuming particular local dimensions. Many arguments concerning certain aspects of monogamy are dependent on these assumptions: For example, the maximal entanglement of two parties excludes a third party to be entangled with either of the former *only* if the systems of the former have the *same* local dimension. Furthermore, it has been shown that in general entanglement measures that quantify maximal entanglement geometrically faithful cannot be monogamous in asymptotic dimensions [24]; this is true also for squashed entanglement.

Considering all these problems in finding feasible entanglement measures which fulfill the strict monogamy relation in arbitrary dimension, it is sensible to relax this strict condition, e.g. [25] or by introducing dimension-dependent factors to find analogue relations, as suggested in [24]. These analogues might not fulfill the *strict* notion of monogamy but capture the main idea of monogamy: That the correlations within one marginal restrict the correlations of all other possible marginals with the former. With this in mind, we define a correlation monotone which, even though it does not fulfill the *strict* monogamy relation, still complies with useful (quasi)-monogamy relations. Even though this (quasi)-monogamy relation is weaker than then CKW inequality for qubits, it provides a dimension-dependent inequality for *arbitrary* dimension. Furthermore we can reproduce a well known result for qubit systems in arbitrary dimension: We show that if two parties with systems of *equal* dimension are maximally entangled, no other party can be entangled with the composite system. Additionally if two parties are *not maximally* entangled but share some entanglement we can still provide non-trivial bounds on the shared correlations with any other party.

That the introduction of dimensional factors enlarges the applicability of monogamy and entropy relations is in itself a noteworthy observation already made in [24], in this article we are however able to contribute entropy and (quasi-) monogamy relations. Let us stress another important point: Even though both areas of research, entropy inequalities and monogamy relations, are usually considered as two distinct subfields, there exists an intimate connection, which becomes clear once we identify them as particular instances of the marginal problem. The marginal problem is solved if for a given set of marginals all complementary sets of marginals, which make up a physical state, are identified [26]. Since both entropy inequalities as well as monogamy relations depend on functions of the marginals, it is not surprising that a connection between them can be made.

This connection becomes particularly obvious by using the correlation tensor of the generalized Bloch representation [27–30]. Another important advantage of using the Bloch vector representation is the fact, that it naturally introduces dimension-dependent factors, which we show to be useful to circumvent certain no-go-theorems. Even though the Bloch picture is an extremely well-established subject, it attracts continued interest up to this day. Most notably the proof of the long standing non-existence conjecture of the absolutely maximally entangled (AME) states for seven qubit systems [31] including a subsequent connection to coding theory and a classification of higher dimensional AME states [32] but also applications in entanglement detection [33–35] and quantum thermodynamics [36]. In this work we are able to contribute to the Bloch formalism with the introduction of the *Split Bloch basis*, an orthogonal operator basis, which allows a concise description of states with low dimensional support in high-dimensional Hilbert spaces. The use of this basis is helpful in the handling of multipartite systems with different local dimensions, since it allows to easily define functions which are invariant under isometric transformations. It is our hope that this article sparks further discussions over the merits of the generalized Bloch decomposition.

This article is structured as follows: In Section II we repeat the basic concepts of the generalized Bloch decomposition and the correlation tensor formalism. Building on these concepts we introduce the split Bloch basis in Section III. The split Bloch basis is an orthogonal operator basis, similar to the generalized Bloch basis. Using this novel tool we define a correlation monotone, which is convex and invariant under isometry transformations. Subsequently several (quasi-)monogamy relations are found (Section IV). Then we turn our attention towards the second part of the paper: entropy inequalities: In Section V we explain why the Bloch decomposition relates the linear entropy of a system to the correlation tensor of the aforementioned system. Following up we briefly review the state of the art on entropy inequalities of the Réyni and Tsallis type and go on to introduce a novel linear inequality for the linear (or Tsallis 2-)entropy. In Section VI we introduce a new quadratic entropy relation for the linear entropy: the *generalized* pseudo-additivity. It originates from the pseudo-additivity of the q-entropies, but is applicable to *all* states instead of only product states as in the case of pseudo-additivity. In the remainder of the section we show that this relation is independent of the known subadditivity [13] and visualize and discuss the body of allowed entropies for tripartite systems. Finally, we sum up our results and remark on open questions in Section VII.

II. INTRO: THE CORRELATION TENSOR FORMALISM

In this section we will shortly introduce the concepts and notions of the traditional (generalized-) Bloch decomposition [27],[30] and the correlation tensor formalism and continue to introduce the *split Bloch basis*, which tackles the problem of expressing low-dimensional quantum states in high-dimensional Hilbert spaces.

Let us start by stating the traditional Bloch decomposition:

Definition 1 *A single partite (qudit) quantum state $\rho \in \mathcal{H}^d$ can always be written in the (generalized-)Bloch decomposition as defined in [30] by:*

$$\rho = \frac{1}{d}\left(\mathbb{1}_d + \sum_{i=1}^{d^2-1} \langle \lambda_i \rangle \, \lambda_i\right) \tag{1}$$

with λ_i being orthogonal, traceless (and canonically assumed hermitian $\lambda_i = \lambda_i^\dagger$) matrices and d being the dimension of the Hilbert space of ρ.

Remark 1 *Note that the Hilbert space we consider is a Hilbert-Schmidt space $\mathcal{H}^d = (\mathbb{C}^d)^* \otimes \mathbb{C}^d$ with the associated scalar product $\langle A|B\rangle = \mathrm{Tr}\,(B^* A)$.*

In large dimensions there is some freedom in the choice of λ_i with the canonical choices being either the generalized Gell-Mann [30, 37] matrices or the (non-hermitian) Heisenberg-Weyl [38] matrices, alongside more unusual choices like the Heisenberg-Weyl observables [39]. The single party case can be naturally extended to multi-partite systems by a tensor product construction.

Definition 2 *Any n-partite quantum state $\rho_\Sigma \in \mathcal{H}^{d_\Sigma} = \otimes_{i=1}^n \mathcal{H}^{d_i}$ where $\Sigma := \{\Sigma_1, \Sigma_2, \cdots, \Sigma_n\}$ is the set of all parties can always be represented as*

$$\rho_\Sigma = \frac{1}{d_\Sigma}\left(\sum_{i_1=0}^{d_1^2-1} \cdots \sum_{i_n=0}^{d_n^2-1} \left\langle \lambda_{i_1}^{\Sigma_1} \otimes \cdots \otimes \lambda_{i_n}^{\Sigma_n} \right\rangle \lambda_{i_1}^{\Sigma_1} \otimes \cdots \otimes \lambda_{i_n}^{\Sigma_n}\right) \tag{2}$$

Here one canonically uses a basis comprised of tensor products of local hermitian Bloch bases, which then allow for a local Bloch vector decomposition. This means the $\lambda_{i_j}^{\Sigma_j}$ are again orthogonal, e.g. $\mathrm{Tr}\left(\lambda_{m_j}^{\Sigma_j}\lambda_{n_j}^{\Sigma_j}\right) = d_j\delta_{mn}$, where d_j is the dimension of the local Hilbert space $\mathcal{H}^{d_j}$; note that $d_\Sigma = \prod_{j=1}^n d_j$. Furthermore all $\lambda_{i_j}^{\Sigma_j}$ are traceless, except for $\lambda_{0_j}^{\Sigma_j} = \mathbb{1}_{d_j}$.

The advantage is that the Bloch components divide into an intuitive set of correlation tensors. For example in tripartite systems this leads to three local Bloch vectors, three correlation matrices and a single three-body correlation tensor. The Bloch representation furthermore has the advantage of giving an economical form for $\mathrm{Tr}(\rho^2)$ through the tracelessness of λ_i.

Definition 3 (Correlation Tensor) *Let ρ_Σ be an n-partite state:*

(i) The correlation tensor of a state $T(\rho_\Sigma)$ is the generalization of the Bloch vector in the qubit Bloch decomposition, it collects all coordinates of the operator basis:

$$[T(\rho_\Sigma)]_{i_1,i_2,\cdots,i_n} := \left\langle \lambda_{i_1}^{\Sigma_1} \otimes \cdots \otimes \lambda_{i_n}^{\Sigma_n} \right\rangle \qquad 1 \le i_j < d_j^2 \tag{3}$$

(ii) We can now define lower order correlation tensors as:

$$T(\rho_v) := T^v \tag{4}$$

Where $v \subseteq \Sigma$ runs over all non-empty subsets of Σ, i.e. its powerset $P(\Sigma) \setminus \emptyset$ and $\rho_v = \mathrm{Tr}_{\bar{v}}\,(\rho_\Sigma)$ is the state of the subsystem of v given by taking the partial trace over its complement $\bar{v}$, i.e. v and $\bar{v}$ are a partition of Σ.

Let us state now a very useful lemma:

Lemma 1 *If ρ_Σ denotes a n-partite system owned by a set of parties $\Sigma = \{\Sigma_1, \ldots, \Sigma_n\}$ with dimension $d_\Sigma = \prod_i d_i$, we can write $\mathrm{Tr}\left(\rho_\Sigma^2\right)$ as :*

$$\mathrm{Tr}(\rho_\Sigma^2) = \frac{1}{d_\Sigma}\left(1 + \sum_{\forall v \in P(\Sigma)} \|T^v\|^2\right). \tag{5}$$

Where $v \subseteq \Sigma$ runs over all non-empty subsets of Σ, e.g. its powerset $P(\Sigma) \setminus \emptyset$. $\sum_v \|T^v\|^2$ is the sum over correlation tensors as defined above (Definition 3).

Proof
The lemma follows directly from the definition of the basis, i.e. since $Tr\left((\lambda_{i_1}^{\Sigma_1} \otimes \cdots \otimes \lambda_{i_n}^{\Sigma_n})(\lambda_{i_1'}^{\Sigma_1} \otimes \cdots \otimes \lambda_{i_n'}^{\Sigma_n})\right) = \delta_{i_1,i_1'} \ldots \delta_{i_n,i_n'} d_\Sigma$ we find

$$\mathrm{Tr}\left(\rho_\Sigma^2\right) = \frac{d_\Sigma}{d_\Sigma^2}\left(\sum_{i_1=0}^{d_1^2-1} \cdots \sum_{i_n=0}^{d_n^2-1} \left\langle \lambda_{i_1}^{\Sigma_1} \otimes \cdots \otimes \lambda_{i_n}^{\Sigma_n} \right\rangle^2\right) = \frac{1}{d_\Sigma}\left(1 + \sum_v \|T^v\|^2\right) \tag{6}$$

III. THE SPLIT BLOCH BASIS

After having repeated the basic concept of the traditional Bloch decomposition, we proceed now to extend this notion to the *split Bloch decomposition* and motivate its introduction: Let us consider the scenario where a low dimensional state is represented in a Bloch basis of a Hilbert space with much larger dimension. In this case the representation is unnecessarily involved. For example, consider the non-normalized state $\rho = \mathrm{diag}(1,1,0,0) \in \mathcal{H}^4$, where diag is the function which maps a vector to a matrix with the vectors entries on the diagonal. Recall the set of operators, that are typically associated with the generalized Bloch decomposition [30]: $\mathcal{H}^d = \mathrm{span}\left(\mathbb{1}_d, \lambda_1, ..., \lambda_{d^2-1}\right)$ where $\mathbb{1}_d$ is the identity on the space and λ_i are required to be traceless and normalized.

The identity is independently of the choice of basis always a part of the set of operators. Returning to the example, we see that the use of the identity is sub-optimal, since the additional ones on the diagonal have to be compensated by additional diagonal basis elements. This simple example already demonstrate a deeper problem concerning canonical Bloch decompositions, i.e. the difficulty to describe *subspaces* of a Hilbert space in a concise way. This problem becomes more apparent for multi-partite states which have different local dimensions: We will later consider a cryptographic scenario where Alice and Bob want to communicate securely, meaning they want to exclude a malicious third party (Eve) to extract any information about the content of their communication. While we can assume the knowledge about the local dimension of Alice and Bob, the local dimension of Eve is arbitrary. To treat this problem, a separation into different subspaces is very helpful (compare Theorem 1).

Now we can ask ourselves: *Is there a Bloch basis which allows a concise description of subspaces?* The answer is the *split Bloch basis*. The idea of the basis is to find a complete set of basis elements of a Hilbert space, which can be divided into subsets which span the subspaces. In the following we will define an orthogonal operator basis similar to the generalized Gellmann matrices. Recall, that the generalized Gellmann basis for a d-dimensional Hilbert space consists of the identity, $d^2 - d$ elements with only *off-diagonal* entries and $d-1$ traceless elements with only *diagonal* entries. The main difference between the split Bloch basis and the Gellmann basis is that we will replace the identity $\mathbb{1}$ with two sub-identities $\bar{\mathbb{1}}$ and the diagonal elements with a set of $d-2$ diagonal elements. The off-diagonal elements need not to be replaced since they already divide into two subsets which live in either subspace.

Let us first describe a operation $\odot$ which describes the split into different subspaces:

Definition 4 *Given a Hilbert-Schmidt space $\mathcal{H}^d = \mathrm{span}\left(\lambda_0, \ldots, \lambda_{d^2-1}\right)$ with the customary Hilbert-Schmidt scalar product, i.e. $\langle A|B\rangle = \mathrm{Tr}(B^*A)$ can always be divide into subspaces such that:*

$$\mathcal{H}^d = \mathcal{H}^c \odot \mathcal{H}^{d-c} := \left(\mathbb{C}^c \oplus \mathbb{C}^{d-c}\right)^* \otimes \left(\mathbb{C}^c \oplus \mathbb{C}^{d-c}\right) \tag{7}$$

$$= \mathcal{H}^c \oplus \mathcal{H}^{d-c} \oplus \left(\left(\mathbb{C}^{d-c}\right)^* \otimes \mathbb{C}^c \oplus (\mathbb{C}^c)^* \otimes \mathbb{C}^{d-c}\right) \tag{8}$$

$$= \mathrm{span}\left(\Lambda_c\right) \oplus \mathrm{span}\left(\Lambda_{d-c}\right) \oplus \mathrm{span}\left(\Sigma\right) \tag{9}$$

Where Λ_c, Λ_{d-c} and Σ first have to be a partition of $\{\lambda_0, \ldots, \lambda_{d^2-1}\}$ and second $|\Lambda_c| = c^2$, $|\Lambda_{d-c}| = (d-c)^2$ and $|\Sigma| = 2dc - 2c^2$ Note that the direct sum in the third line is the internal *direct sum, since $\lambda_i \in \mathcal{H}^d$ $\forall i$. The internal is however isomorphic to the external direct sum.*

Definition 5 (The Split Bloch Basis) *Given a Hilbert-Schmidt space $\mathcal{H}^d$ with the customary Hilbert-Schmidt scalar product, i.e. $\langle A|B\rangle = \mathrm{Tr}(B^*A)$, we want to find a basis $\mathcal{B}_{split} = \{\lambda_i \,|\, \forall i\} \cup \{\omega_j \,|\, \forall j\} \cup \{\nu_k \,|\, \forall k\}$, such that $\mathcal{H}^d = \mathcal{H}^c \odot \mathcal{H}^{d-c}$ and $\lambda_i, \omega_j, \nu_k \in \mathcal{H}^d$ while $\mathcal{H}^c = \mathrm{span}\left(\{\lambda_i \,|\, \forall i\}\right)$ and $\mathcal{H}^{d-c} = \mathrm{span}\left(\{\omega_j \,|\, \forall j\}\right)$. First we will define non-canonical operators, similar to the canonical generalized Gellmann matrices, then we use them to define a split Bloch basis: $\mathcal{B}_{split}$:*

(i) Assuming the standard computational basis $\mathbb{C}^d = \mathrm{span}\left(|0\rangle, \ldots, |d-1\rangle\right)$, let us define a set of operators, which span the Hilbert space. It consist of:
two sub-identities

$$\lambda_{00} = \bar{\mathbb{1}}_c \quad = \sum_{l=0}^{c-1} |l\rangle\langle l| \tag{10}$$

$$\omega_{00} = \bar{\mathbb{1}}_{d-c} = \sum_{l=c}^{d-1} |l\rangle\langle l| \ , \tag{11}$$

$d-2$ diagonal elements:

$$\lambda_{kk} = \sqrt{\frac{c}{k+k^2}} \left(\sum_{l=0}^{k-1} |l\rangle\langle l| - k\,|k\rangle\langle k| \right) \qquad 1 \le k \le c-1 \tag{12}$$

$$\omega_{kk} = \sqrt{\frac{d-c}{k+k^2}} \left(\sum_{l=0}^{k-1} |l+c\rangle\langle l+c| - k\,|k+c\rangle\langle k+c| \right) \qquad 1 \le k \le d-c-1 \ , \tag{13}$$

$\frac{d(d-1)}{2}$ symmetric off-diagonal elements

$$\lambda_{kl} = \sqrt{\frac{c}{2}} \left(|k\rangle\langle l| + |l\rangle\langle k| \right) \qquad 0 \le k < l \le c-1 \tag{14}$$

$$\omega_{kl} = \sqrt{\frac{d-c}{2}} \left(|k\rangle\langle l| + |l\rangle\langle k| \right) \qquad c-1 \le k < l \le d-1 \tag{15}$$

$$\nu_{kl} = \sqrt{\frac{d-c}{2}} \left(|k\rangle\langle l| + |l\rangle\langle k| \right) \qquad 0 \le k \le c-1 < l \le d-1 \tag{16}$$

and $\frac{d(d-1)}{2}$ anti-symmetric off-diagonal elements

$$\hat{\lambda}_{kl} = \sqrt{\frac{c}{2}} \left(-\mathbf{i}\,|k\rangle\langle l| + \mathbf{i}\,|l\rangle\langle k| \right) \qquad 0 \le k < l \le c-1 \tag{17}$$

$$\hat{\omega}_{kl} = \sqrt{\frac{d-c}{2}} \left(-\mathbf{i}\,|k\rangle\langle l| + \mathbf{i}\,|l\rangle\langle k| \right) \qquad c-1 \le k < l \le d-1 \tag{18}$$

$$\hat{\nu}_{kl} = \sqrt{\frac{d-c}{2}} \left(-\mathbf{i}\,|k\rangle\langle l| + \mathbf{i}\,|l\rangle\langle k| \right) \qquad 0 \le k \le c-1 < l \le d-1 \tag{19}$$

Note that $\mathbf{i}$ does not stand for an index but rather $\mathbf{i}^2 = -1$.

(ii) With these elements we are able to find a basis $\mathcal{B}_{split}$ for $\mathcal{H}^d$:

$$\mathcal{B}_{split} := \left(\{\lambda_{kl} \,|\, \forall k,l\} \cup \{\hat{\lambda}_{mn} \,|\, \forall m,n\} \right) \cup \left(\{\omega_{kl} \,|\, \forall k,l\} \cup \{\hat{\omega}_{mn} \,|\, \forall m,n\} \right) \cup \left(\{\nu_{kl} \,|\, \forall k,l\} \cup \{\hat{\nu}_{mn} \,|\, \forall m,n\} \right) \tag{20}$$

$$:= \{\lambda'_i \,|\, 0 \le i \le c^2-1\} \cup \{\omega'_i \,|\, 0 \le i \le (d-c)^2-1\} \cup \{\nu'_i \,|\, 0 \le i \le 2dc-2c^2-1\} \tag{21}$$

In the second line of the above equation we simplified the notation by concatenating the indices, we only require $\lambda'_0 = \lambda_{00}$ and $\omega'_0 = \omega_{00}$ all other indices may be assigned freely. Note that the basis is split naturally into three parts. Two of them span two Hilbert-Schmidt subspaces, i.e. $\mathcal{H}^c = \mathrm{span}\left(\{\lambda'_i \,|\, \forall i\}\right)$ and $\mathcal{H}^{d-c} = \mathrm{span}\left(\{\omega'_i \,|\, \forall i\}\right)$. The third part spans a subspace which is however not *a Hilbert-Schmidt space since* in general *it can not be written as a tensor product of $\mathbb{C}^d$ with its dual, i.e. $\mathrm{span}(\nu'_i \,|\, 0 \le i \le 2dc-2c^2-1) \neq (\mathbb{C}^d)^* \otimes \mathbb{C}^d \ \forall d, c$. From*

now on we will use $\{\mu^i \,|\, 0 \leq i \leq d^2 - c^2 - 1\} = \{\omega_i' \,|\, 0 \leq i \leq (d-c)^2 - 1\} \cup \{\nu_i' \,|\, 0 \leq i \leq 2dc - 2c^2 - 1\}$ *with* $\mu_0 = \omega_o = \bar{\mathbb{1}}_{d-c}$ *and take* $\lambda_i' \to \lambda_i \; \forall i$ *for simplicity of notation. We will however mention when we use the split Bloch basis although it can be understood from context. In fact, whenever* μ_i*'s appear it should be understood that we are using the split Bloch basis.*

Note that we have chosen the normalization of the subspaces differently, i.e. $\mathrm{Tr}\,(\lambda_i \lambda_j) = \delta_{ij}\, c$ and $\mathrm{Tr}\,(\mu_i \mu_j) = \delta_{ij}\,(d-c)$. This ensures that the normalization of the subspace $\mathcal{H}^c$ is independent of the total dimension.

It is still necessary to show that we indeed constructed a orthogonal operator basis, e.g. that all elements of the basis are orthogonal $\langle \lambda_i |\, \lambda_{j\neq i} \rangle = 0$, $\langle \mu_i |\, \mu_{j\neq i} \rangle = 0$, $\langle \lambda_i |\, \mu_j \rangle = 0$ and that they actually span $\mathcal{H}^d$. This is however easy to see: Any scalar product of pairs of operators with only off-diagonal elements is trivially zero, the same is true for any scalar product of off-diagonal and diagonal operators. Furthermore, any scalar product of diagonal operators in the separate subspaces is zero due to the tracelessness of all operators, except the (sub-)identity. Finally, any scalar product of any diagonal operators of the different subspaces is zero, due to the fact that they are non-overlapping block matrices. The fact that we have d^2 orthogonal elements already suffice to span $\mathcal{H}^d$, i.e. c diagonal elements in $\mathcal{H}^c$, $d-c$ diagonal elements in $\mathcal{H}^{d-c}$ add up to the regular d diagonal elements of the canonical Bloch basis of $\mathcal{H}^d$ and the off-diagonal are, apart from normalization, the same.

We now see that the split Bloch basis allows for a concise representation states with low-dimensional support in a d-dimensional system. For example, take $|\psi\rangle = \frac{1}{\sqrt{2}}(|0\rangle + |1\rangle) \in \mathbb{C}^d$. This state has a split Bloch representation of $\langle \lambda_{01} \rangle = 1$ being the only traceless Bloch matrix with non-zero expectation value. The canonical Bloch representation would have to compensate the first entry λ_0 by additional diagonal Bloch matrices. In addition, keeping the squared trace constant it would also imply an increasing value of $\langle \lambda_{01} \rangle = \sqrt{2d}$ using the above normalization.

After having defined the split Bloch basis, we can repeat the definition of the correlation tensor (Definition 3) and the lemma connecting the trace of the squared state with the Euclidean norm of the correlation tensor (Lemma 1). First we describe only bipartite states in the split Bloch basis, the generalization is however straight-forward (see Remark 4).

Remark 2 *Given a bipartite state* $\rho_{AB} \in \mathcal{H}^{d_A d_B}$ *where the parts have* different *local dimension; w.l.o.g.* $d_A < d_B$. *We will use the split basis* $\mathcal{B}_{split}$ *to divide the bigger Hilbert space* $\mathcal{H}^{d_B} = \mathcal{H}^{d_A} \odot \mathcal{H}^{d_B - d_A}$, *such that the local dimension of one of the Hilbert-Schmidt subspaces coincides with the local dimension of the smaller space, i.e.* $\mathcal{H}^{d_A d_B} = \mathcal{H}^{d_A} \otimes \left(\mathcal{H}^{d_A} \odot \mathcal{H}^{d_B - d_A}\right)$.

$$\rho_{AB} = \sum_{i=0}^{d_A^2-1} \left(\frac{1}{d_A^2} \left(\sum_{j=0}^{d_A^2-1} \langle \lambda_i^A \otimes \lambda_j^B \rangle \, \lambda_i^A \otimes \lambda_j^B \right) + \frac{1}{(d_B - d_A)\, d_A} \left(\sum_{j=0}^{d_B^2 - d_A^2 - 1} \langle \lambda_i^A \otimes \mu_j^B \rangle \, \lambda_i^A \otimes \mu_j^B \right) \right) \tag{22}$$

Note that only λ_0^A, λ_0^B *and* μ_0^B *have finite trace, all other elements are traceless. Any state is properly normalized, i.e.* $\mathrm{Tr}\,(\rho_{AB}) = 1$. *Since the only elements with a finite trace are* $\mathbb{1}_{d_A} \otimes \bar{\mathbb{1}}_{d_A}$ *and* $\mathbb{1}_{d_A} \otimes \bar{\mathbb{1}}_{d_B - d_A}$ *we find:*

$$\mathrm{Tr}\,(\rho_{AB}) = \frac{\langle \mathbb{1}_{d_A} \otimes \bar{\mathbb{1}}_{d_A} \rangle}{d_A^2} \mathrm{Tr}\,(\mathbb{1}_{d_A} \otimes \bar{\mathbb{1}}_{d_A}) + \frac{\langle \mathbb{1}_{d_A} \otimes \bar{\mathbb{1}}_{d_B - d_A} \rangle}{(d_B - d_A)\, d_A} \mathrm{Tr}\,(\mathbb{1}_{d_A} \otimes \bar{\mathbb{1}}_{d_B - d_A}) \tag{23}$$

$$= \langle \mathbb{1}_{d_A} \otimes \bar{\mathbb{1}}_{d_A} \rangle + \langle \mathbb{1}_{d_A} \otimes \bar{\mathbb{1}}_{d_B - d_A} \rangle = 1 \tag{24}$$

Note that in the standard Bloch decomposition the Bloch coefficient of the identity is fixed to one by normalization of the density matrix, in our case only the sum *of the Bloch coefficients of the partial identities adds up to one.*

Now let us investigate the correlation tensor formalism in the split Bloch basis; again we will use a bipartite state as an example:

Definition 6 *Given a bipartite state* $\rho_{AB} \in \mathcal{H}^{d_A} \otimes \mathcal{H}^{d_B}$ *with* $d_B > d_A$ *expressed in the split Bloch basis. Now we split the correlation tensor into parts :*

$$\left[T_{SD}(\rho_{AB})\right]_{ij} := \langle \lambda_i^A \otimes \lambda_j^B \rangle \qquad i,j \in \{1, \ldots, d_A^2 - 1\} \tag{25}$$

$$\left[\tilde{T}(\rho_{AB})\right]_{ij} := \langle \lambda_i^A \otimes \mu_j^B \rangle \qquad i \in \{1, \ldots, d_A^2 - 1\}\,;\, j \in \{1, \ldots, d_B^2 - d_A^2 - 1\} \tag{26}$$

$T^{SD}(\rho_{AB})$ *describes the correlations in* $\mathcal{H}^{d_A} \otimes \mathcal{H}^{d_A}$ *and* $\tilde{T}(\rho_{AB})$ *describes the remaining correlations in* $\mathcal{H}^{d_A} \otimes \mathcal{H}^{d_B}$. *The lower order correlation tensors are, in this case, just the local Bloch vectors.*

Finally we can find an expression for Lemma 1 in the split Bloch basis:

Remark 3 *We can write the trace of a squared bipartite state $\rho_{AB} \in \mathcal{H}^{d_A} \otimes \mathcal{H}^{d_B}$ of different local dimension, e.g. $d_A < d_B$:*

$$\mathrm{Tr}\left(\rho_{AB}^2\right) = \frac{1}{d_A^2}\left(\langle \mathbb{1}_{d_A} \otimes \bar{\mathbb{1}}_{d_A}\rangle + \sum_{v\in P(\{A,B\})} \|T_{SD}^v\|^2\right) + \frac{1}{(d_B - d_A)\, d_A}\left(\langle \mathbb{1}_{d_A} \otimes \bar{\mathbb{1}}_{d_B-d_A}\rangle + \sum_{v\in\{B,AB\}} \|\tilde{T}^v\|^2\right) \tag{27}$$

As we have seen the split Bloch basis preserves the advantages of the Bloch basis. However, it has additional advantages one of which is the possibility to express the (operator) Schmidt basis in terms of the split Bloch basis:

Lemma 2 (The Schmidt decomposition) *For pure states $|\psi\rangle_{AB} \in \mathbb{C}^{d_A} \otimes \left(\mathbb{C}^{d_A} \oplus \mathbb{C}^{d_B-d_A}\right)$ with $d_B > d_A$, there exists* some *split Bloch basis such that we find the Schmidt decomposition as:*

$$\left(|\psi\rangle\langle\psi|\right)_{AB} = \sum_{i,j=0}^{\min(d_A,d_B)-1} \left\langle \lambda_i^A \otimes \lambda_j^B \right\rangle \lambda_i^A \otimes \lambda_j^B \tag{28}$$

where $\left\langle \lambda_0^A \otimes \lambda_0^B \right\rangle = 1$. The proof of this lemma can be found in the appendix.

Let us finish this chapter with a short note on the n-partite generalization:

Remark 4 (Generalization) *Until now, we have only considered bipartite states. However, this choice is only due to the fact that the notation becomes very cumbersome in the n-partite scenario. The generalization to multipartite states is straightforward: Formally we can just repeat the step from Definition 1 to Definition 2, i.e. replacing the Bloch basis by tensor products of* local *Bloch bases, which can be split or not. Note that the powerset construction we have chosen allows to scale the definitions concerning the split Bloch basis to n-partite systems easily by simply using the set of the n-parties.*

IV. MONOGAMY OF CORRELATIONS FROM THE BLOCH PICTURE

We proceed in this section by utilizing the correlation tensor formalism to derive some quasi-monogamy relations for (quantum-)correlations. The key idea is to focus on the relevant parts of the correlation tensor and drop all non-essential terms. This choice of a subset of the correlation tensor will lead to a dimension-dependent quasi-monogamy relation. In order to capture the correlations between two subsystems A, B of a bipartite system we define the following quantity to measure these correlations:

Definition 7 (Correlation Monotone) *Let ρ_{AB} be an arbitrary bi-partite system and w.l.o.g. $d_A \leq d_B$, we define a correlation monotone $\mathcal{T}_{A|B}(\rho_{AB})$:*

$$\mathcal{T}_{A|B}(\rho_{AB}) := \frac{1}{g_{A|B}} \max_{\{\lambda_j^B\}} \left(\sum_{i=1}^{d_{min}^2-1} \sum_{j=1}^{d_{min}^2-1} \left\langle \lambda_i^A \otimes \lambda_j^B \right\rangle^2 \right) \tag{29}$$

Where $d_{min} = \min(d_A, d_B)$ is the minimum of the dimensions of the subsystems A and B. Furthermore, $\mathrm{Tr}\left(\lambda_i^A \lambda_j^A\right) = \mathrm{Tr}\left(\lambda_i^B \lambda_j^B\right) = \delta_{ij}\, d_{min}$. Note that the maximization is obsolete if the local dimension of ρ_A and ρ_B is the same. If the local dimensions are different the maximization is over arbitrary basis changes on the bigger subspace. If $d_B > d_A$ then $\rho_B \in \mathcal{H}^{d_A} \odot \mathcal{H}^{d_B-d_A}$ will be described by the split Bloch basis such that one part of the split matches the local dimension of ρ_A. The optimization is such that the correlations are maximal between the same dimensional spaces of ρ_A and ρ_B.

$\mathcal{T}_{A|B}$ should be read as "the correlations between the systems A and B". This monotone has a natural operational interpretation: For any given complete set of observables on A, it is the maximum amount of correlations achievable over any d_A-dimensional subspace of B. Due to the symmetric nature of the Schmidt decomposition, for pure states this coincides with the squared 2-norm of the correlation tensor, i.e. $\mathcal{T}_{A|B}\left(|\psi_{AB}\rangle\langle\psi_{AB}|\right) = \frac{1}{g_{A|B}}||T^{AB}||^2$. The particular choice of normalization is left unspecified by intention. We will write in the following $g_{A|B}$ without further specification. In principle the exact choice is a matter of taste.

Let us now state a useful lemma, which gathers some important properties of our monotone:

Lemma 3 *For a general (possibly mixed) state ρ_{ABE} be the following relations for the correlation monotone are true:*

(i)

$$\mathcal{T}_{A|B} = \mathcal{T}_{B|A} \tag{30}$$

(ii) and:

$$\frac{g_{A|B}}{g_{A|BE}} \mathcal{T}_{A|B}(\rho_{ABE}) \leq \mathcal{T}_{A|BE}(\rho_{ABE}) \tag{31}$$

Proof
add (i): Follows directly from the definition.

add (ii): Simply using the fact that $\|T^{AB}\|^2 \leq \|T^{AB}\|^2 + \|T^{AE}\|^2 + \|T^{ABE}\|^2$ *together with the definition of* $\mathcal{T}$ *recovers the above equation.*

The main result of this section is the following theorem that demonstrates how correlations within a tripartite system are constrained by a quasi-monogamy relation.

Theorem 1 *Let* $\rho_{ABE} \in \mathcal{H} = \mathcal{H}^{d^2} \otimes \mathcal{H}^{d_E}$ *be an arbitrary tripartite state owned by* A, B *and* E *with local dimensions* $d_A = d_B = d$ *and* d_E*:*

(i): The correlation of a composite system ρ_{AB} *with an arbitrary system* ρ_E *limits the correlation of its marginals with the same:*

$$\mathcal{T}_{A|E}\left(\rho_{ABE}\right) + \mathcal{T}_{B|E}\left(\rho_{ABE}\right) \leq \frac{g_{AB|E}}{\min\left(g_{A|E}, g_{B|E}\right)} \mathcal{T}_{AB|E}\left(\rho_{ABE}\right) \tag{32}$$

(ii): The correlation of any state $\rho_{AB} \in \mathcal{H}^{d^2}$ *with an arbitrary state* ρ_E *is restricted by:*

$$\mathcal{T}_{AB|E}\left(\rho_{ABE}\right) \leq \frac{d^4 - 1 - 2\left(\left\|T^A\right\|^2 + \left\|T^B\right\|^2\right) - 2g_{A|B}\mathcal{T}_{A|B}}{g_{AB|E}} \tag{33}$$

The proof of this theorem can be found in the appendix.

We point out that Theorem 1 (i) is reminiscent of the Coffman-Kundu-Wootters inequality [18]. It was the first example of a monogamy relation. For three qubits the CKW inequality is used almost synonymous with the term monogamy. The form of Theorem 1 (i) is the same, except for a dimensional correction factor, hidden in the normalization, on the right hand side and our quantity $\mathcal{T}_{\Omega|\Sigma}$ replacing the concurrence. Even though this result was inspired by the notion of monogamy of entanglement ([14, 18–21]) we have to differentiate from these well known relations.

First, our results primarily discuss *correlations* instead of entanglement. Our quantity $\mathcal{T}_{\Omega|\Sigma}$ can easily be rewritten into an entanglement *monotone* by subtracting the maximal value allowed by a separable state, however we have not proven the LOCC non-increasingness of $\mathcal{T}_{\Omega|\Sigma}$. Therefore we can not assume it to be an entanglement *measure*, unlike the concurrence [40] used in Coffman-Kundu-Wootters [18].

Second, the functional form of our relation is different since it involves dimension-dependent constants. We consider this to be acceptable, since the most well known monogamy inequalities are also inherently dimension-dependent. They may not contain explicit dimension factors, but in fact they are dimension-dependent since they only hold for the qubit case. Already in the case of the slightly larger qutrit system a counter example is known [23], that can be extended to the case of arbitrary dimension [24]. Our dimension-dependent factors, hidden in the normalization constant $g_{*|*}$, in turn allow our relations to hold in any dimension.

We call Theorem 1 (ii) a quasi-monogamy relation, since it captures the fundamental idea which monogamy relations aim to describe: That the correlations of Alice and Bob limit the amount of possible shared correlations of Eve with either of the two remaining systems. In fact, Theorem 1 (ii) evaluated for maximally entangled Alice and Bob turns out to coincide with the upper bound of $\mathcal{T}^{sep}$ for product states. Thus generalising a known result for the CKW inequality, that two maximally entangled parties with *equal* dimension can not be entangled with any other party. We point out that our result has a functional form in *arbitrary* dimension.

But even if Alice and Bob are not maximally entangled, the bound (Theorem 1 (ii)) is still limiting the correlations Eve can have with the system. We assume that Alice and Bob have the same local dimension, e.g. $d_A = d_B = d$,

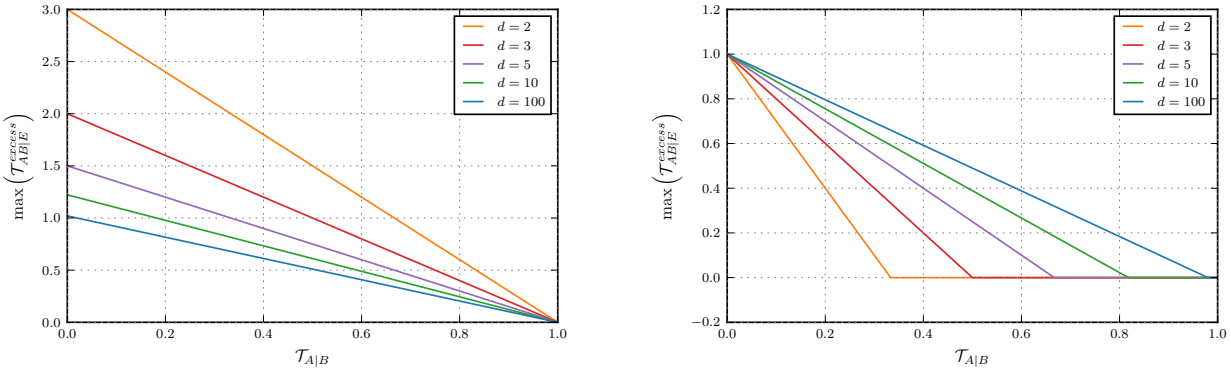

(a) Locally maximally mixed states, i.e. only correlations contributing to the purity $\|T^A\|^2 + \|T^B\|^2 = 0$.

(b) Local Bloch vectors at maximal possible local norm, i.e. $\|T^A\|^2 + \|T^B\|^2 = \min\left(2d-2, \left(d^2-1\right)\left(1-\mathcal{T}_{A|B}\right)\right)$

Figure 1: The (scaled) shared entanglement of Eve with Alice and Bob $\mathcal{T}^{excess}_{AB|E} = d\left(\mathcal{T}_{AB|E} - 1\right)$ is restricted by the shared correlations between the latter $\mathcal{T}_{A|B}$ even if Eve holds a purification for the composite system of Alice and Bob, e.g. $d_E = d^2$. Note that $\mathcal{T}^{excess}_{AB|E}$ is normalized by the bound of separable states $g_{AB|E} = \left(d^2-1\right)\left(d_E - 1\right)$ and weighed with d.

normalize by the bound for separable states $g_{AB|E} = \mathcal{T}^{sep}_{AB|E}$ with $\mathcal{T}^{sep}_{AB|E} = \left(d^2-1\right)\left(d_E-1\right) \geq \mathcal{T}_{AB|E}\left(\rho_{AB}\otimes\rho_E\right)$ and define $\mathcal{T}^{excess}_{AB|E} := d\left(\mathcal{T}_{AB|E} - 1\right)$. $\mathcal{T}^{excess}_{AB|E}$ measures how much entanglement Eve shares with the composite system of Alice and Bob scaled by the local dimension d. Note that we estimate entanglement rather than correlations due to the fact that we subtract the bound for separable states $1 = \mathcal{T}^{sep}_{AB|E}/g_{AB|E}$. The scaling is only used to make $\mathcal{T}^{excess}_{AB|E}$ comparable for different dimensions.

Considering the worst case scenario, that Eve holds a purification to Alice and Bob's system (see the proof of Theorem 1 in the Appendix), i.e. $d_E = d^2$, we plot (Fig. 1) the maximal value of $\mathcal{T}^{excess}_{AB|E}$ for $0 \leq \mathcal{T}_{A|B} \leq 1$ for different dimensions. Note that the range of $\mathcal{T}_{A|B}$ corresponds to a normalization of $g_{A|B} = d^2 - 1$. We consider two different scenarios, i.e. the local correlation tensors $\|T^A\|^2$ and $\|T^B\|^2$ are either minimal or maximal. If they are minimal (Fig. 1a), either due to ignorance of the local states or because the state is proportional to the identity, we see that only maximal entanglement between Alice and Bob, i.e. $\mathcal{T}_{A|B} = 1$ excludes entanglement with Eve. This is however true independent of the local dimension d of Alice's and Bob's system. The other scenario is also interesting (Fig. 1b): If it is possible to certify that $\|T^A\|^2 + \|T^B\|^2$ is maximal it suffices that Alice and Bob share some correlations to exclude any entanglement with Eve. This is however highly dependent on the local dimension d: Unsurprisingly the lower the local dimension the greater the advantage of knowing the correlation tensor norms of the local systems. In fact we can see that the advantage for $d = 100$ is minute even for maximal local correlation tensor norms. The factors influencing the bound $\|T^A\|^2$, $\|T^B\|^2$ and $\mathcal{T}_{A|B}$ are however related, i.e. $0 \leq \|T^A\|^2 + \|T^B\|^2 \leq \min\left(2d-2, \left(d^2-1\right)\left(1-\mathcal{T}_{A|B}\right)\right)$. For the proof of these bounds consult the appendix (Lemma 6).

Let us finish this section again with a short note on the n-partite generalization:

Remark 5 *Note that this correlation monotone can be used to describe multi-partite systems as well: Let $\rho_{A_1,\ldots,A_n}$ be a multi-partite system with $\Omega \subset \{A_1 \ldots A_n\}, \Sigma \subset \{A_1 \ldots A_n\}$ and $\Omega \cap \Sigma \neq \emptyset$. If Σ, Ω are composite systems, i.e. it is possible to describe them as tensor product of local Bloch bases, then we want to consider the correlations of all possible subsystems of Σ with all subsystems of Ω. Therefore, if the index is replaced with a multi-index $\lambda^{\Sigma}_i \to \lambda^{\Sigma}_{i_1,\ldots,i_{|\Sigma|}}$ and $\lambda^{\Omega}_j \to \lambda^{\Omega}_{j_1,\ldots,j_{|\Omega|}}$, we need the cross sum over the new indices in the parts both to be greater then one: $\sum_k i_k \geq 1 \wedge \sum_l j_l \geq 1$. In the language of correlation tensors this is of course equal to the sum of the squared correlation tensor norms $\sum_{v\in\Gamma}\|T^v\|^2$ with $\Gamma := P\left(\Omega \cup \Sigma\right) \setminus \left(P\left(\Omega\right) \cup P\left(\Sigma\right)\right)$, since this set contains exactly the correlation tensor elements that have at least one element in each of the two subsets Ω and Σ. Finally, note that if the subsystems of the bi-partition have the* same *dimension $d_\Sigma = d_\Omega$ the correlation tensors are defined as Definition 3 and the maximization is obsolete, if they have* different *dimension $d_\Sigma \neq d_\Omega$ the split Bloch basis will be used and the sum will be over $\|T^v_{SD}\|^2$ as defined in Definition 6. The maximization can be found by arbitrary basis change in the bigger space.*

V. LINEAR ENTROPY INEQUALITIES FROM THE BLOCH PICTURE

In this section we will demonstrate that correlation tensor norm constraints (often also called Bloch vector length constraints) can be reinterpreted as entropy inequalities. This equivalence is best seen in the Bloch picture: The natural relation of $\mathrm{Tr}(\rho^2)$ to the correlation tensors of the Bloch representation allows us to rewrite existing relations between marginals in the Bloch picture into entropy inequalities of suitable members of several parametrized entropic families. The two most famous of these are the additive Rényi α-family [4], given by

$$\mathcal{S}_\alpha(\rho) := \frac{1}{1-\alpha}\log \mathrm{Tr}(\rho^\alpha), \tag{34}$$

alongside the non-additive Tsallis q-family [5] defined by

$$\mathcal{S}^q(\rho) := \frac{1}{q-1}\left(1-\mathrm{Tr}(\rho^q)\right). \tag{35}$$

Both families retrieve the von Neumann entropy in the case of $\alpha/q \to 1$. In the case of $\alpha = q = 2$ we can use the simple representation of $\mathrm{Tr}\left(\rho^2\right)$ in form of correlation tensor norms (compare Lemma 1) to find simple forms of these entropies:

Remark 6 *Given n-partite quantum state $\rho_\Sigma \in \mathcal{H}^{d_\Sigma} = \otimes_{i=1}^n \mathcal{H}^{d_i}$ where $\Sigma := \{\Sigma_1, \Sigma_2, \cdots, \Sigma_n\}$ is the set of all parties we find the Tsallis 2 or linear entropy as:*

$$\mathcal{S}_L(\rho_\Sigma) := \left(1-\mathrm{Tr}(\rho_\Sigma^2)\right) \tag{36}$$

$$= 1 - \frac{1}{d_\Sigma}\left(1 + \sum_{\forall v \in P(\Sigma)} \|T^v\|^2\right) \tag{37}$$

Note that we simply used Lemma 1 to replace $\mathrm{Tr}(\rho_\Sigma^2)$.

Entropy inequalities are an extensively studied subject already in the context of classical information theory, where entropy relations are readily available [2]. The first attempts to recreate the classical results in quantum information have been achieved by Lieb and Ruskai [41], who showed the famous strong subadditivity relation (SSA)

$$\mathcal{S}_1(\rho_{ABC}) + \mathcal{S}_1(\rho_C) \leq \mathcal{S}_1(\rho_{AC}) + \mathcal{S}_1(\rho_{BC}), \tag{38}$$

for the von Neumann entropy. The hope to extend this result to the remaining parameter space of any of these two families has been impaired by broadly applicable no-go results. It is known that the Tsallis q-familiy can not satisfy SSA except for $q = 1$ [42]. In contrast the weaker notion of subadditivity holds for quantum Tsallis entropies with $q \geq 1$ [13]. Similarly, the case of the Rényi entropy has been mostly settled by [6], who demonstrated that for $\alpha \in (0,1) \cup (1,\infty)$ SSA can not hold. The results of [6] go far beyond SSA. They limit the parameter space where SSA or even a similar relation may hold severely. In the interval $(0,1)$ non-negativity is the only possible relation and in $(1,\infty)$ no homogeneous, thus linear, entropy inequality may exist. For the Rényi 0-entropy linear inequalities do exist [7], however SSA is not among them. As a reaction to this setback many authors consider alternative or generalized versions of SSA [12]. In a similar spirit the Bloch picture allows us to construct relations that resemble dimension-dependent versions of SSA.

Theorem 2 *For a tripartite quantum system ρ_{ABC} we find the following entropy inequality for the linear entropy $\mathcal{S}_L\left(\rho_{ABC}\right) = 1 - \mathrm{Tr}\left(\rho_{ABC}^2\right)$:*

$$\mathcal{S}_L\left(\rho_{ABC}\right) + \frac{1}{d_A d_B}\mathcal{S}_L\left(\rho_C\right) \leq \frac{1}{d_B}\mathcal{S}_L\left(\rho_{AC}\right) + \frac{1}{d_A}\mathcal{S}_L\left(\rho_{BC}\right) + \frac{d_A d_B + 1 - d_A - d_B}{d_A d_B} \tag{39}$$

The proof of the theorem can be found in the appendix.

This theorem can be considered as providing a substitute for SSA in the $q = 2$ case, where SSA is known not to hold [42]. Alternatively, we could have chosen to express $\mathrm{Tr}(\rho^2)$ in terms of 2^{-S_2} instead of S_L. This formulation leads to a non-linear entropy inequality for the Rényi entropy with $\alpha = 2$. We point out that such a reformulation is not in conflict with the established no-go result about homogeneous Rényi α-entropy relations [6] for $\alpha \in (1,\infty)$, since 2^{-S_2} is non-linear. The proof of Theorem 2 in the appendix however employs the very same techniques as the

proofs of the monogamy relations in Section IV. Generally speaking all proofs are inspired by the Bloch formalism. Essentially, we set some elements of the correlation tensor to zero. The resulting statement depends on the choice which correlation tensors are kept and which are discarded. Interestingly, these very different types of results seem to be complementary to each other in the Bloch picture. The correlation tensor formalism allows us to harness tools like purity and combine it with the Schmidt decomposition in a straightforward way. Additionally, once we know that a certain state does not exhibit correlations in a particular sector of the correlation tensor, we can develop tailor-made entropy relations that are expected to be tight with respect to the chosen state.

Before closing this section, we need to asses the utility of our newly derived linear entropy inequalities. It is natural to ask how they compare to other well-known entropy inequalities. It was possible to classify all possible classical entropy inequalities by a well known result, that showed that all classical entropy inequalities are representable as a convex cone of properly chosen elementary entropy vectors [2]. Similar arguments were used to study the von Neumann entropy [3]. In contrast, benchmarking q-entropy inequalities is not a straightforward endeavour, since to the best of our knowledge no comparable complete classifications exist. Audenaert's (weak) subadditivity of q-entropies [13] seems to be one of the natural competitors

$$\mathcal{S}^q(\rho_{AB}) \leq \mathcal{S}^q(\rho_A) + \mathcal{S}^q(\rho_B). \tag{40}$$

In the following we want to demonstrate that Theorem 2 and Eq. (39) does not follow trivially from the above Eq. (40). Since Eq. (39) involves tripartite terms and Eq. (40) does not, our first step is to pad Audenaert's subadditivity by an extra system and set $q = 2$ to make both relations comparable, thus we rewrite both into

$$\mathcal{S}_L(\rho_{ABC}) \leq \mathcal{S}_L(\rho_{AC}) + \mathcal{S}_L(\rho_B) \tag{41}$$

$$\mathcal{S}_L\left(\rho_{ABC}\right) \leq \frac{1}{d_B}\mathcal{S}_L\left(\rho_{AC}\right) + \frac{1}{d_A}\mathcal{S}_L\left(\rho_{BC}\right) - \frac{1}{d_A d_B}\mathcal{S}_L\left(\rho_C\right) + \frac{d_A d_B + 1 - d_A - d_B}{d_A d_B}. \tag{42}$$

The above are bounds on the same quantity $\mathcal{S}_L(\rho_{ABC})$. Now the only remaining question whether one bound is sharper than the other. This question depends on the state and the dimension. Let us set for example $d_A = d_B = d_C = 2$, then the question whether Eq. (42) is sharper than Eq. (41) is equivalent to

$$\frac{1}{2}\mathcal{S}_L(\rho_{AC}) + \mathcal{S}_L(\rho_B) - \frac{1}{2}\mathcal{S}_L(\rho_{BC}) + \frac{1}{4}\mathcal{S}_L\left(\rho_C\right) > \frac{1}{4}. \tag{43}$$

Phrased like this it is obvious, that this is true for all highly mixed states. For the maximally mixed state $\rho = \frac{1}{d_A d_B d_C}\mathbb{1}$ each single party marginal fulfills $S_L(\mathrm{Tr}_{ij}(\frac{1}{8}\mathbb{1})) = \frac{1}{2}$, while all two party marginals $S_L(\mathrm{Tr}_j(\frac{1}{8}\mathbb{1})) = \frac{3}{4}$. This means that for the maximally mixed state the above evaluates to the true statement $\frac{5}{8} > \frac{1}{4}$. This gives one example where our dimension-dependent SSA is sharper than (weak) subadditivity and thus independent. Similar results will hold for an ε-ball of states surrounding the maximally mixed state.

VI. A QUADRATIC ENTROPY INEQUALITY FOR THE LINEAR ENTROPY FROM THE BLOCH PICTURE

We know that in the special case of $q = \alpha = 1$, the Shannon [2] or von Neumann [3] entropy inequalities all describe a convex cone. All possible inequalities are described by linear combinations of certain elementary inequalities. This is a remarkably easy and elegant situation. Unfortunately similar results do not seem available for the remainder of the Tsallis family. Since the Tsallis 2-entropy features values between 0 and 1, we can nonetheless represent physical realizations in a hypercube of dimension $2^n - 1$, which allows a particularly instructive visualization for $n = 2$.

In the discussion of Section V, we were asking what Tsallis 2-entropy or linear entropy relations were possible for a tripartite system. In absence of complete classifications, we had to resort to a direct comparison with the most famous equation known to us: subadditivity. In this discussion we briefly consider the question of how q-entropies may be classified and find a new non-linear entropy inequality for the linear entropy.

Generally speaking, not many linear inequalities are available for q-entropies. Apart from the subadditivity [13], the triangle inequality [44] and the trivial choice of non-negativity not a lot is known. We know for a fact, that SSA does never hold for $q \neq 1$ [12]. There are some further information theoretic results such as Fannes type bounds and Lesche stability [44], but we are not aware of any further linear inequalities discussed in literature.

However, in the special case of $q = 2$ we can say more. Our Theorem 2 delivers a new, albeit dimension-dependent, linear entropy inequality for $q = 2$ and there may very well be more independent linear inequalities.

Even though we are not aware of any well-known non-linear entropy inequality we can construct a non-trivial example. As an Ansatz we can consider the most simple non-linear situation: the quadratic case. For tensor products

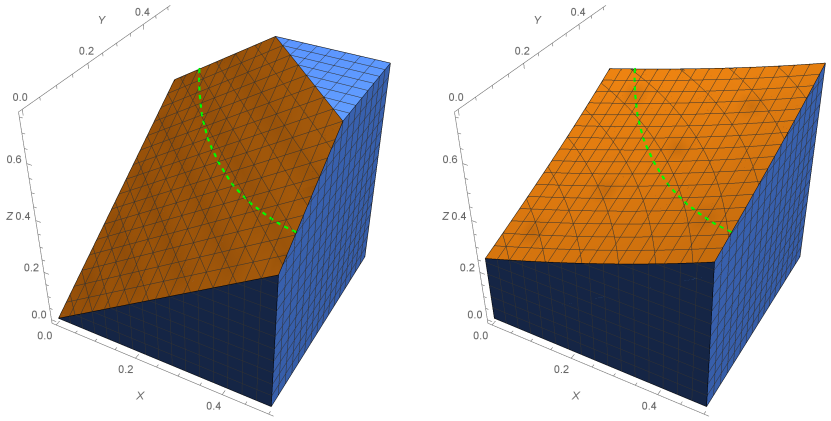

(a) (Weak) Subadditivity (b) Generalized Pseudo-Additivity

Figure 2: Comparison of different entropy inequalities for $d_A = d_B = 2$. On the X-Y plane we have plotted the values for $\mathcal{S}_L(A)$ and $\mathcal{S}_L(B)$, the Z-axis describes the maximal attainable value of $\mathcal{S}_L(AB)$ allowed by the corresponding entropy inequality. This means that a lower Z-value in the plots corresponds to the the respective inequality being sharper for the corresponding marginal values $\mathcal{S}_L(A)$ and $\mathcal{S}_L(B)$. Above the green dashed line in Fig. 2a and Fig. 2b our generalized pseudo-additivity is sharper than subadditivity, below the line the subadditivity is the sharper entropy inequality.

we have a clear candidate. It is known in the literature that a q-entropy fulfills the so-called pseudo-additivity [45],[12]

$$S_q(\rho_A \otimes \rho_B) = S_q(\rho_A) + S_q(\rho_B) + (1-q)S_q(\rho_A)S_q(\rho_B). \tag{44}$$

This gives q a clear interpretation as a parametrization of the corresponding Tsallis entropies non-additivity. Furthermore, it is a quadratic relation between a composite system and its marginals. Quadratic functions are non-linear but still simple enough to work with. The caveat is that pseudo-additivity only holds for product states $\rho_A \otimes \rho_B$. In the next theorem we show, that with simple Bloch picture techniques we can remedy this drawback for $q = 2$.

Theorem 3 *For all ρ_{AB} the the linear entropy or Tsallis 2-entropy can be bounded as:*

$$1 - \frac{d_A d_B}{4}\left(1 - \mathcal{S}_L(\rho_{AB}) + \frac{1}{d_A d_B}\right)^2 \leq \mathcal{S}_L(\rho_A) + \mathcal{S}_L(\rho_B) - \mathcal{S}_L(\rho_A)\mathcal{S}_L(\rho_B). \tag{45}$$

The proof can be found in the Appendix.

Using the purity bound we are able to turn the equality in Eq. (44) into an inequality and thus managed to also cover entangled or correlated composite systems ρ_{AB} instead of the product state appearing on the left hand side of Eq. (44). This turns the pseudo-additivity into a general non-linear inequality for linear entropy that is applicable to all states.

That this inequality is independent of subadditivity can be seen through the example of the maximally mixed state $\frac{1}{4}\mathbb{1}_{AB}$ for $d_A = d_B = 2$. Clearly, in this case $\mathcal{S}_L(\frac{1}{4}\mathbb{1}_{AB}) = \frac{3}{4}$, while its marginals attain the values $\mathcal{S}_L(\frac{1}{2}\mathbb{1}_A) = \mathcal{S}_L(\frac{1}{2}\mathbb{1}_B) = \frac{1}{2}$. Thus $\frac{3}{4} \leq \frac{1}{2} + \frac{1}{2}$ fulfills subadditivity $\mathcal{S}^q(\rho_{AB}) \leq \mathcal{S}^q(\rho_A) + \mathcal{S}^q(\rho_B)$, but is not sharp. On the other hand Eq. (45) evaluates to $\frac{3}{4} = 1 - \left(\frac{5}{4} - \frac{3}{4}\right)^2 \leq \frac{1}{2} + \frac{1}{2} - \frac{1}{4} = \frac{3}{4}$. Therefore, Eq. (45) does *not only hold*, it is *even tight*. We can conclude that it is an independent equation. A purely linear description of the entropy inequalities for the linear entropy seems impossible. Therefore we have to forfeit the hope to achieve a linear description in analogy to [2] of the linear entropy.

For a more geometric picture of the entropy space in the tripartite scenario refer to (see Fig. 2). There the relation of the marginals $\mathcal{S}_\mathcal{L}(A)$ and $\mathcal{S}_\mathcal{L}(B)$ to $\mathcal{S}_\mathcal{L}(AB)$ is plotted. We have depicted the attainable value of $\mathcal{S}_\mathcal{L}(AB)$ for subadditivity and our generalized pseudo-additivity. A lower value on the Z-axis corresponds to the inequality being sharper with respect to the corresponding pair of marginal entropies $\mathcal{S}_\mathcal{L}(A)$ and $\mathcal{S}_\mathcal{L}(B)$.

The region of validity for subadditivity resembles a cube cut apart diagonally (see Fig. 2a). The cut reveals a facet. In contrast the upper surface delimiting the generalized pseudo-additivity curves inward (see Fig. 2b). Together with the fact that edges are explicitly realizable it furthermore proves the non-convexity of the admissible entropy manifold. With respect to standard subadditivity, we find a non-trivial behaviour that depends on dimensional factors and on

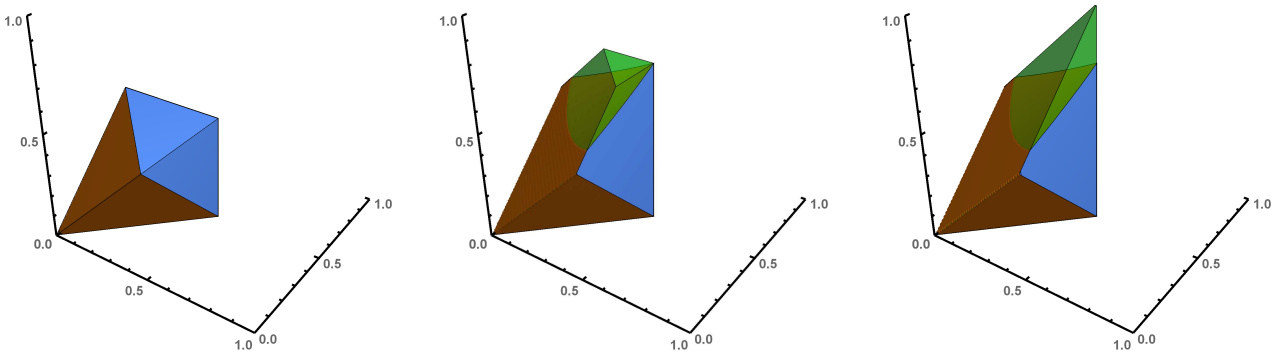

(a) $d_A = d_B = 2$ and $d_C = 2$ (b) $d_A = d_B = 2$ and $d_C = 4$ (c) $d_A = d_B = 2$ and $d_C = 100$

Figure 3: Every plotted point in the orange-blue body corresponds to a triple $(\mathcal{S}_L(A), \mathcal{S}_L(B), \mathcal{S}_L(C))$ of a tripartite systems marginal entropies that are admissible in both subadditivity and generalized pseudo-additivity. The green region is depicted transparent and contains the points that are only admissible in subadditivity but not generalized pseudo-additivity. Thus the green region marks the region where generalized pseudo-additivity is sharper than (weak) subadditivity.

the exact values of the involved entropic quantities. We have plotted as a dashed green line the intersection of both inequalities. The regions above the dashed line are stronger than subadditivity, while those towards the bottom and close to the origin are weaker (see Figs. 2a and 2b). This shows that depending on the involved state one or the other relation may be sharper. The exact size of these regions depends on the exact interrelations of the involved dimensions.

To analyze the dimensional dependence of standard subadditivity and generalized pseudo-additivity refer to Fig. 3. In Fig. 3 we have plotted the body of admissible marginal entropies that fulfill all three equations given by subadditivity (green) and those that as well satisfy the three equations given by permutations of Eq. (45) (orange-blue). If all dimensions are equal, generalized pseudo-additivity (see Eq. (45)) is not stronger than subadditivity. This is why Fig. 3a only shows the cone defined by subadditivity. In fact Fig. 3a represents a zoomed out version of Fig. 2a.

Already for $d_A = d_B = 2$ and $d_C = 3$ generalized pseudo-additivity is sharper for some regions. The upper blue facet of the body in Fig. 3a curves inward with increasing d_C in total analogy to Fig. 2b. In Figs. 3b and 3c the upper part of the body turns orange indicating that it has become a non-linear surface.

The region where Eq. (45) is stronger than subadditivity grows with $|d_i - d_j|$. In fact the cone described by only subadditivity grows with $|d_i - d_j|$, while the one defined by pseudo-additivity seems to saturate at $\min(d_i, d_j)^2$. This is visible in Figs. 3b and 3c, where the orange-blue body stopped growing.

One can sum up, that generalized pseudo-additivity is relevant for systems with asymmetric dimensions. It clearly rules out the possibility to rely on purely linear descriptions, as the extremal points between the non-linear inequality are realizable and the non-linear surface in Figs. 3b and 3c is slightly non-convex.

VII. CONCLUSION

We have demonstrated that the correlation tensor formalism is a powerful tool to derive dimension-dependent statements about two seemingly different areas of research: monogamy relations and entropy inequalities.

First, we have introduced the *split Bloch basis*, a sparse Bloch representation for quantum states with low-dimensional support. While all physical quantum states are of course expected to be full rank and thus an empty kernel, this tool can nonetheless be very useful for theoretical techniques that make use of purification and Schmidt decompositions.

Using this representation we have shown that a natural monotone for quantifying correlations indeed exhibits monogamy in arbitrary dimensions. In particular, any amount of bipartite correlation between them non-trivially restricts the correlations of any external party with the system and maximal correlation implies decoupling from any external party.

Complementary, by using the very same techniques with some slightly different choices, we derived a number of inequalities for the well-known linear (or Tsallis 2-)entropy. First, we have a new linear inequality, a dimension-

dependent analogue to strong subadditivity. Second and maybe more interesting, we provide a non-linear but simple inequality for the linear entropy.

We find that, while in the case of symmetric dimension subadditivity is strictly stronger than our inequality, it is nonetheless sharper for asymmetric dimensions.

An open question is whether our results could be made sharper. The key technique in all our theorems is the relation of the purity $\mathrm{Tr}(\rho^2)$ to correlation tensor norms. Typically we employ purity here, however a sharper bound may lead to better results. Possible candidates could be found in either [46] or [47], where more involved relations for $\mathrm{Tr}(\rho^2)$ are given. Similarly, in (B9) we simply set $\|T^{AB}\|^2$ to zero for the derivation of the generalized pseudo-additivity. It may be that a sharper bound is possible here. Furthermore, the reliance on the connection between $\mathrm{Tr}(\rho^2)$ and the Bloch parameterization during the proof of the generalized subadditivity limits the relation to the linear entropy. It would be certainly desirable to obtain a similarly general result for all q-entropies. Another interesting direction may be the derivation of non-trivial restrictions for correlation tensor elements from q-entropy inequalities.

It is still unclear if a complete geometric classification is possible, but it will be certainly more complicated than the entropy cones of the von Neumann entropy. Still, one could hope to at least find a more complex body that contains all entropic relations at once.

VIII. ACKNOWLEDGMENTS

We especially thank Felix Huber for pointing out an error in the first arxiv version. We thank Nicolai Friis, Milan Mosonyi and Matej Pivoluska for their comments. PA, CK and MH acknowledge support of funding from the Austrian Science Fund (FWF) through the START project Y879-N27 and the joint Czech-Austrian project MultiQUEST (I 3053-N27 and GF17-33780L). CK especially thanks Babsi for being the best and dearest and excuses for not having had the opportunity to thank Barbara Weberndorfer accordingly in his thesis. He does sincerely hope time travel may one day allow to correct this error.

Appendix A: Monogamy of Correlation Relations

Lemma 4 (The Schmidt decomposition) *For pure states $|\psi\rangle_{AB} \in \mathcal{H}^{d_A} \otimes \left(\mathcal{H}^{d_A} \oplus \mathcal{H}^{d_B - d_A}\right)$ with $d_B > d_A$ we find the Schmidt decomposition as:*

$$\left(|\psi\rangle\langle\psi|\right)_{AB} = \sum_{i,j=0}^{\min(d_A,d_B)-1} \left\langle \lambda_i^A \otimes \lambda_j^B \right\rangle \lambda_i^A \otimes \lambda_j^B \tag{A1}$$

Proof
We will simply prove the above statement by explicitly constructing the standard Schmidt basis from our Split Bloch basis: First let us state the standard Schmidt decomposition for pure states $|\psi\rangle_{AB} = \sum_{i=0}^{\min(d_A,d_B)-1} c_i |ii\rangle$ in operator form:

$$\left(|\psi\rangle\langle\psi|\right)_{AB} = \sum_{i,j=0}^{\min(d_A,d_B)-1} c_i c_j \, |ii\rangle\langle jj| \tag{A2}$$

Let us construct first the diagonal $|i\rangle\langle i|$ in the local Bloch bases. Note that the construction in the split Bloch basis and the canonical Gellmann matrix basis is analogue, since the λ_{ij} and $\hat{\lambda}_{ij}$ of the split Bloch basis are simply the embedded Gellmann matrices in the bigger space. For simplicity we will concatenate the index of the diagonal Bloch basis elements, e.g. $\lambda_{ii} = \lambda_i$

$$\sqrt{d}\,|0\rangle\langle 0| = \lambda_0 + \frac{1}{d-1}\lambda_{d-1} + \sum_{k=2}^{d-1} \alpha_{d-k}\lambda_{d-k} + \alpha_{d-i-1}\lambda_i \tag{A3}$$

$$\sqrt{d}\,|i\rangle\langle i| = \frac{1}{i}\left(\lambda_0 + \frac{1}{d-1}\lambda_{d-1} + \sum_{k=2}^{d-i-1} \alpha_{d-k}\lambda_{d-k} - \alpha_{d-i-1}\lambda_i\right) \qquad | \, i \in \{1,\ldots,d-2\} \tag{A4}$$

$$\sqrt{d}\,|d-1\rangle\langle d-1| = \frac{1}{d-1}\left(\lambda_0 + \lambda_{d-1}\right) \tag{A5}$$

with $\alpha_{d-k} = \Pi_{j=1}^{k-1}(1 + \frac{1}{d-j})/d - k$ and d the local dimension of the Hilbert space. The diagonal elements of the bipartite basis are simply found as the tensor product $|ii\rangle\langle ii| = |i\rangle\langle i|_A \otimes |i\rangle\langle i|_B$ for all $i \in \{0,\ldots,d_{min}-1\}$. Where $d_{min} = \min(d_A, d_B)$. For the off-diagonal elements we find:

$$|ii\rangle\langle jj| + |jj\rangle\langle ii| = \frac{1}{2d_{min}}\left(\lambda_{ij}^A \otimes \lambda_{ij}^B + \hat{\lambda}_{ij}^A \otimes \hat{\lambda}_{ij}^B\right) \qquad | \, i \neq j \tag{A6}$$

this is true since:

$$\lambda_{ij}^A \otimes \lambda_{ij}^B = |ij\rangle\langle ji| + |ji\rangle\langle ij| + |ii\rangle\langle jj| + |jj\rangle\langle ii| \tag{A7}$$

and:

$$\hat{\lambda}_{ij}^A \otimes \hat{\lambda}_{ij}^B = |ij\rangle\langle ji| + |ji\rangle\langle ij| - |ii\rangle\langle jj| - |jj\rangle\langle ii| \tag{A8}$$

Note that we already assumed that the computational bases in which we expressed the Schmidt basis and the split Bloch basis are the same. This is not necessarily the case, however, any two computational bases are connected by unitary transformations.

Theorem 1 *Let $\rho_{ABE} \in \mathcal{H} = \mathcal{H}^{d^2} \otimes \mathcal{H}^{d_E}$ be an arbitrary tripartite state owned by A, B and E with local dimensions $d_A = d_B = d$ and d_E:*

(i): The correlation of a composite system ρ_{AB} with an arbitrary system ρ_E limits the correlation of its marginals with the same:

$$\mathcal{T}_{A|E}\left(\rho_{ABE}\right) + \mathcal{T}_{B|E}\left(\rho_{ABE}\right) \leq \frac{g_{AB|E}}{\min\left(g_{A|E}, g_{B|E}\right)} \mathcal{T}_{AB|E}\left(\rho_{ABE}\right) \tag{A9}$$

(ii): The correlation of any state $\rho_{AB} \in \mathcal{H}^{d^2}$ with an arbitrary state ρ_E is restricted by:

$$\mathcal{T}_{AB|E} \leq \frac{d^4 - 1 - 2\left(\left\|T^A\right\|^2 + \left\|T^B\right\|^2\right) - 2g_{A|B}\mathcal{T}_{A|B}}{g_{AB|E}} \tag{A10}$$

Proof
add (i): By the definition of $\mathcal{T}_{A|E}$, $\mathcal{T}_{B|E}$ and $\mathcal{T}_{AB|E}$ we have

$$\begin{aligned}\min\left(g_{A|E}, g_{B|E}\right)\left(\mathcal{T}_{A|E} + \mathcal{T}_{B|E}\right) &\leq g_{A|E}\,\mathcal{T}_{A|E} + g_{B|E}\,\mathcal{T}_{B|E} &\text{(A11)}\\ &= \left\|T^{AE}\right\|^2 + \left\|T^{BE}\right\|^2 \leq \left\|T^{AE}\right\|^2 + \left\|T^{BE}\right\|^2 + \left\|T^{ABE}\right\|^2 = g_{AB|E}\mathcal{T}_{AB|E} &\text{(A12)}\end{aligned}$$

add (ii): This proof makes use of the split Bloch decomposition. First we need to state that for every ρ_{ABE} with a fixed marginal $\rho_{AB} = \sigma$ there exists a purification $|\psi_{ABEE'}\rangle$. A purification is however not unique, i.e. all purifications are connected by an isometry: $|\psi'\rangle_{ABEE'} = \mathbb{1} \otimes V\,|\psi\rangle_{ABEE'} \in \mathcal{H}^{d^2} \otimes \mathcal{H}^{d'>d_{min}}$ with the isometry $V : \mathcal{B}\left(\mathcal{H}^{d_{min}}, \mathcal{H}^{d'}\right)$.

Using these considerations allows us to use the Schmidt decomposition for pure states as well as the fact that $\mathrm{Tr}\left(\left(|\psi\rangle\langle\psi|\right)^2_{ABEE'}\right) = 1$. Furthermore it is very useful to use the split Bloch basis. For sake of brevity let us introduce the shorthand subscript $EE' \to \tilde{E}$ and thus $c_0 = \left\langle \lambda_0^{AB} \otimes \lambda_0^{\tilde{E}} \right\rangle^2$ and $c_0' = \left\langle \lambda_0^{AB} \otimes \mu_0^{\tilde{E}} \right\rangle^2$.

$$\begin{aligned}\mathrm{Tr}\left(\left(|\psi\rangle\langle\psi|\right)^2_{AB\tilde{E}}\right) = 1 = \frac{1}{d^4}&\left(c_0 + \|T^A\|^2 + \|T^B\|^2 + \|T^{\tilde{E}}_{SD}\|^2 + \|T^{AB}\|^2 + \|T^{A\tilde{E}}_{SD}\|^2 + \|T^{B\tilde{E}}_{SD}\|^2 + \|T^{AB\tilde{E}}_{SD}\|^2\right)\\ &+ \frac{1}{\left(d_{\tilde{E}} - d^2\right)d^2}\left(c_0' + \|\tilde{T}^{\tilde{E}}\|^2 + \|\tilde{T}^{A\tilde{E}}\|^2 + \|\tilde{T}^{B\tilde{E}}\|^2 + \|\tilde{T}^{AB\tilde{E}}\|^2\right) &\text{(A13)}\end{aligned}$$

By simply rewriting this equation we find:

$$\begin{aligned}\|T^{A\tilde{E}}_{SD}\|^2 + \|T^{B\tilde{E}}_{SD}\|^2 + \|T^{AB\tilde{E}}_{SD}\|^2 = d^4 &- \left(c_0 + \|T^A\|^2 + \|T^B\|^2 + \|T^{\tilde{E}}_{SD}\|^2 + \|T^{AB}\|^2\right)\\ &- \frac{d^2}{\left(d_{\tilde{E}} - d^2\right)}\left(c_0' + \|\tilde{T}^{\tilde{E}}\|^2 + \|\tilde{T}^{A\tilde{E}}\|^2 + \|\tilde{T}^{B\tilde{E}}\|^2 + \|\tilde{T}^{AB\tilde{E}}\|^2\right) &\text{(A14)}\end{aligned}$$

Now we can use the Schmidt decomposition, i.e.:

$$\begin{aligned}\frac{1}{d^2}\left(1 + \|T^A\|^2 + \|T^B\|^2 + \|T^{AB}\|^2\right) &= \frac{1}{d^2}\left(c_0 + \|T^{\tilde{E}}_{SD}\|^2\right) + \frac{1}{\left(d_{\tilde{E}} - d^2\right)d^2}\left(c_0' + \|\tilde{T}^{\tilde{E}}\|^2\right) &\text{(A15)}\\ \|T^{\tilde{E}}_{SD}\|^2 = 1 + \|T^A\|^2 + \|T^B\|^2 + \|T^{AB}\|^2 - c_0 &- \frac{1}{\left(d_{\tilde{E}} - d^2\right)}\left(c_0' + \|\tilde{T}^{\tilde{E}}\|^2\right) &\text{(A16)}\end{aligned}$$

Plugging this in above we find:

$$\begin{aligned}\|T^{A\tilde{E}}_{SD}\|^2 + \|T^{B\tilde{E}}_{SD}\|^2 + \|T^{AB\tilde{E}}_{SD}\|^2 = d^4 &- \left(c_0 + 2\|T^A\|^2 + 2\|T^B\|^2 + 2\|T^{AB}\|^2 + 1 - c_0\right)\\ &- \underbrace{\frac{d^2 - 1}{\left(d_{\tilde{E}} - d^2\right)}\left(c_0' + \|\tilde{T}^{\tilde{E}}\|^2\right) - \frac{d^2}{\left(d_{\tilde{E}} - d^2\right)}\left(\|\tilde{T}^{A\tilde{E}}\|^2 + \|\tilde{T}^{B\tilde{E}}\|^2 + \|\tilde{T}^{AB\tilde{E}}\|^2\right)}_{\Delta} &\text{(A17)}\end{aligned}$$

Due to Lemma 2 we know there exists a basis such that $\Delta = 0$, since the $\mathrm{Tr}\left(\rho^2_{AB}\right)$ is invariant under changing the local Bloch basis, this is achieved by maximizing the left hand side:

$$\begin{aligned}\max_{\{\lambda_i^{\tilde{E}}\}}\left(\|T^{A\tilde{E}}_{SD}\|^2 + \|T^{B\tilde{E}}_{SD}\|^2 + \|T^{AB\tilde{E}}_{SD}\|^2\right) &= d^4 - 1 - 2\left(\|T^A\|^2 + \|T^B\|^2 + g_{A|B}\mathcal{T}_{A|B}\right) &\text{(A18)}\\ g_{AB|\tilde{E}}\mathcal{T}_{AB|\tilde{E}}\left(|\psi_{AB\tilde{E}}\rangle\langle\psi_{AB\tilde{E}}|\right) &= d^4 - 1 - 2\left(\|T^A\|^2 + \|T^B\|^2 + g_{A|B}\mathcal{T}_{A|B}\right) &\text{(A19)}\end{aligned}$$

Finally due to Lemma 3 (ii) we find:

$$g_{AB|E}\mathcal{T}_{AB|E}\left(\left(|\psi\rangle\langle\psi|\right)_{AB\tilde{E}}\right) \leq g_{AB|\tilde{E}}\mathcal{T}_{AB|\tilde{E}}\left(\left(|\psi\rangle\langle\psi|\right)_{AB\tilde{E}}\right) = d^4 - 1 - 2\left(\|T^A\|^2 + \|T^B\|^2 + g_{A|B}\mathcal{T}_{A|B}\right) \tag{A20}$$

and since $\mathcal{T}_{AB|E}$ is independent of E' we can take the partial trace in the argument over E', i.e. $\mathcal{T}_{AB|E}\left(\left(|\psi\rangle\langle\psi|\right)_{AB\tilde{E}}\right) = \mathcal{T}_{AB|E}\left(\mathrm{Tr}'_E\left(\left(|\psi\rangle\langle\psi|\right)_{AB\tilde{E}}\right)\right) = \mathcal{T}_{AB|E}\left(\rho_{ABE}\right)$.

$$g_{AB|E}\mathcal{T}_{AB|E}\left(\rho_{ABE}\right) \leq d^4 - 1 - 2\left(\|T^A\|^2 + \|T^B\|^2 + g_{A|B}\mathcal{T}_{A|B}\right) \tag{A21}$$

Lemma 6 *The sum of correlation tensor norms in Theorem 1 (ii) is bounded from above by:*

$$\|T^A\|^2 + \|T^B\|^2 \leq \min\left(2d-2, \left(d^2-1\right)\left(1-\mathcal{T}_{A|B}\right)\right)$$

and from below by:

$$\|T^A\|^2 + \|T^B\|^2 \geq \max\left(0, \frac{d^2}{d_E} - 1 - \left(d^2-1\right)\mathcal{T}_{A|B}\right)$$

Proof

We will start by proving the upper bound for $\|T^A\|^2 + \|T^B\|^2$. A very simple connection can be found by using purity:

$$d^2 - 1 \geq \|T^A\|^2 + \|T^B\|^2 + \|T^{AB}\|^2 \tag{A22}$$

$$d^2 - 1 - g_{A|B}\mathcal{T}_{A|B} \geq \|T^A\|^2 + \|T^B\|^2 \tag{A23}$$

$$\left(d^2-1\right)\left(1-\mathcal{T}_{A|B}\right) = \|T^A\|^2 + \|T^B\|^2 \tag{A24}$$

Now by varying $0 \leq \mathcal{T}_{A|B} \leq 1$ we can estimate the entanglement Eve possesses. However due to the fact that the squared Euclidean norm of a correlation tensor is realized by a pure state, another bound has to be considered:

$$2d - 2 \geq \|T^A\|^2 + \|T^B\|^2$$

Thus we found an upper bound for:

$$\min\left(2d-2, \left(d^2-1\right)\left(1-\mathcal{T}_{A|B}\right)\right) \geq \|T^A\|^2 + \|T^B\|^2$$

For the lower bound we will use:

$$\frac{1}{d_E}\left(1 + \|T^E\|^2\right) = \frac{1}{d^2}\left(1 + \|T^A\|^2 + \|T^B\|^2 + \|T^{AB}\|^2\right)$$

$$\frac{d^2}{d_E} - 1 \leq \|T^A\|^2 + \|T^B\|^2 + \|T^{AB}\|^2$$

$$\frac{d^2}{d_E} - 1 - g_{A|B}\mathcal{T}_{A|B} \leq \|T^A\|^2 + \|T^B\|^2$$

$$\frac{d^2}{d_E} - 1 - g\left(d^2-1\right)\mathcal{T}_{A|B} \leq \|T^A\|^2 + \|T^B\|^2$$

We know however that $\|T^A\|^2 + \|T^B\|^2 > 0$ thus we find the lower bound as :

$$\max\left(0, \frac{d^2}{d_E} - 1 - \left(d^2-1\right)\mathcal{T}_{A|B}\right)$$

Which concludes our proof.

Appendix B: Entropy Inequalities

Theorem 2 *For a tripartite quantum system ρ_{ABC} we find the following entropy inequality for the linear entropy $\mathcal{S}_L\left(\rho_{ABC}\right) = 1 - \mathrm{Tr}\left(\rho_{ABC}^2\right)$:*

$$\mathcal{S}_L\left(\rho_{ABC}\right) + \frac{1}{d_A d_B}\mathcal{S}_L\left(\rho_C\right) \leq \frac{1}{d_B}\mathcal{S}_L\left(\rho_{AC}\right) + \frac{1}{d_A}\mathcal{S}_L\left(\rho_{BC}\right) + \frac{d_A d_B + 1 - d_A - d_B}{d_A d_B} \tag{B1}$$

Proof
We rewrite the entire system into the relevant subsystems

$$d_A d_B d_C \operatorname{Tr}\left(\rho_{ABC}^2\right) = 1 + \|T^A\|^2 + \|T^B\|^2 + \|T^C\|^2 + \|T^{AB}\|^2 + \|T^{AC}\|^2 + \|T^{BC}\|^2 + \|T^{ABC}\|^2 \tag{B2}$$

$$= \left(1 + \|T^A\|^2 + \|T^C\|^2 + \|T^{AC}\|^2\right) + \left(1 + \|T^B\|^2 + \|T^C\|^2 + \|T^{BC}\|^2\right) - \left(1 + \|T^C\|^2\right) \tag{B3}$$

$$= d_A d_C \operatorname{Tr}\left(\rho_{AC}^2\right) + d_B d_C \operatorname{Tr}\left(\rho_{BC}^2\right) - d_C \operatorname{Tr}\left(\rho_C^2\right). \tag{B4}$$

We can rewrite $\operatorname{Tr}(\rho^2)$ *into* S_L *by its definition (see Eq. (36)) and obtain*

$$1 - \mathcal{S}_L\left(\rho_{ABC}\right) + \frac{1}{d_A d_B}\left(1 - \mathcal{S}_L\left(\rho_C\right)\right) \geq \frac{1}{d_B}\left(1 - \mathcal{S}_L\left(\rho_{AC}\right)\right) + \frac{1}{d_A}\left(1 - \mathcal{S}_L\left(\rho_{BC}\right)\right), \tag{B5}$$

or equivalently our claim

$$\mathcal{S}_L\left(\rho_{ABC}\right) + \frac{1}{d_A d_B}\mathcal{S}_L\left(\rho_C\right) \leq \frac{1}{d_B}\mathcal{S}_L\left(\rho_{AC}\right) + \frac{1}{d_A}\mathcal{S}_L\left(\rho_{BC}\right) + \frac{d_A d_B + 1 - d_A - d_B}{d_A d_B}. \tag{B6}$$

Theorem 3 *For all* ρ_{AB} *and the linear entropy or Tsallis 2-entropy we have*

$$1 - \frac{d_A d_B}{4}\left(1 - \mathcal{S}_L(\rho_{AB}) + \frac{1}{d_A d_B}\right)^2 \leq S_L(\rho_A) + S_L(\rho_B) - S_L(\rho_A) S_L(\rho_B). \tag{B7}$$

Proof
We prove the desired equation by showing a kind of "sub-multiplicativity" $f(\mathcal{S}_L(\operatorname{Tr}(\rho_{AB})^2)) \leq \mathcal{S}_L(\operatorname{Tr}(\rho_A \otimes \rho_B)^2)$ *of* $\mathcal{S}_L$ *under the tensor product. For this we express* $\operatorname{Tr}(\rho_{AB})^2$ *in the Bloch picture. We make use of the relation* $\operatorname{Tr}\left(\rho_A^2\right) = \frac{1}{d_A}\left(1 + \|T^A\|^2\right)$ *to obtain*

$$\operatorname{Tr}(\rho_{AB})^2 = \frac{1}{d_A d_B}\left(1 + \|T^A\|^2 + \|T^B\|^2 + \|T^{AB}\|^2\right) \tag{B8}$$

$$= \frac{1}{d_A d_B}\left(1 + \left(d_A \operatorname{Tr}\left(\rho_A^2\right) - 1\right) + \left(d_B \operatorname{Tr}\left(\rho_B^2\right) - 1\right) + \|T^{AB}\|^2\right) \tag{B9}$$

$$\geq \frac{1}{d_A d_B}\left(d_A \operatorname{Tr}\left(\rho_A^2\right) + d_B \operatorname{Tr}\left(\rho_B^2\right) - 1\right) \tag{B10}$$

$$= \frac{1}{d_A d_B}\left(d_A d_B \operatorname{Tr}\left(\left(\rho_A \otimes \rho_B\right)^2\right)\left(\frac{1}{d_B \operatorname{Tr}\left(\rho_B^2\right)} + \frac{1}{d_A \operatorname{Tr}\left(\rho_A^2\right)}\right) - 1\right) \tag{B11}$$

Finally by the Arithmetic-Geometric mean inequality $a + b \geq 2\sqrt{ab}$ *we got*

$$\operatorname{Tr}(\rho_{AB}^2) \geq \frac{1}{d_A d_B}\left(d_A d_B \operatorname{Tr}\left(\left(\rho_A \otimes \rho_B\right)^2\right)\left(\frac{1}{d_B \operatorname{Tr}\left(\rho_B^2\right)} + \frac{1}{d_A \operatorname{Tr}\left(\rho_A^2\right)}\right) - 1\right) \tag{B12}$$

$$= \frac{1}{d_A d_B}\left(d_A d_B \operatorname{Tr}\left(\left(\rho_A \otimes \rho_B\right)^2\right)\left(\frac{2}{\sqrt{d_A d_B \operatorname{Tr}\left(\rho_A^2\right)\operatorname{Tr}\left(\rho_B^2\right)}}\right) - 1\right) \tag{B13}$$

$$= \frac{2}{\sqrt{d_A d_B}}\sqrt{\operatorname{Tr}\left(\left(\rho_A \otimes \rho_B\right)^2\right)} - \frac{1}{d_A d_B} \tag{B14}$$

or alternatively $\operatorname{Tr}\left(\left(\rho_A \otimes \rho_B\right)^2\right) \leq \frac{d_A d_B}{4}\left(\operatorname{Tr}\left(\rho_{AB}^2\right) + \frac{1}{d_A d_B}\right)^2$.

The pseudo-additivity [45],[12] for $q = 2$ *is*

$$S_L(\rho_A) + S_L(\rho_B) - S_L(\rho_A) S_L(\rho_B) = S_L(\rho_A \otimes \rho_B) = 1 - \operatorname{Tr}\left(\left(\rho_A \otimes \rho_B\right)^2\right) \tag{B15}$$

$$\geq 1 - \frac{d_A d_B}{4}\left(\operatorname{Tr}\left(\rho_{AB}^2\right) + \frac{1}{d_A d_B}\right)^2, \tag{B16}$$

leaving us with

(B17)

$$S_L(\rho_A) + S_L(\rho_B) - S_L(\rho_A) S_L(\rho_B) \geq 1 - \frac{d_A d_B}{4}\left(1 - \mathcal{S}_L(\rho_{AB}) + \frac{1}{d_A d_B}\right)^2 \tag{B18}$$

[1] C.E. Shannon and W. Weaver, The Mathematical Theory of Communication, University of Illinois Press, (1963)
[2] R.W. Yeung, IEEE Trans. Inf. Theory **43** 6 19241934 (1997)
[3] N. Pippenger, IEEE Trans. Inf. Theory **49** 4 773789 (2003)
[4] A. Rényi, Proc. Fourth Berkeley Symp. on Math.Statist. and Prob., **547561** (1960)
[5] C. Tsallis, J.Stat.Phys, 52, **479-487**,(1988)
[6] N. Linden, M. Mosonyi and A. Winter, Proc. R. Soc. A, (2013) ; arXiv: 1212.0248
[7] J. Cadney, M. Huber, N. Linden, A. Winter, Lin. Alg. Appl.,vol. 452, pp. 153-171 (2014) ; arXiv: 1308.0539
[8] T. Yamano, Physica A, **305**, 486-496 (2002)
[9] C. Tsallis, Introduction to Nonextensive Statistical Mechanics Approaching a Complex World - Springer (2009)
[10] S. Thurner and R. Hanel, AIP Conference Proceedings 965, 68 (2007); arXiv: 0709.1685
[11] S. Thurner and C. Tsallis, EPL (Europhysics Letters), Volume 72, Number 2; arXiv: 0506140
[12] D Petz, D Virosztek, Mathematical Inequalities and Applications, Vol. 18, No. 2, 01.04.2015, p. 555-568 ; arXiv-preprint: 1403.7062
[13] KMR. Audenaert, Journal of Mathematical Physics, (2007) ; arXiv: 0705.1276
[14] B. Terhal, IBM Journal of Research and Development **48.1** (2004), ; arXiv: 0307120
[15] H.K. Lo and H.F. Chau, Science **2050-2056**, 283.5410 (1999) ; arXiv: 9803006
[16] P.W. Shor and J. Preskill, Phys. Rev. Lett. **85**, 441 (2000) ; arXiv: 0003004
[17] C.H. Bennett and G. Brassard, Proceedings of the IEEE International Conference on Computers, Systems, and Signal Processing (IEEE Press, New York, 1984), **175-179**
[18] V. Coffman, J. Kundu and WK. Wootters, Phys. Rev. A **61**, 052306 (2000) ; arXiv: 9907047
[19] T.J. Osborne and F. Verstraete, Phys. Rev. Lett. **96**, 220503 (2006) ; arXiv: 0502176
[20] M. Christandl and A. Winter, Journal of Mathematical Physics **45**, 829 (2004) ; arXiv: 0308088
[21] M. Koashi and A. Winter, Phys. Rev. A **69**, 022309 (2004) ; arXiv: 0310037
[22] A. Streltsov, G. Adesso, M. Piani and D. Bruß, Phys. Rev. Lett. **109**, 050503 (2012) ; arxiv: 1112.3967
[23] Yong-Cheng Ou, Phys. Rev. A **75**, 034305 (2007) ; arXiv: 0612127
[24] C. Lancien, S. Di Martino, M. Huber, M. Piani, G. Adesso and A. Winter, Phys. Rev. Lett. **117**, 060501 (2016) ; arXiv: 1604.02189
[25] G. Gour and Y. Guo , (2017), arXiv-preprint: 1710.03295
[26] A. Klyachko, (2004), arXiv-preprint: 0409113
[27] F. Bloch, Phys. Rev. **70**, 460-474 (1946)
[28] G. Kimura,Phys. Lett. A **31** 4, 339 (2003);
[29] G. Kimura, A. Kossakowski, Open Sys. Information Dyn. **12**, 207 (2005);
[30] RA. Bertlmann and P. Krammer, J. Phys. A **41**, 23 (2008) ; arXiv: 0806.1174
[31] F. Huber, O. Gühne, and J. Siewert, Phys. Rev. Lett. **118**, 200502 (2017) ; arXiv: 1608.06228
[32] F. Huber, C. Eltschka, J. Siewert and O. Gühne, (2017), arXiv-preprint: 1708.06298
[33] C. Klöckl and M. Huber, Phys. Rev. A **91**, 042339, (2015) ; arXiv: 1411.5399
[34] A. S. M. Hassan, P. S. Joag, Quant. Inf. Comp., **8**, No. 8-9 0773-0790 (2008);
[35] J. I. de Vicente, M. Huber, Phys. Rev. A **84**, 062306 (2011);
[36] N. Friis, M. Huber and M. Perarnau-Llobet, Phys. Rev. E **93**, 042135 (2016); arXiv: 1511.08654
[37] On a historical note it is not entirely clear to us who to attribute the generalized Gell-Mann matrices to. The d = 3 construction is due to Gell-Mann, however who is responsible for the first generalization is unclear to us. We could trace back the mention of the generalized Gell-Mann matrices to: F. T. Hioe and J. H. Eberly. , Phys. Rev. Lett., **47** 838-841, (1981). We are happy about any comments on earlier work unknown to us.
[38] H. Weyl, Zeitschrift für Physik, 46(1):146,(1927)
[39] A. Asadian, P. Erker, M. Huber and C. Klöckl, Phys. Rev. A, **94** 010301 (R) (2016) ; arXiv: 1512.05640
[40] W.K. Wootters, Phys. Rev. Lett. **80**, 2245 (1998) ; arXiv: 9709029
[41] EH. Lieb and MB. Ruskai, Journal of Mathematical Physics **14**, 1938 (1973)
[42] S. Furuichi, Journal of Mathematical Physics **47**, 023302 (2006) ; arXiv: 0405600
[43] H Araki and EH Lieb, Communications in Mathematical Physics **18**, 2, 160170 (1970)
[44] A.E. Rastegin, J. Stat. Phys. **143** 11201135,(2011) ; arxiv: 1012.5356
[45] S. Abe, Physics Letters A, Volume 271, **74-79**, (2000) ; arXiv: 0005538
[46] C. Eltschka and J. Siewert, Phys. Rev. Lett. **114**, 140402 (2015) ; arXiv: 1407.8195
[47] C. Eltschka and J. Siewert, (2017), arXiv-preprint: 1708.09639

4 Finite-Function-Encoding Quantum States

4.1 Summary

We introduce a class of quantum states, called finite-function-encoding (FFE) states, that extend the qubit hypergraph construction—phase encodings of binary logical functions—to the encoding of d-valued logical functions in qudit systems. Not all FFE states can be described by a graph. This is because graphs correspond to polynomial functions, and while all binary logical functions are polynomial, this property does not extend to arbitrary dimension: in prime dimensions every logical function can be expressed as a polynomial, but in non-prime dimensions this is no longer the case.

We complete the definition of the states associated with polynomial functions in arbitrary dimensions. To that end, we define a new class of graphs, called tensor-edge hypergraphs (TEH). The states associated to them generalize the previously studied qudit hypergraph states and allow for the representation of all polynomial functions in arbitrary dimensions. However, through the investigation of the stabilizer formalism and local equivalence, we observe that polynomial and non-polynomial functions are connected by local unitary transformations. This motivates the consideration of the full class of FFE states rather than restricting attention to the subclass of states associated with polynomial functions. Although FFE states encompass a larger set than graph states, several structural features of graph states are preserved within FFE states. We develop a stabilizer formalism and study local equivalence by introducing a group of finite-function-encoding Pauli (FP) operations, which map FFE states to FFE states. This approach is analogous to the use of the Clifford group in the context of qubit graph states, where a finitely generated subgroup of the unitary group preserves the set of graph states and serves to generate the stabilizer group, thereby enabling a compact description of the states. In our setting, we similarly use FP operations to generate stabilizers of FFE states and obtain a closed-form characterization. We identify an additional structural constraint in the generators of the stabilizer group that distinguishes tensor-edge hypergraph states from general FFE states. We then study local equivalence classes under two types of operations: local unitary (LU) transformations and local finite-function-encoding Pauli (LFP) transformations. Historically, there has been a long-standing conjecture that the local Clifford group constitutes the full set of LU operations preserving the set of qubit graph states, but this has been shown to be false. In a similar vein, we identify LU transformations that are not contained within LFP, further highlighting the distinction between these two groups of operations. While the general classification problem is computationally hard, we obtain a complete classification under local unitary (LU) and local finite-function-encoding Pauli (LFP) transformations for all two-qutrit and two-ququart FFE states. This analysis provides structural insights and reveals a connection between the classification of bipartite maximally entangled FFE states and the classification problem for Butson-type Hadamard matrices. Although this connection does not resolve the Hadamard classification problem, it establishes a correspondence that may be exploited in future work. This framework extends the methods available for the study and classification of high-dimensional entangled states in quantum information theory.

In the broader generalization perspective of this thesis, FFE preserves the operational idea to encode functions in phases of quantum states while allowing the form to change: polynomiality marks where graphical intuition remains valid, and relaxing it reveals a larger non-graphical family that nonetheless retains stabilizer-like structure and useful control.

4.2 Own Contribution

The idea for this paper was proposed by my supervisor, Marcus Huber, who was also actively involved in the development and writing of the manuscript. Giuseppe Vitagliano, who was a postdoctoral researcher in Marcus Huber's group and the last author of the paper, coordinated the collaboration, contributed to all major aspects of the project, and played a key role in guiding its overall direction and maintaining conceptual coherence. David Lyons, professor at Lebanon Valley College at the time, collaborated on the project together with his students Alexander J. Heilmann and Ezekiel W. Wertz. In addition to their general participation, they worked in particular on the analysis of continuous local stabilizers. Matej Pivoluska was a postdoctoral researcher at Masaryk University in Brno during the time of writing. Alongside his involvement in various aspects of the project, he contributed in particular to establishing the lower bound on the number of local equivalence classes. As first author, I was involved in all stages of the project. My primary responsibilities included implementing the code for the brute-force search over local equivalence classes and contributing to the definition and characterization of tensor-edged hypergraph states.

Finite-Function-Encoding Quantum States

Paul Appel[1,2], Alexander J. Heilman[3], Ezekiel W. Wertz[3], David W. Lyons[3], Marcus Huber[1,2], Matej Pivoluska[4,5], and Giuseppe Vitagliano[1,2]

[1]Atominstitut, Technische Universität Wien, Stadionallee 2, 1020 Vienna, Austria
[2]Institute for Quantum Optics and Quantum Information – IQOQI Vienna, Austrian Academy of Sciences, Boltzmanngasse 3, 1090 Vienna, Austria
[3]Mathematics and Physics, Lebanon Valley College, 101 North College Avenue, Annville, Pennsylvania, 17003, United States of America
[4] Institute of Computer Science, Masaryk University, Botanická 68a, 60200 Brno, Czech Republic
[5] Institute of Physics, Slovak Academy of Sciences, Dúbravská cesta 5807/9, 845 11 Karlova Ves, Slovakia

We introduce finite-function-encoding (FFE) states which encode arbitrary d-valued logic functions, i.e., multivariate functions over the ring of integers modulo d, and investigate some of their structural properties. We also point out some differences between polynomial and non-polynomial function encoding states: The former can be associated to graphical objects, that we dub tensor-edge hypergraphs (TEH), which are a generalization of hypergraphs with a tensor attached to each hyperedge encoding the coefficients of the different monomials. To complete the framework, we also introduce a notion of finite-function-encoding Pauli (FP) operators, which correspond to elements of what is known as the generalized symmetric group in mathematics. First, using this machinery, we study the stabilizer group associated to FFE states and observe how qu*d*it hypergraph states introduced in Ref. [1] admit stabilizers of a particularly simpler form. Afterwards, we investigate the classification of FFE states under local unitaries (LU), and, after showing the complexity of this problem, we focus on the case of bipartite states and especially on the classification under local FP operations (LFP). We find all LU and LFP classes for two qutrits and two ququarts and study several other special classes, pointing out the relation between maximally entangled FFE states and complex Butson-type Hadamard matrices. Our investigation showcases also the relation between the properties of FFE states, especially their LU classification, and the theory of finite rings over the integers.

1 Introduction

Higher-dimensional quantum systems have become a common research interest in many fields of quantum information theory. It has been shown that they exhibit potential advantages due to higher security of cryptography protocols [2–5], better key rates in QKD [6–8], reduced circuit complexity [9], improved quantum error correction [10] and magic state distillation [11, 12]. At the same time, the complexity of the geometry of high-dimensional quantum states makes a *general* treatment of states rapidly unfeasible. This warrants the search for subsets of states which are sufficiently complex to inherit the advantages of higher dimensional quantum systems, while at the same time are easily described. Identifying these sets is motivated by the fact that for many tasks only some states are useful, while most states are not [13]. Hypergraph states are a prominent example of such a useful set of states. Graph states and stabilizer states have become a central pillar of contemporary research into quantum information processing: appearing as underlying resources in measurement based quantum computation [14]; being of central importance to quantum algorithms [15]; and providing general insight into many body entanglement [16] and special instances of the marginal problem [17]. Hypergraph states [18] have received a lot of attention recently, from analytic Bell violations [19] to providing more general resources for quantum computation [20–22].

Paul Appel: paul.appel@gmail.com
David W. Lyons: lyons@lvc.edu
Marcus Huber: marcus.huber@tuwien.ac.at
Matej Pivoluska: pivoluskamatej@gmail.com
Giuseppe Vitagliano: giuseppe.vitagliano@gmail.com

Qu*b*it hypergraph states can be seen as an encoding of Boolean functions into the relative phases of many-qubit quantum states [18, 23, 24].

In this work, we focus on this encoding and provide a framework to encode higher valued logical functions in higher dimensional quantum states. For simplicity, we will call these functions *finite functions* and the states *finite function encoding (FFE) states,* respectively. This approach turns out to be more general than trying to generalize graphs to higher dimensions, i.e., only a subset of functions, namely polynomial functions, can be associated to a graph, i.e., a pair of a set of vertices and a set of edges. Note, that we use "graph" to mean the general object and *not* simple graphs, which is often done in physics.

Let us now discuss two potential applications of the framework: the investigation of higher dimensional algorithms and the potential to compress quantum circuits. The encoding of Boolean functions in quantum states is one of the main ingredients in ground-breaking qubit quantum algorithms by Deutsch and Jozsa [25] and Grover [26]. Our idea is that encoding higher dimensional finite functions into larger a Hilbert space could be harnessed for the improved efficiency of quantum algorithms, just as the intrinsic dimensionality of photon entanglement can be harnessed for improved communication [7, 8, 27, 28]. Furthermore, higher-dimensional logic might prove to have an additional advantage in actual implementations of quantum algorithms thanks to its intrinsically higher expressivity—using higher dimensional Hilbert spaces allows us to encode multiple logical qubits used in a quantum circuit into a single physical system, thus reducing the number of non-local gates a quantum computer has to perform. This reduction in the number of non-local operations is highly desirable, since they still pose a fundamental challenge in practical implementations of quantum computation: In the quantum case each two-qubit gate represents an entangling operation, which is still the fundamental challenge in practical quantum computation and therefore cannot be considered a negligibly cheap resource. Using higher dimensional logic, many of the two-qubit gates could in principle be replaced by local gates acting on higher-dimensional quantum systems, which has a potential to greatly simplify the actual implementations using the practical quantum processors of the NISQ era. It is for this reason that first investigations have been started into higher-dimensional quantum computation [29, 30].

While there are many more potential applications, we are first interested in providing the underlying framework itself. To that end, we define the finite-function-encoding (FFE) states in section 2 and introduce a group of finite-function-encoding Pauli (FP) operators (section 2.1), which in turn are used to develop a stabilizer formalism for the FFE states (section 2.2). The structure of these stabilizers is unsurprisingly more complicated than the one for qudit hypergraph states introduced in Ref.[1]: Only a subset of FFE states, namely those with stabilizers that can be decomposed as products of operators that commute, are related to the qudit hypergraph states. In section 3, we discuss the intricacies of associating graphs to functions. First, from the fact that in non-prime dimensions not every finite function is a polynomial function, we observe that *only* polynomial functions can be associated to graphs. Next, we discuss how polynomials are encoded into graphs, and we define a new graph, the tensor-edge hypergraph (TEH), to encode arbitrary polynomials. Finally, we discuss, how these TEHs are a generalization of the previously defined qudit hypergraphs [1]. In section 4 we investigate the equivalence of FFE states under local operations, namely the previously defined finite-function-encoding Pauli operators and more general unitary operations. First, we give a bound on the number of equivalence classes under local finite-function-encoding Pauli (LFP) operations, which shows that the number of classes becomes rapidly unfeasible to compute both with increasing local dimension and number of parties involved. We then focus on the bipartite scenario and give a full LFP and local unitary (LU) classification for dimensions $d = 3, 4$ and find partial results for dimension $d = 6$. We observe that bipartite maximally entangled FFE states are closely related to complex Hadamard matrices of Butson type [31]. Using the theory of Hadamard matrices, we are able to identify several entanglement classes of FFE states and make a partial classification of states with low Schmidt rank, focusing on states which are maximally entangled in lower-dimensional subspaces.

2 Definition of Finite-Function-Encoding quantum states

Motivation for this work begins with the observation that n-qubit quantum graph and hypergraph states naturally encode Boolean functions [18, 23, 24]. This motivates a generalization to encode multi-valued logical functions, which we call finite functions for brevity, in the phase of multi-qudit states of arbitrary local Hilbert space dimension d. At first glance, this generalization looks straightforward: A uni-variate Boolean function f_2 takes inputs from the set $\{0, 1\}$ and maps to itself, i.e., $f_2 \colon \{0, 1\} \to \{0, 1\}$, while a uni-variate multi-valued logical function f_d is the map $f_d \colon \{0, \ldots, d-1\} \to \{0, \ldots, d-1\}$. However,

the underlying structure of these sets is different: Whenever d is prime, the set $\{0,\dots,d-1\}$ together with addition and multiplication modulo d is a *finite field* $\mathbb{F}_d$, when d is non-prime it is the *ring of integers modulo d*, denoted $\mathbb{Z}_d$. The main difference to finite fields is that in rings *not every* element has a multiplicative inverse, which has some profound implications, i.a., for the possibility to express a function f_d as a polynomial. Before we discuss the polynomiality of functions f_d further, let us first understand how they are encoded into quantum states. An intuitive way to think about finite functions f_d is by representing every function uniquely by the tuple of its image, i.e., $f_d \leftrightarrow (f(0), f(1), \dots, f(d-1))$. This tuple is then encoded in a quantum state $|f_d\rangle$ by associating the phase of a computational basis element labeled $|i\rangle$ with $f_d(i)$; $|f_d\rangle = (\omega_d)^{f(0)}|0\rangle + (\omega_d)^{f(1)}|1\rangle + \cdots + \omega_d^{f(d-1)}|d-1\rangle$, where $\omega_d = e^{2\pi i/d}$ is the d-th principal complex root of unity. However, encoding uni-variate functions corresponds only to local quantum states. More interesting are the n-partite quantum states with local dimension d, which encode n-variate d-valued finite functions $f_d : \mathbb{Z}_d^n \to \mathbb{Z}_d$. Again, we can identify the function f_d with its image as $f_d \leftrightarrow (f_d(\mathbf{e}))_{\forall \mathbf{e}\in\mathbb{Z}_d^n}$ and proceed to identify the image with a pure quantum state.

$$|f_d\rangle = \frac{1}{\sqrt{d^n}} \sum_{\mathbf{x}\in\mathbb{Z}_d^n} \omega_d^{f_d(\mathbf{x})} |\mathbf{x}\rangle\,, \tag{1}$$

where $\omega_d = e^{2\pi i/d}$ is again the d-th principal complex root of unity. To simplify the notation, we will drop the subscript of ω_d and f_d whenever the local dimension is clear from the context. We call these states *finite-function-encoding* (FFE) states.

2.1 Finite-Function-Encoding Pauli Operations

Let us now define two sets of operators which together we call *finite-function-encoding* Pauli (FP) operators: Given a function $h\colon (\mathbb{Z}_d)^n \to \mathbb{Z}_d$, we will write Z_h to denote the diagonal operator

$$Z_h = \sum_{\mathbf{x}\in(\mathbb{Z}_d)^n} \omega_d^{h(\mathbf{x})} |\mathbf{x}\rangle\langle\mathbf{x}|\,. \tag{2}$$

The ordinary 1-qubit Pauli Z operator is the special case for $h\colon \mathbb{F}_2 \to \mathbb{F}_2$ given by $h(0) = 0, h(1) = 1$. Note, that the sum of two functions is represented by the product of respective function-encoding Z operators, i.e., $Z_{f+g} = Z_f Z_g$. Similarly, by applying a Z_f gate to a FFE state $|g\rangle$ one obtains

$$Z_f |g\rangle = |f+g\rangle\,.$$

Now let us define the *finite-function-encoding Pauli X* operations. In this case, since we want a unitary operation, we have to consider only the permutations and associate a X-type operator to each of them. Given a permutation $\pi \in \mathrm{Sym}(\mathbb{Z}_d^n)$, where $\mathrm{Sym}(\mathbb{Z}_d^n)$ is the symmetric group over $\mathbb{Z}_d^n$, we will write X_π for the operator

$$X_\pi = \sum_{\mathbf{x}\in\mathbb{Z}_d^n} |\pi(\mathbf{x})\rangle\langle\mathbf{x}|\,, \tag{3}$$

The ordinary d-dimensional Pauli X operator is obtained in the case $\pi = \kappa^+$, where

$$\kappa^+\colon k \mapsto k+1 \pmod d, \tag{4}$$

is a d-cycle. We will write $\pi_i\colon \mathbb{Z}_d^n \to \mathbb{Z}_d^n$ to denote the permutation π acting on the ith variable, i.e., $\pi_i(\mathbf{x}) := (x_1, x_2, \dots, \pi(x_i), \dots, x_n)$ and we write X_{π_i} to denote the corresponding (local) operator acting on the i-th qudit of a n-qudit state.

The action of a finite-function-encoding Pauli X_π operator on the FFE state $|f\rangle$ is

$$X_\pi |f\rangle = \frac{1}{\sqrt{d^n}} \sum_{\mathbf{x}} \omega_d^{f(\mathbf{x})} |\pi(\mathbf{x})\rangle = \frac{1}{\sqrt{d^n}} \sum_{\pi^{-1}(\mathbf{y})} \omega_d^{f(\pi^{-1}(\mathbf{y}))} |\mathbf{y}\rangle = \frac{1}{\sqrt{d^n}} \sum_{\mathbf{y}} \omega_d^{f(\pi^{-1}(\mathbf{y}))} |\mathbf{y}\rangle\,, \tag{5}$$

where the sum over $\mathbf{x} := \pi^{-1}(\mathbf{y})$ is the same as the sum over $\mathbf{y}$, since π is a permutation.

We call the group generated by X_π and Z_h operators the *finite-function-encoding Pauli (FP) group*; in mathematical literature, this group is called the *generalized symmetric group*. The FP group is not Abelian: the multiplication rules and commutation relations between these operators are given by

$$Z_f Z_g = Z_g Z_f = Z_{f+g} \tag{6a}$$

$$X_\pi X_\sigma = X_{\pi\circ\sigma} \tag{6b}$$

$$X_\pi Z_{h\circ\pi} = Z_h X_\pi \tag{6c}$$

At the single-particle level, we call the corresponding group the *Local finite-function-encoding Pauli (LFP) group*, i.e., the group generated by X_π and Z_h for single variable functions h. The LFP group is also a non-commutative group with similar commutation relations as Eq. (6) and is a generalization of the Heisenberg-Weyl group of single qudits.

2.2 Stabilizers of FFE States

In this section, we construct stabilizers for FFE states. In particular, we make use of finite-function-encoding Pauli operations to generalize the Pauli stabilizer formalism for hypergraph states [1, 18]. We present a construction of a stabilizer set that uniquely determines an arbitrary FFE state, and we show that a property called *internal commutativity* is satisfied if and only if the FFE state can be obtained with local finite-function-encoding Pauli operations from the qudit hypergraph states defined in Ref. [1].

Recall that graph states are determined by a discrete Abelian group of local Pauli operators, generated by $X_i \bigotimes_{j\neq i} Z_j$, where X_i and Z_j are local operators acting on the i-th and j-th subsystem. Hypergraph states are also determined by an Abelian discrete group of stabilizers of a similar form, but this time, with controlled-Z operators, which are no longer local [1, 18], but still commute with the X operators. Here, we show that FFE states are also determined by Abelian groups of operators having a similar form, but in general the finite-function-encoding Pauli Z operators will not commute with the X operators. The latter *internal commutativity*, as we are going to prove, is satisfied only for a special class of FFE states, that are LFP equivalent to the qudit hypergraph states.

Given a function $f\colon \mathbb{Z}_d^n \to \mathbb{Z}_d$ and a n-$d$it permutation $\pi\colon \mathbb{Z}_d^n \to \mathbb{Z}_d^n$, let $S_{f,\pi}$ denote the operator

$$S_{f,\pi} = X_\pi Z_{f\circ\pi - f}. \tag{7}$$

It is straightforward to check that $S_{f,\pi}$ stabilizes $|f\rangle$, that is

$$S_{f,\pi}\,|f\rangle = |f\rangle\,.$$

For a fixed f, these $(d^n)!$ operators $S_{f,\pi}$ (over all $(d^n)!$ permutations π of n-$d$its) constitute the FP stabilizer group of $|f\rangle$. This group is not Abelian, but it has some useful Abelian subgroups. In particular, we will show that there is an Abelian subgroup of FP stabilizers with the property that the FFE state from which they are constructed is the unique simultaneous $+1$-eigenstate of the set of n generators of the subgroup. It is easy to see that $S_{f,\pi}$ and $S_{f,\sigma}$ commute whenever π and σ commute. In particular, $S_{f,\pi_i}, S_{f,\sigma_j}$, where the permutations act on different qudits always commute. If we fix an arbitrary d-cycle κ_i for each subsystem i, the set of operators $\{S_{f,\kappa_i}\}_{i=1}^n$ uniquely determines $|f\rangle$, among all n-qudit states, as their simultaneous $+1$-eigenstate.

Proposition 1. *The state $|f\rangle$ is the unique simultaneous $+1$-eigenvector of the set of n FP operators $\{S_{f,\kappa_i}\colon 1 \le i \le n\}$, where for each i, κ_i is a d-cycle.*

The proof can be found in Appendix B. In the above construction, the choice of the d-cycles κ_i is left free.

Now, we are interested in another property of the stabilizers: *internal commutativity*. In other words, we are interested to find a set of stabilizing operators that determine a state $|f\rangle$ uniquely and also *internally commute*, i.e., $X_{\kappa_i} Z_{f\circ\kappa_i - f} = Z_{f\circ\kappa_i - f} X_{\kappa_i}\ \forall i$. This will be done by looking at the previous construction and studying which functions give rise to internally commuting stabilizing operators:

Lemma 1. *Let κ be a d-cycle. Then $X_{\kappa_i} Z_h = Z_h X_{\kappa_i}$ if and only if $h(\mathbf{x})$ does not depend on the value of x_i.*

Proof. From the general commutativity relation (6c) we have,

$$X_{\kappa_i} Z_h = Z_h X_{\kappa_i} \iff h\circ\kappa_i(\mathbf{x}) = h(\mathbf{x}). \tag{8}$$

This implies

$$\forall c \in \mathbb{F}_d : h(x_1,\ldots,x_{i-1},c,x_{i+1},\ldots,x_n) = h(x_1,\ldots,x_{i-1},\kappa_i(c),x_{i+1},\ldots,x_n),$$

which, together with κ_i being a d-cycle, implies that h is independent of x_i. In particular, we have that X_{κ_i} and Z_h act non-trivially on the Hilbert spaces of different parties, and we can write their product in a tensor product form. ∎

Due to this, it turns out that internally commuting stabilizers exist only for a subset of functions:

Proposition 2. *Let $\{S_{f,\kappa_i}\}_{i=1}^n$ be a set of stabilizers which uniquely determines a state $|f\rangle$ and let the $\kappa_i = \pi_i^{-1}\kappa_i^+\pi_i$ be fixed d-cycles. The stabilizers $S_{f,\kappa_i} = X_{\kappa_i}Z_{f\circ\kappa_i - f}$ commute internally if and only if the function f can be written as*

$$f = f' \circ \pi_1 \circ \cdots \circ \pi_n, \tag{9}$$

where f' has degree at most 1 in each variable.

The proof can be found in the Appendix B. This result shows, that functions that have degree at most 1 in each variable indeed have a special property that is lost in the case of general FFE states. Those are precisely LFP (and hence LU) equivalent to the qudit hypergraph states defined in Ref. [1] (see also table 1 and the discussion above it). Thus, the latter have stabilizers with a simpler structure than those of general FFE states. Nevertheless, the above construction is still a direct generalization of the qubit stabilizers formalism and one can still recover a similar structure. For example, as an additional minor result we present in Appendix C a family of states having continuous unitary stabilizers, with a construction that generalizes that of Ref. [32, 33].

3 Definition of Tensor-Edge Hypergraph (TEH)

Now, let us return to polynomiality of the finite functions. As mentioned before, Boolean functions can be encoded in *graph* states. Thus, we find a mapping from Boolean functions to *simple* graphs. However, this mapping turns out *not* to hold for d-valued finite functions. In fact, the association to a graph is inherently connected to the polynomial representation of the function. While in $\mathbb{F}_d$ every function f_d can be represented by a polynomial, this is *not* the case in $\mathbb{Z}_d$. As an example, consider a function $f : \mathbb{Z}_4 \to \mathbb{Z}_4$ and its image $(0, 2, 0, 3)$. In order to find its polynomial representation, consider a polynomial over $\mathbb{Z}_4$, which can be in general written as $p(x) = c_0 + c_1x + c_2x^2 + c_3x^3$. Now, set $f(i) = p(i)$ to find the coefficients c_i:

$$\begin{aligned}
0 &= c_0 && \pmod 4\\
2 &= c_0 + c_1 + c_2 + c_3 && \pmod 4\\
0 &= c_0 + 2c_1 + 4c_2 + 8c_3 && \pmod 4\\
3 &= c_0 + 3c_1 + 9c_2 + 27c_3 && \pmod 4
\end{aligned}$$

A quick calculation shows that; $c_0 = 0, c_1 = 0, c_2 = 2 - c_3$ and finally $2c_3 = 1$. Clearly this last equation has no solution since 2 has no multiplicative inverse in $\mathbb{Z}_4$. Thus, there exist functions in $\mathbb{Z}_d$ which can *not* be represented by a polynomial. In this light, we will use term *polynomial functions* for functions which have a polynomial representation. Generally, the polynomial representation of polynomial functions is *not* unique. In fact, many equivalent polynomials can be chosen to represent the same polynomial function. The uniqueness of the polynomial representative can be recovered by choosing a suitable normal form of a polynomial, which typically restricts both the degree of the *monomials* and the value of the coefficients. Importantly, there exist polynomial normal forms for any $\mathbb{Z}_d$ and any number of variables n [34, 35]. Note, that graphs in general are not associated to the polynomial function directly, but to its polynomial representative. Thus, without picking a normal form, many equivalent graphs can be associated to a single state.

In finite fields, every function is a polynomial function and there exists a canonical normal form. Thus, a distinction of functions, polynomial functions and their polynomial representatives is unnecessary. However, in our case, the choice of normal form has a direct influence on the sparsity of the tensor we associate to the edges. We opt for a normal form which has many "local" monomials, i.e., terms whose corresponding state can be generated by local operations, and as few monomials present as possible. Our choice of normal form recovers the well known representation of polynomial functions for prime dimensions, i.e., the representation by polynomials with every variable of degree smaller than d, with coefficients as well smaller than d. However, for non-prime dimensions these restriction do not suffice. For a more detailed review of the normal form of polynomial functions over $\mathbb{Z}_d$ we employ see appendix A.

Remark 1. *Note, that it is possible to define a finite field as well for prime powers $d = p^k$. The construction for prime powers is slightly more complicated: The finite field is* not *equivalent to $\mathbb{Z}_{p^k}$, like in the prime case, but there exists a finite field with p^k elements unique up to isomorphism. We will not concern ourselves with these constructions in this work, since we are more interested to understand the*

structure of finite encoding functions, considering the difference between finite fields and rings of integers (mod d).

Before we continue our investigation of FFE states, we like to define a subset of these states which can be associated with a new kind of graph we call tensor-edge hypergraph (TEH). We observe that the association of a graph is directly connected to the polynomial representation of the finite function. Thus, we want to encode polynomials into graphs; where the graph is a pair $G = (V, E)$, with $V = \{1, 2, \ldots, n\}$ a set of vertices and E is a set of edges and a polynomial p is a function of the form $p(x_1, \ldots, x_n) = \sum_{i_1,\ldots,i_n} c_{i_1\ldots i_n} x_1^{i_1} \ldots x_n^{i_n}$, where each $x_1^{i_1} \ldots x_n^{i_n}$ is called a monomial. The main idea is to encode the variables in the vertices and the coefficients of each monomial in the edges. Starting with the simplest example, a bi-variate monomial, we explain the restrictions of this encoding and define increasingly more complex edges to encode more complex polynomials in them.

A given a polynomial p is encoded into a graph by identifying each variable with a vertex and each edge with a non-zero coefficient of a monomial. Consider the monomial $p(x_1, x_2) = x_1x_2$ This monomial is described by a *simple* graph, with a edge between two vertices. To see how this notion has to be expanded for more complex polynomials, let us consider another polynomial $p(x_1, x_2, x_3) = x_1x_2 + x_1x_2x_3$. Clearly, a simple graph does not suffice because of the second monomial in the polynomial. However, by simply allowing the edges to be n-tuples incorporates monomials with n variables. In this case, the graph is called a hypergraph and the edges are called hyperedges. Next, let us consider a polynomial of the form $p(x_1, x_2) = x_1x_2 + 2x_1x_2x_3$. Again, we have to adjust the definition of the edges to be able to describe the different values of the coefficients. To that end, a weight (or multiplicity) is added to each edge, that describes the coefficient of each monomial; these graphs are called weighed (hyper-)graphs. Finally, consider the polynomial $p(x_1, x_2) = x_1x_2 + x_1x_2^2$: To include monomials with higher exponents, again, the notion of the edge has to be extended. A tensor edge is a pair of a n-tuple of vertices α, and a n-th order tensor C^α describing the coefficients of the monomials composed of variables in α. Note, that the tensor will describe several monomials and not just a single one. Thus, we need to collect the monomials which have the same variables, e.g., for a polynomial $p(x_1, x_2, x_3) = x_1x_2 + x_1x_2^2 + x_1x_2x_3 + 2x_1^2x_2x_3$ we would group the first two and the latter two terms together. The monomials which are not present, i.e., their coefficient is zero, correspond to zero entries in the tensor. The physical motivation for this grouping is the fact that encoding monomials with the same set of variables with non-zero exponents requires interaction between the subsystems corresponding to these variables; see Remark 2. An illustrative example of these concepts is given in Figure 1.

With these *tensor-edge* hypergraphs we are finally able to encode arbitrary polynomials with $c_{0\ldots0} = 0$ into graphs. In the light of the encoding of quantum states, this restriction is irrelevant since the $c_{0\ldots0}$ corresponds to a global phase, i.e., $\omega^{p(\mathbf{x})} = \omega^{c_{0\ldots0}+p'(\mathbf{x})} = \omega^{c_{0\ldots0}}\omega^{p'(\mathbf{x})}$. Although we allow "local" edges, i.e., edges that encode monomials with only a single variable, we like to point out that these can be avoided by LFP operations in the context of encoding of quantum states. Let us give a *formal* definition of the tensor-edge hypergraphs. A n-vertex *tensor-edge hypergraph (TEH)* is a pair $G = (V, E)$, where $V = [n]$ is the set of vertices and E is a set of tensor edges. A tensor edge is a pair (α, C^α) where $\alpha \subset [n]$ and C^α is a tensor defined by grouping related monomials, i.e., we decompose a polynomial in the monomial basis as

$$p(\mathbf{x}) = \sum_{\mathbf{e}} c_{\mathbf{e}} \mathbf{x}^{\mathbf{e}} \tag{10}$$

for some coefficients $c_{\mathbf{e}} \in \mathbb{Z}_d$, $\mathbf{x} = (x_1, x_2, \ldots, x_n)$, $\mathbf{e} = (e_1, e_2, \ldots, e_n) \in \mathbb{Z}_d^n$ and $\mathbf{x}^{\mathbf{e}} := x_1^{e_1}, \ldots, x_n^{e_n}$.

Now, we can gather the terms in the monomial expansion (10) by terms that share the same variables with non-zero exponents. With this partitioning of terms, equation (10) becomes

$$p(\mathbf{x}) = \sum_{\alpha\subset[n]} \sum_{\substack{\mathbf{b}\in\mathbb{Z}_d^n:\\ \mathrm{supp}(\mathbf{b})=\alpha}} C_{\mathbf{b}}^{\alpha} \mathbf{x}^{\mathbf{b}} \tag{11}$$

where $[n] = \{1, 2, \ldots, n\}$ and we sum over all vectors with $\mathrm{supp}(\mathbf{b}) = \alpha$, i.e., all vectors which have support equal to α.

Clearly, TEHs are a generalization of simple graphs and hypergraphs. Table 1 gives a summary of how various classes of simple graphs, hypergraphs, and their generalizations, which we refer to collectively as graphs on n vertices, are special cases of TEHs. Likewise, quantum states corresponding to the various classes of graphs are special cases of TEH states. The table is organized by value of d and the following restrictions:

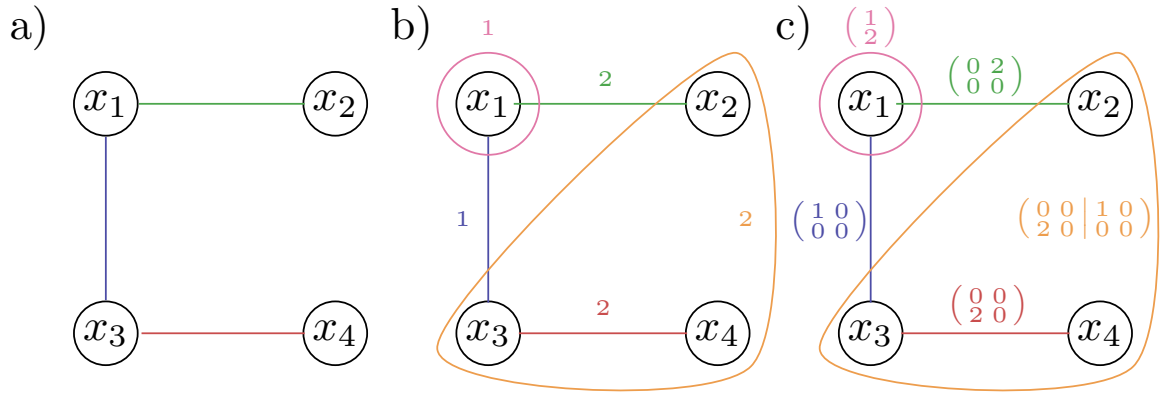

Figure 1: Here are examples of graphical representations of polynomial functions. Vertices correspond to variables of the depicted functions, (hyper-)edges differ based on the generality of description needed for a given function. a) A simple graph corresponding to a function $p(x_1, x_2, x_3, x_4) = x_1x_2+x_1x_3+x_3x_4$. Each monomial of $p(x_1, x_2, x_3, x_4)$ corresponds to an edge between vertices. b) A hypergraph corresponding to a function $p(x_1, x_2, x_3, x_4) = x_1+2x_1x_2+x_1x_3+2x_3x_4+2x_2x_3x_4$. Each monomial of $p(x_1, x_2, x_3, x_4)$ corresponds a hyperedge. The coefficients of each monomial are represented as weight associated to each hyperedge. c) A TEH state corresponding to $p(x_1, x_2, x_3, x_4) = x_1 + 2x_1^2+2x_1x_2^2+x_1x_3+2x_3^2x_4+2x_2^2x_3x_4 + x_2x_3x_4^2$. Here, multiple monomials of $p(x_1, x_2, x_3, x_4)$ can correspond to the same hyperedge, since the hyperedges capture only information about which variables are present in a single monomial. To also encode coefficients of the monomials present in $p(x_1, x_2, x_3, x_4)$ one needs to associate tensors C^α to each hyperedge α. Powers of each variable in monomial correspond to the list of indices in C^α, while its coefficient value corresponds to the value of the corresponding tensor element. Since the rank of the tensor depends on the number of nodes connected to the edge, in the case of the hyperedge connecting x_2, x_3 and x_4 (depicted in yellow), the corresponding tensor of rank 3 is represented as two matrices. The left matrix corresponds to monomials containing x_4, and the right matrix corresponds to monomials containing x_4^2.

(1) Even though $d > 2$, all variables in all monomials in p are limited to exponents $0, 1$.

(2) All monomials in the expansion of p have at most two variables with nonzero exponents.

graph/state type	restriction on d	restriction on p	references
TEH	none	none	(this paper)
qudit hypergraph	none	(1)	[1]
hypergraph	$d = 2$	none	[18, 33, 36]
qudit graph	none	(1) and (2)	[37, 38]
simple graph	$d = 2$	(2)	[14, 39]

Table 1: Comparison of various types of graphs and their generalizations and their corresponding quantum states.

Remark 2. *Using this monomial expansion, we can recreate the "simple" recipe analogous to hypergraph states to prepare these TEH states, i.e., we can give a modular preparation scheme. With this notation, the FFE state $|p\rangle$ that encodes the polynomial function $p = \sum_{\mathbf{e}} c_{\mathbf{e}}\mathbf{x}^{\mathbf{e}}$ can be also expanded in terms of monomial Z operators:*

$$|p\rangle = \frac{1}{\sqrt{d^n}} \sum_{\mathbf{x}\in(\mathbb{Z}_d)^n} \omega_d^{p(\mathbf{x})} |\mathbf{x}\rangle = Z_p |+\rangle^{\otimes n} = \left(\prod_{\mathbf{e}} (Z_{\mathbf{x}^{\mathbf{e}}})^{c_{\mathbf{e}}}\right) |+\rangle^{\otimes n}, \tag{12}$$

where $|+\rangle = \frac{1}{\sqrt{d}}(|0\rangle + |1\rangle + \cdots + |d-1\rangle)$ and $\mathbf{x}^{\mathbf{e}} = x_1^{e_1}x_2^{e_2}\cdots x_n^{e_n}$. We use the label $Z_{\mathbf{x}^{\mathbf{e}}}$ for the associated FP operation, which can be understood as a generalization of the qudit controlled-Z gate. Note, that the canonical qudit controlled-Z corresponds to monomials with $\mathbf{x}^{\mathbf{e}}$ with $\max(e_i) \leq 1$.

4 Local equivalence of Finite-Function-Encoding states

In this section, we investigate the equivalence of finite-function-encoding states under LU and LFP operations. Aside from the foundation's point of view, the question is important for understanding the potential of FFE states as resources for, e.g., quantum computation. Deciding whether multipartite quantum states are equivalent under local operations is one of the central questions of quantum information theory. It has been studied for different subsets of quantum states and operations. The most prominent example is the paradigm of local operations and classical communications (LOCC) [40–42], which is motivated by an operational perspective. A simpler problem is the classification under local unitary (LU) operations, which however is still relevant for characterizing resources for quantum computation. Note, that the problem of characterizing *all* LU equivalence classes is notoriously difficult, even when the set of states considered is very restricted [43, 44]. Already for the comparably simpler qubit hypergraph states a complete characterization of equivalence classes under local unitaries is an open problem[1], and thus relaxed problems are investigated, e.g., equivalence under the restricted set of local so-called Clifford unitaries, i.e., unitaries that map Pauli matrices into Pauli matrices [45]. Another example is that of k-uniform states [17, 46–49] , i.e., $n-$partite states with all k-party marginals maximally mixed, and their extremal case of so-called absolutely maximally entangled (AME) states [17, 46–48, 50, 51], (i.e. n-party $k-$uniform states with $k = \lfloor \frac{n}{2} \rfloor$). Given certain n and d, the classification of k-uniform states is a long-standing open problem. Besides even deciding whether such states exist for given n, d and k, it is also hard to decide whether, e.g., two AME states are LU inequivalent.

Here, in addition to equivalence under general LU operations, we study equivalence of FFE states under LFP operations, since these always map a FFE state into a FFE state. A similar classification problem arises in the theory of Hadamard matrices, where so-called Butson type Hadamard matrices, are classified up to operations that correspond to our LFP operations [31]. Note, that even this very restricted classification is known to be very complex [31, 52, 53]. First, we show that the problem of identifying all LFP equivalence classes becomes quickly infeasible with increasing dimension d as well as the number of parties n involved by bounding the number of equivalence classes $\ell_{d,n}$ from below. Second, we investigate in some detail the classification of bipartite states, where we give a full LFP and LU classification for prime dimension $d = 3$ and composite dimension $d = 4$. We observe, that LFP operations can transform TEH states into generic FFE states, i.e., they connect polynomial and non-polynomial function encoding non-trivially. Furthermore, we show that, in composite dimension, most of the equivalence classes do not contain a TEH state. Third, we identify all equivalence classes in $d = 6$ which contain a TEH state. These specific studies showcase once more the difficulty to give a *full* classification of local equivalences for FFE states. However, for many tasks a complete classification is not necessary and whether two *particular* states are locally equivalent is more relevant. Deciding whether two states are LFP equivalent is a far easier task than the general classification. However, a simple brute-force algorithm still needs $\mathcal{O}(d!^n)$ steps. In other words, even this simpler problem becomes infeasible already for a relatively small n and d. Still, this problem can be tackled with the help of LFP invariants, which we also discuss. This way, we can investigate the structure of certain particular classes of bipartite FFE states, which include maximally entangled states, and connect it to the theory of complex Hadamard matrices of Butson type.

4.1 The LFP classification problem

Here, we investigate the classification problem of FFE states under LFP operations. We give a lower bound on the number of equivalence classes, showcasing that a general classification becomes quickly infeasible with the dimension and the number of parties. Secondly, we introduce a set of LFP invariants which can aid in deciding if two particular states are non-equivalent under LFP operations.

4.1.1 A lower bound on the number of LFP classes

Before we investigate the local Pauli equivalence of FFE states, let us introduce some useful quantities. Recall that every finite function $f\colon \mathbb{Z}_d^n \to \mathbb{Z}_d$ is completely described by a tuple of its image, i.e. $f \leftrightarrow (f(\mathbf{e}))_{\mathbf{e}\in\mathbb{Z}_d^n}$. By giving this tuple some more structure we can define an *image* tensor M_f in the $\mathbb{Z}_d$-module $\mathbb{Z}_d^{\otimes n}$ (analogous of a vector space defined over the ring of integers $\mathbb{Z}_d$).

$$M_f = (f(e_1, \ldots, e_n))_{e_1,\ldots,e_n \in \mathbb{Z}_d} \tag{13}$$

[1] see https://oqp.iqoqi.univie.ac.at/local-equivalence-of-graph-states

This image tensor is intimately related to the coefficients of the FFE state: the state's coefficient tensor T_f is obtained by taking the *element wise* exponential function EXP

$$T_f = \mathrm{EXP}\left(\frac{2\pi i}{d} M_f\right). \tag{14}$$

Clearly, both M_f and T_f describe the state completely. To simplify the notation, we sometimes identify M_f with f when clear from the context. Let us now discuss how M_f and T_f are transformed under the action of a LFP operation: The action of a local X_π gate is a permutation of certain entries of M_f and T_f. However, since the permutation is local, only a subset of these entries can be changed. In fact, let us assume that a permutation acts on the first system, which exchanges the values of 0 and 1 and leaves other values unchanged. We find that in M_f, elements $f(0, e_2, \ldots, e_n)$ are exchanged with $f(1, e_2, \ldots, e_n)$, while all e_i stay the same. From this, we can easily generalize and see that a local X_π operation acts as a permutation of rows, or columns both in M_f and T_f if they are matrices, i.e., in case of $n = 2$, and as a permutation of their higher-dimensional counterparts if they are higher-order tensors. A Z_h operation is *local* if the function $h(x_1, \ldots, x_n)$ is univariate. For example, consider Z_h acting on a first qudit only, this means that it transforms $f(0, e_2, \ldots, e_n)$ to $f(0, e_2, \ldots, e_n) + h(0)$, $f(1, e_2, \ldots, e_n)$ to $f(1, e_2, \ldots, e_n) + h(1)$ and so forth. In terms of M_f this means that we add a constant term to certain rows or columns or their higher-dimensional counterparts. For T_f this translates into multiplication of the corresponding rows and columns by constant phases. Note, that these operations are a subset of operations which define equivalence classes of complex Hadamard matrices [31]. In fact, we can define a normal form under LFP similarly as in Hadamard matrix theory, where the coefficient tensor of the state is such that

$$(T_f)_{i_1,0,\ldots,0} = (T_f)_{0,i_2,\ldots,0} = \cdots = (T_f)_{0,\ldots,0,i_n} = 1. \tag{15}$$

Following the terminology of Hadamard matrices, we call this normal form *dephased*. In the case of $n = 2$ we call the submatrix $(T_f)_{i_1,i_2}$ for $i_1, i_2 \in \{1, \ldots, d-1\}$ the *core*. Clearly, every FFE state can be transformed into its dephased form by a set of *unique* local Z_h operations. Thus, requiring that the state is in its dephased form fixes the local Z_h operation. However, this leaves the ambiguity on the X_π operations, i.e., there is not a single unique normal form. Furthermore, although making permutations of the non-zero entries of the normal form leads to LFP equivalent states, one can also permute the T_f out of the dephased form and then return to it with a different Z_h operation, leading potentially to a new LFP equivalent state. Thus, to find all states LFP equivalent to a given state, e.g., in the case $n = 2$ where T_f is a matrix, we have to scan all permutations of rows and columns, and then apply the corresponding Z_h operations to bring the state back into the dephased form. Using these simple preliminary observations, we can derive a conceptually-simple algorithm to find the orbits of states under LFP operations. Starting from a dephased state, we can apply permutations followed by a return to the dephased form. Once, all permutations have been applied, all equivalent states are found. Unfortunately, the number of permutations increases rapidly with d and n: a rough estimate of the complexity of the algorithm is $\mathcal{O}((d!)^n)$. Because of this inherent complexity, the method becomes infeasible already for very small values of d and n. However, we are able to use it in order to divide all 3^9 bipartite qutrit FFE states into 9 LFP equivalence classes and all 4^{16} bipartite ququart FFE states into 807 LFP classes, which are described in detail in Appendix G.

Furthermore, this method provides a lower bound on the number of LFP classes of n-partite FFE states in dimension d, since it gives an upper bound on the number of states in each LFP class.

Proposition 3. *A lower bound on the number of LFP equivalence classes $\ell_{d,n}$ for a n-partite qudit FFE state is*

$$\ell_{d,n} \geq \left\lceil \frac{d^{d^n - n(d-1) - 1}}{(d!)^n} \right\rceil \tag{16}$$

Proof. As calculated above, each normalized LFP class can have at most $(d!)^n$ states, together with the fact that there are $d^{d^n - n(d-1) - 1}$ dephased n partite d dimensional states gives the lower bound on the number of classes. ∎

This is not a tight bound, as the size of the classes is typically much smaller than $(d!)^n$. The case studies with $n = 2$ and $d = 3, 4$ confirm this. Our lower bounds evaluate to $\ell_{3,2} \geq 3$ and $\ell_{4,2} \geq 456$, while the real number of classes are $\ell_{3,2} = 9$ and $\ell_{4,2} = 807$. The bound is useful to demonstrate that increasing the value of either d or n deems the full characterization impractical, as $\ell_{5,2} \geq 10596382$ and $\ell_{3,3} \geq 16142521$.

4.1.2 Invariants under LFP unitaries

With a different approach, one can look for functions of T_f or M_f, which are invariant under the action of LFP operations, to provide sufficient criteria for LFP inequivalence of particular states. Thus, given two FFE states, such invariants can be helpful in deciding whether they are *not equivalent*.

As a simple example of an LFP invariant, let us consider the sum of all elements of the image tensor M_f:

$$S(f) = \sum_{x_1,\ldots,x_n} f(x_1,\ldots,x_n) \mod d. \tag{17}$$

The LFP invariance of $S(f)$ can be easily proven by considering that X-type operations only change the order of summation and Z-type operations acting on variable x_i change $S(f)$ to $S(f+h) = S(f) + S(h)$, with $h(\mathbf{x})$ a univariable function of an arbitrary variable x_i. Furthermore, $S(h) = 0 \mod d$, since for each $k \in \{0,\ldots,d-1\}$ images $h(x_1,\ldots,x_{i-1},k,x_{i+1},\ldots,x_n)$ have the same value for all $x_1,\ldots,x_{i-1},x_{i+1},\ldots,x_n \in \{0,\ldots,d-1\}$. This means that $S(h)$ can be written as $d^{n-1}\sum_{k\in\{0,\ldots,d-1\}} h(0,\ldots,0,k,0,\ldots,0)$, which is equal to 0 modulo d.

A more elaborate LFP invariant can be defined using a set of certain sums in the following way. First one chooses an index j and splits $S(f)$ into d sums, $S_{x_j=k}(f)$, one for each possible value $k \in \{0,\ldots,d-1\}$. Then, one considers the set of all such sums indexed by j, which is also invariant under LFPs. Formally, for each index $j \in \{1,\ldots,n\}$, we define the sets

$$I_j := \{S_{x_j=k}(f)\}_{k=0}^{d-1}, \tag{18}$$

where

$$S_{x_j=k}(f) = \sum_{\forall i\neq j, x_i=0}^{d-1} f(x_1,\ldots,x_{j-1},k,x_{j+1},\ldots,x_n). \tag{19}$$

Again, for each index j, the set I_j above is invariant under LFP operations. Similarly to $S(f)$ one can see that X-type operations on variable x_i, where $i \neq j$ only change the order of summands in each partial sum $S_{x_j=k}(f)$, while X-type operation on x_j exchanges some $S_{x_j=k}(f)$ with $S_{x_j=k'}(f)$ within the set I_j. Concerning Z-type operations, one can use a similar argument as in the case of $S(f)$ and conclude that for each k and j the partial sum $S_{x_j=k}(f)$ after a Z-type LFP operation can be calculated as $S_{x_i=k}(f+h)$, where h is univariate and thus $S_{x_i=k}(h) = 0 \mod d$. Note, that for bipartite systems (which is the application we consider below) M_f is a matrix and correspondingly the invariant $S(f)$ is just the sum of all matrix elements, the invariant set I_0 contains sums of all elements in each matrix row, while I_1 contains sums of all elements in each matrix column. Note that also in the theory of Hadamard matrices a similar invariant set has been defined (cf. Eq. (34) in Appendix D) and has been very helpful to distinguish equivalence classes [54] (see also Appendix D).

4.2 Local unitary equivalence of bipartite FFE states

Now we focus our attention on the easiest non-trivial case, i.e, the bipartite scenario. Two bipartite pure states are locally unitary equivalent, if and only if they have the same Schmidt decomposition, which can be obtained by performing a singular value decomposition of their coefficient matrices [40]. The singular value decomposition allows for a simple algorithm to decide whether two FFE states are LU equivalent, and it can also provide a witness of LFP inequivalence. The converse is not true, and in fact we can explicitly observe that there are states that are LU equivalent but not LFP equivalent. For example, matrix transposition and complex conjugation on T_f do not change the LU class, but sometimes map states into two different LFP classes.

Remark 3. *A bipartite d-dimensional FFE states represented by coefficient matrices T_f, T_f^T and T_f^* are locally unitary equivalent, since they have all the same singular value decomposition.*

In the following, we investigate LFP equivalence for small dimensions and in particular the structure of the maximally entangled FFE states, identify states with maximally entangled subspaces and finally give a full characterization of LFP and LU equivalence for dimension $d = 3, 4$ while characterizing all TEH states in $d = 6$.

4.2.1 Maximally entangled states

For general dimensions, we can start by looking at bipartite maximally entangled states. This is on the one hand interesting for potential practical applications of FFE states, and on the other hand it elucidates the difficulties of fully describing LFP classes of FFE states. Let us introduce some language: A $d \times d$ square matrix is called a *Butson type* Hadamard matrix $H(d,q)$ if $HH^\dagger = d\mathbb{1}_d$ where all elements are q-th roots of unity and $\mathbb{1}_d$ is the identity matrix in dimension d. Then, let us recall that a bipartite pure state is maximally entangled whenever the marginals are maximally mixed. In our case, this means that a FFE state $|f\rangle$ is maximally entangled whenever $\frac{1}{d}\sum_{k=0}^{d-1}\omega_d^{f(k,i)-f(k,j)} = \delta_{i,j}$, where $\delta_{i,j}$ is the Kronecker delta. In other words, the (unnormalized) coefficient matrix of the state is unitary, i.e., $dT_f T_f^\dagger = \mathbb{1}_d$ holds. Thus, maximally entangled FFE states correspond to Hadamard matrices, and more specifically to those of type $H(d,d)$. An exemplary maximally entangled FFE state is precisely a traditional bipartite qudit graph state, namely the state that encodes the function $f_d(x,y) = xy$. In this case, the coefficient matrix of the state is the finite Fourier transform F_d. Furthermore, all states obtained by applying LFP operations to the $f_d(x,y) = xy$ are also maximally entangled. In fact, Hadamard matrices themselves are also classified up to rows and columns permutations and multiplication by a diagonal matrix of complex phases. From the point of view of finite functions, we see that in particular we can compose the above monomial as $\pi_1(x)\pi_2(y)$ with arbitrary permutations and still get a maximally entangled FFE state.

From the known results on complex Hadamard matrices, we are able to provide a characterization of the maximally entangled FFE states for low dimensions. We also observe that a full characterization for arbitrary d cannot be given in simple terms, since the characterization of complex $H(d,d)$ matrices remains, despite decades of efforts, an open problem. So far, full characterization is given for $d = 4$ and for (small) prime dimensions $p \leq 17$. For those prime dimensions, it is known that the Fourier transform matrix represents the unique LFP class (corresponding to maximally entangled FFE states in our language [53]).

The cases $d = 4$ and $d = 6$ are also instructive to report, since they are useful to clarify to some extent the additional structure that arises for composite dimensions. For the case $d = 4$, all Hadamard matrices of type $H(4,4)$ are well classified, and it is known that there exists a single continuous 1-parameter family of them [31] (see also Appendix D). To fit in our definition of FFE states, we additionally require the entries to be only 4-th root of unity, and making this additional restriction results in having exactly 2 LFP inequivalent maximally entangled FFE states, which we label as $|f_4\rangle$ and $|f_{2\times 2}\rangle$, because the two corresponding coefficient matrices are respectively $\frac{1}{4}F_4$ and $\frac{1}{4}F_2 \otimes F_2$. Additionally, we can ask whether both those matrices have representative polynomial functions $p_f : \mathbb{Z}_4^2 \to \mathbb{Z}_4$, and it turns out that this is the case. The two functions are $f_4 = xy$, and $f_{2\times 2} = xy^2 + x^2y + 2xy$. See also Table 4.

It is interesting to notice that these two TEH states are LU equivalent, but not connected by any of the unitary transformations mentioned in Remark 3. This follows from the fact, that there are two LFP inequivalent Hadamards of type $H(4,4)$, and the simple observation that $F_4 = (F_2 \otimes F_2)(F_2 \otimes F_2)^\dagger F_4$. Thus, we can see that

$$|f_4\rangle = \mathbb{1}_4 \otimes \left[F_4^T (F_2 \otimes F_2)^*\right] |f_{2\times 2}\rangle\,, \tag{20}$$

which means that two TEH states belonging to different LFP classes are connected by a particular local unitary, coming from a product of Hadamard matrices. At the level of the coefficient matrices, it can be seen (cf. Eq. (31) in Appendix D) that the operation connecting the two LFP classes is a Hadamard product with a particular matrix. After making this simple observation, we can further notice that the same local unitary above maps other LFP inequivalent FFE states into each other. See also the results of our brute-force calculations in $d = 4$ afterwards.

For $d = 6$ the theory of Hadamard matrices becomes already extremely complicated and not all $H(6,6)$ matrices are known. For example, analogously to $d = 4$, a continuous family is known which includes F_6 and $F_3 \otimes F_2$. These two matrices are however, contrary to the analogous $d = 4$ case, LFP equivalent [52]. It is also curious to observe that the state with the coefficient matrix $\frac{1}{6}F_3 \otimes F_2$ is not a TEH state. In other words, the corresponding function $f_{3\times 2}$ (cf. Eq. (33)) is not a polynomial. This can be observed by direct interpolation or also by listing all polynomials $p_f : \mathbb{Z}_6^2 \to \mathbb{Z}_6$ (see Table 5). It is also interesting to observe that there is a special matrix $S_6 \in H(6,6)$ which does not belong to any continuous family and is also connected to other mathematical problems [2]. The function s_6 (cf. Eq. (33)) is also not a polynomial. In fact, we can see from Table 5 that the only TEH maximally entangled state has a coefficient matrix given by $\frac{1}{6}F_6$. As in the $d = 4$ case, we can construct local unitaries that map FFE states in different LFP classes into each other. In this case $(F_3 \otimes F_2)^\dagger F_6$ does not work since $|f_6\rangle$

[2] It was in fact found by Tao in relation to the so-called Fuglede's conjecture. See Ref. [55] for further details.

and $|f_{3\times 2}\rangle$ are in the same LFP class [52]. However, for example the following local unitary mappings

$$\begin{aligned} |s_6\rangle =& \mathbb{1}_6 \otimes \left[S_6^T (F_3 \otimes F_2)^*\right] |f_{3\times 2}\rangle \\ |s_6\rangle =& \mathbb{1}_6 \otimes S_6^T F_6^* \, |f_6\rangle \end{aligned} \tag{21}$$

do the job, since $|f_{3,2}\rangle$ and $|s_6\rangle$ are in different LFP classes and so are $|f_6\rangle$ and $|s_6\rangle$. To conclude this discussion, we refer to [31, 53] and references therein for further details about Butson type Hadamard matrices [3].

4.2.2 States with low Schmidt rank

Let us now focus on LFP classes with lower Schmidt rank. A natural question is whether it is possible to find bipartite states of dimension d that have Schmidt rank r and are maximally entangled in a subspace of dimension r. In the case that r divides d, it is easy to see that this is true by making a constructive proof that uses: (i) if $d = k \cdot r$ we can see the d-dimensional system is composed of a k and a r-dimensional part; (ii) a r-th complex root of unity is also a d-th root of unity. Then, one example of states with the required properties are those with coefficient matrices proportional to $F_r \otimes J_k$ and $J_k \otimes F_r$ respectively, where J_k is the k-dimensional matrix with every coefficient equal to 1. Building upon this idea, we can make a more general construction, that actually enables us to find several LU classes with non-maximal Schmidt rank. A first simple observation is the following:

Lemma 2. *FFE states with Schmidt rank smaller than r can be obtained from representative functions of the type*

$$f_r(x, y) = g_A(x) g_B(y), \tag{22}$$

where either g_A or g_B is a function with only r distinct outputs.

Proof. Let us fix the function g_A to have r distinct outputs. Then, we have that the coefficient matrix T_f has at most r distinct rows. Thus, the rank of $T_f T_f^\dagger$ can be at most r, which is also the rank of the single-particle reduced density matrix of $|f_r\rangle$. ∎

It is interesting to study more details on the LU and LFP classification in the case of $f_r(x, y)$ given by Eq. (22) with, say, g_A having r outputs and g_B having d outputs. In this case, it is always possible to map the state to another one such that $g_B(y) = y$ using LFP unitaries. Then, the coefficient matrix becomes proportional to a so-called *Vandermonde matrix*, which makes it easier to partially characterize the LU classification of the corresponding FFE states. We make some observations in the following, corroborated by the discussion in Appendix E.

Lemma 3. *The state $|f_r\rangle$ corresponding to a function $f_r(x, y)$ as in Eq. (22) with g_B having d distinct outputs has exactly Schmidt rank r. In the case of r being a divisor of d and each of the different r outputs of f_r appearing exactly d/r times, $|f_r\rangle$ is maximally entangled in a r-dimensional subspace.*

Proof. See Appendix E. ∎

This construction uses precisely the ideas outlined above. In general, there are several $d \times d$ FFE states maximally entangled in a r-dimensional subspace whenever r divides d. Obviously, all of them will be in the same LU class, but they can be in different LFP classes. In fact, some LFP classes can be distinguished by the invariant set (18): For example, if we consider odd dimensions d and take a function of the form $f(x, y) = g_A(x)y$ and we sum over the column index we get always zero, i.e., $I_1(f) = \{0, \ldots, 0\}$, while if we take the "transposed" function $f^T(x, y) = x g_A(y)$ we get that $I_1(f^T)$ contains nonzero elements whenever $\sum_y g_A(y) \neq 0$. Another natural question is whether (and for which d) we can find some $|f_r\rangle$ that are also represented by a polynomial function. The answer is that at least one canonical rank-r maximally entangled TEH state always exists, as we observe in the following:

Proposition 4. *Bipartite TEH states of dimension $d \times d$ that have Schmidt rank r and are maximally entangled in a r-dimensional subspace exist whenever r divides d. One example is given by the state $|m_{d/r}\rangle$, where*

$$m_{d/r}(x, y) = \frac{d}{r} xy. \tag{23}$$

[3] See also https://chaos.if.uj.edu.pl/~karol/hadamard/ and https://wiki.aalto.fi/display/Butson/Butson+Home for an up-to-date catalog of complex Hadamard matrices

Proof. The function $m_{d/r}(x,y)$ is a product of $g_A(x) = \frac{d}{r}x$ and $g_B(y) = y$, where g_A has its outputs as the element of the subgroup $\mathbb{Z}_r \subset \mathbb{Z}_d$, i.e., it is an r-output function with each output appearing exactly d/r times, due to the cyclicity of the function. The statement then follows directly from Lemma 3. ∎

Note that the coefficient matrix of $|m_{d/r}\rangle$ given above is precisely $T_{d/r} = \frac{1}{d}F_r \otimes J_{d/r}$, which can be seen as the canonical form under LFP. Examples of such states for $d = 6$ are given in Table 5.

The particular case of $d = p^m$ being a prime power with $m > 1$ is also special from the point of view of entanglement classes of FFE states. In that case, we can write any integer in $x \in \{0, \ldots, d-1\}$ in its p-ary expansion as $x = a_0 p^0 + \cdots + a_{m-1}p^{m-1}$, i.e., we can write any d-it as a m-tuple of p-its: $x \equiv (a_0, \ldots, a_{m-1}) := \mathbf{a}$, where the a_j's are in $\mathbb{Z}_p$. Correspondingly, the single d-dimensional Hilbert space associated to x can be viewed as a multi-qu$p$it space, i.e., as a tensor product $\mathcal{H}_p^{\otimes m}$, where $\mathcal{H}_p$ are p-dimensional. In turn, this fictitious multipartite structure leads to more richness also in the entanglement classes of FFE states. For example, we can observe in the following that more possibilities exist to construct TEH states that have Schmidt rank $r < d$ and are maximally entangled in the corresponding r-dimensional subspace.

Proposition 5. *When $d = p^m$ with $m > 1$, states associated to the functions*

$$\begin{aligned} m_{p^{m-1}}(x,y) &= x^{p^{m-1}}y, \\ m^T_{p^{m-1}}(x,y) &= xy^{p^{m-1}}, \end{aligned} \tag{24}$$

are maximally entangled in a p-dimensional subspace. Furthermore, these two states belong to different LFP classes.

Proof. The statement comes again from Lemma 3 and the fact that $m_{p^{m-1}}$ and $m^T_{p^{m-1}}$ are composed by a p-output function $g_A(x) = x^{p^{m-1}}$ and a d-output function $g_B(y) = y$. Furthermore, each of the p outputs of $g_A(x)$ appears exactly $d/p = p^{m-1}$ times. To see this, let us consider the function $x^{p^{m-1}}$. We have that $(x+p)^{p^{m-1}} = \sum_{k=0}^{p^{m-1}} \binom{p^{m-1}}{k} x^{p^{m-1}-k}p^k$. It is a consequence of Kummer's Theorem (see Lemma 5 in Appendix E) that $\binom{p^{m-1}}{k}p^k \equiv 0 \mod p^m$ for $0 < k$. Consequently, we have that $(x+p)^{p^{m-1}} = x^{p^{m-1}}$, meaning that the function $g_A(x)$ has a property of cyclicity of order p. To see that g_A has p distinct values, let x, y be in the range $0 \le x, y \le p-1$ and suppose that $g_A(x) = g_A(y)$. Then the difference $x^{p^{m-1}} - y^{p^{m-1}}$ is divisible by p^m. Since p is prime and $x, y < p$, it must be that $x = y$. To distinguish the LFP classes, we can use the invariant (18): We have $I_1(m_{p^{m-1}}) = \{0, \ldots, 0\}$, while $I_1(m^T_{p^{m-1}})$ contains nonzero elements as soon as $\sum_y y^{p^{m-1}} \neq 0$. ∎

The construction in Lemma 3 does not work for constructing this type of low rank maximally entangled states when the dimension $d = p$ is a prime number. Still, the general construction in Lemma 2 contains actually far more low rank classes. In particular, we have seen that single power functions $g_A(x) = cx^k$ in some cases have nice cyclic structures that have implications in the LU classification problem. In Appendix E, we provide a similar example for the case of prime dimensions, where a few rank-2 classes can be found in this way. Thus, we have seen that the construction as in Lemmas 2 and 3 provides FFE states for which the LU classification problem is essentially reduced to a combinatorial problem of studying the outputs of finite functions. Furthermore, for functions associated to states belonging to the same LU class, one can use the LFP invariants of Sec. 4.1.2 to make a (partial) LFP classification.

4.2.3 Application of brute-force algorithms for small dimensions

Here, let us summarize shortly the results of a general LU/LFP classification, which can be made for very small dimensions. First, for $d = 2$ we can easily see that there are just two LU classes: the separable states, corresponding to functions of the form $f(x,y) = f_A(x) + f_B(y)$ and the maximally entangled states, corresponding to the function $f(x,y) = xy$. For $d = 3$ and $d = 4$ it is also still feasible to use a brute-force algorithm to derive all LFP classes. Then, by performing the singular value decomposition of a representative matrix of each class, we can also find all the LU classes with this brute-force method. Another, slightly more efficient, brute-force algorithm can be used to find all the LU classes in the bipartite case: It is sufficient to scan all possible $(d-1)\times(d-1)$ "core" matrices and calculate the traces of their powers up to the d-th. In this way, one can classify all possible characteristic polynomials of $T_f T_f^\dagger$, and thereby list all possible LU classes. This algorithm can provide a quicker answer to the problem in $d = 3$ and $d = 4$, but is still unfeasible for higher dimensions due to the extremely high number of core matrices to scan. See appendix F for more details and an explicit example in $d = 3$.

In the following, we summarize the results for small dimensions that also lead to statements valid in general. The case $d = 3$ is exemplary of prime dimensions, and we know that in this case all finite functions are polynomials. In Table 3 in Appendix G we summarize the list of LFP classes, grouped by the Schmidt rank. Note the presence of classes as in Eq. (41). For the LU classes, we can easily observe that these 9 LFP qutrit classes collapse into 6 LU classes and that, in fact, the operations mapping LFP inequivalent states of the same LU class are just those mentioned in Remark 3.

Next, the case of $d = 4$ is particularly interesting because we can still fully solve it and see the additional complications that arise for non-prime dimensions, and at the same time the richness of structure that arises when the dimension is a prime-power. We find that the number of LFP equivalence classes is 682, while only 15 of them have a TEH state in them. A summary of the LFP classes with a TEH state representative, ordered by different Schmidt ranks, is presented in Table 4 in Appendix H. Furthermore, the number of LU equivalence classes is 127 (cf. Table 2) and only 7 of them have a TEH state representative. What is more interesting, is that now there exist LU operations different from those listed in Remark 3 that connect different LFP classes. In fact, these LU operations are precisely those of the form $\mathbb{1}_4 \otimes \left[F_4^T (F_2 \otimes F_2)^*\right]$ (plus eventually further LFPs), which however connect not just the maximally entangled states between each other, but also states in other LU classes. Another peculiarity of the $d = 4$ case (also compared to the $d = 6$) is that there is more than a single LFP class of TEH states which are maximally entangled in a lower dimensional subspace. Namely, besides the polynomial $m_2(x, y) = 2xy$ which corresponds to a state maximally entangled in a 2-dimensional subspace (as in Proposition 4), there are also 2-dimensional maximally entangled states, with corresponding functions given by x^2y and xy^2, precisely as in Proposition 5.

For $d = 5$ and $d = 6$, it is already not possible to perform a full brute-force LFP/LU classification. However, in the $d = 6$ case it is possible to list all possible polynomial functions and thereby make a LFP/LU classification of TEH states, which is summarized in Table 5 in Appendix I. Noticeable in this case is that there exists only a single maximally entangled class, corresponding to the function xy, and that the only lower-dimensional maximally entangled states are given by the construction as in Proposition 4, namely there is a 2-dimensional maximally entangled state corresponding to the function $3xy$ and a 3-dimensional maximally entangled state corresponding to the function $2xy$. In Table 2 below, we summarize the characterization of the LU and LFP classes discussed above, for dimensions $d = 3, 4, 5, 6, 7$.

Using these case studies, we can draw certain general conclusions concerning the structure of FFE states. The investigation of composite dimensions shows that polynomial and non-polynomial functions are related by LFP operations, and thus a simple characterization of the operations connecting all polynomial functions seems elusive. This problem is intimately connected to the question of polynomiality of finite functions over rings [34]. Furthermore, when considering LU operations, we can observe the number of unitaries, which collapse different LFP classes to a single LU class, increase with growing dimension. While in the case of $d = 3$ complex conjugation and transpose were sufficient to characterize all LU operations which connect LFP classes, in $d = 4$ more LU operators were necessary. This implies that the structure of the LU operations which are necessary becomes increasingly difficult. Finally, the connection with the theory of complex Hadamard matrices gives access to a rich theory. However, many even basic properties of these matrices remain unknown and are the subject of ongoing research. Seeing these complications already in the bipartite scenario hints at the increasing complexity of entanglement structures in the multipartite scenario. On the other hand, any progress in the classification of Butson type Hadamard matrices will be directly translatable to results on FFE states.

dim	# of LFP cl.	# of LU cl.	# of LFP ineq. MES	# LFP cl. for TEH	# LU cl. for TEH
2	2	2	1	2	2
3	9	6	1	9	6
4	807	127	2	17	7
5	$> \boxed{\frac{5^{14}}{576}}$	?	1	$> \boxed{\frac{5^{14}}{576}}$	?
6	$> \boxed{\frac{6^{21}}{400}}$	?	≥ 4 [53]	27	12
7	$> \boxed{\frac{7^{34}}{518400}}$	?	1	$> \boxed{\frac{7^{34}}{518400}}$	?

Table 2: In this table we summarize the number of LFP and LU equivalence classes for FFE and TEH states and give a number of LFP inequivalent maximally entangled states(MES).

5 Conclusions and outlook

In this work, we introduced a framework that aims to exploit a potential interplay between high-dimensional logic and quantum theory, both at a purely theoretical level and towards applications in quantum information. Motivated by generalizing the notion of qubit hypergraph state to the realm of high-dimensional quantum logic [9], we define a set of quantum states which encode arbitrary multivariate, d-valued logical functions into their phases. Naturally, the construction resembles very much that of qudit hypergraph states, previously introduced in Ref. [1]. However, we took here the angle of arbitrary function-encodings, generalizing the construction of qubit hypergraph states, which encode all binary-logical functions, rather than that of generalizing the notion of controlled Pauli operations. In fact, in our framework the natural generalization of Pauli operations is represented by elements of the generalized symmetric group, which we term finite-function-encoding Pauli operators, and are a much wider class of operations than the traditional qudit Heisenberg-Weyl group. We observe in some detail how our notion generalizes that of [1] with several consequences. First, we point out that it is possible to associate certain graphical objects to states only when the encoded function is a polynomial. Such a generalized hypergraph, that we call tensor-edge hypergraph has a tensor attached to every edge, in order to have a one-to-one association with arbitrary polynomial terms. Secondly, we also observe how the stabilizer group of FFE states is generally more complicated than that of qudit hypergraph states. We observe that the property of internal commutativity of stabilizers can be maintained only for the latter set of states (up to LFP equivalence). In the central part of our investigation, we studied the problem of LU classification of FFE states. Besides it being a traditionally relevant problem in quantum information, also related to the classification of resources for applications, it showcases the complex structure of FFE states and their relation to the properties of functions over finite rings of integers. Generalizing the idea of relating entanglement classes with (hyper)graph-theoretic properties (i.e., (hyper)edges and their possible multiplicities), we studied how entanglement classes of FFE states are associated to the properties of the underlying finite functions. This showed the interplay of our framework with important problems in combinatorics and number theory, like the classification of complex Hadamard matrices [31].

Several open questions arise naturally from our study. For example, finding the Clifford group associated to our finite-function-encoding Pauli operations seems pertinent to extend our framework, as well as studying the associated local Clifford classification problem of FFE states. In general, while our definitions and constructions work for any number of parties, the bulk of our present results are actually situated in the realm of bipartite states. While already here one can see interesting structures and identify open problems, we believe the most interesting road ahead concerns results on multipartite states. We expect that multipartite entanglement classification of FFE states will be, on the one hand, closely related to recent constructions of k-uniform states [17, 48], embedding those in a larger scenario containing far more structure. On the other hand, we expect that this will open up a plethora of consequent research towards applications of FFE states, for example for error correction, quantum algorithms and quantum computing in general. In particular, we see measurement-based quantum computing as a promising potential application. In this scheme of quantum computation, the main resource is a multipartite entangled state, given in advance, and quantum gates are implemented via local measurements.

Aside from these we expect that a deep investigation into multipartite FFE states will be strongly related with, and potentially have interesting implication for, several number theory problems, such as in particular, those related to complex Hadamard matrices and generalized permutation matrices.

Thus, it is very intriguing to explore further the connections between the mathematics of finite functions and the formalism of quantum theory with this angle, deepening further the applications of combinatorics and number theory to quantum information theory. Similarly, perhaps in a bit of a more speculative perspective, one can think that progresses in implementations of FFE states in higher-dimensional quantum computation might find applications in solving complex combinatorial problems.

In conclusion, the encoding of finite functions into higher dimensional quantum states yields a rich interplay of mathematical and physical tools. Our construction, despite its complexity, can still exploit a very rich and structured mathematical machinery to dig into the complex realm of multipartite, high-dimensional quantum states. Furthermore, prominent abstract mathematical questions also gain physical relevance when applied to our framework. On the one hand, our construction naturally embeds the theory of finite functions into quantum mechanics, thus relating combinatorial structures to properties of quantum states and their physical implementation. On the other hand, with concurrent developments in manipulating higher-dimensional quantum systems, it is of main practical importance to classify and distill relevant resources for different tasks. In this sense, our construction also opens exciting explorations for potential practical applications, for example in the context of quantum computation, of a very abstract

mathematical theory.

Acknowledgements

We thank Mariami Gachechiladze, Stefan Bäuml, Ludovico Lami and Otfried Gühne for discussions and Ferenc Szöllősi for useful correspondence. P.A., G.V. and M.H. acknowledge funding from the Austrian Science Fund (FWF) through the START project Y879-N27, the Lise-Meitner project M 2462-N27 and the Zukunftskolleg project ZK 3. M.P. acknowledges the support of VEGA project 2/0136/19 and GAMU project MUNI/G/1596/2019. D.L. acknowledges funding from the National Science Foundation (NSF) through grants PHY-1713868 and PHY-2011074.

References

[1] F. E. S. Steinhoff, C. Ritz, N. I. Miklin, and O. Gühne. Qudit hypergraph states. *Physical Review A*, 95(5):052340, May 2017. DOI: 10.1103/PhysRevA.95.052340.

[2] D. Bruß and C. Macchiavello. Optimal Eavesdropping in Cryptography with Three-Dimensional Quantum States. *Physical Review Letters*, 88(12):127901, March 2002. DOI: 10.1103/PhysRevLett.88.127901.

[3] Nicolas J. Cerf, Mohamed Bourennane, Anders Karlsson, and Nicolas Gisin. Security of Quantum Key Distribution Using d-level systems. *Physical Review Letters*, 88(12):127902, March 2002. DOI: 10.1103/PhysRevLett.88.127902.

[4] M. Huber and M. Pawlowski. Weak randomness in device independent quantum key distribution and the advantage of using high dimensional entanglement. *Physical Review A*, 88:032309, 2013. DOI: 10.1103/PhysRevA.88.032309.

[5] Daniele Cozzolino, Beatrice Da Lio, Davide Bacco, and Leif Katsuo Oxenløwe. High-dimensional quantum communication: Benefits, progress, and future challenges. *Advanced Quantum Technologies*, 2(12):1900038, 2019. DOI: 10.1002/qute.201900038.

[6] Nurul T Islam, Charles Ci Wen Lim, Clinton Cahall, Jungsang Kim, and Daniel J Gauthier. Provably secure and high-rate quantum key distribution with time-bin qudits. *Science advances*, 3(11): e1701491, 2017. DOI: 10.1126/sciadv.1701491.

[7] Mirdit Doda, Marcus Huber, Gláucia Murta, Matej Pivoluska, Martin Plesch, and Chrysoula Vlachou. Quantum key distribution overcoming extreme noise: Simultaneous subspace coding using high-dimensional entanglement. *Phys. Rev. Applied*, 15:034003, Mar 2021. DOI: 10.1103/PhysRevApplied.15.034003.

[8] Xiao-Min Hu, Chao Zhang, Yu Guo, Fang-Xiang Wang, Wen-Bo Xing, Cen-Xiao Huang, Bi-Heng Liu, Yun-Feng Huang, Chuan-Feng Li, Guang-Can Guo, Xiaoqin Gao, Matej Pivoluska, and Marcus Huber. Pathways for entanglement-based quantum communication in the face of high noise. *Phys. Rev. Lett.*, 127:110505, Sep 2021. DOI: 10.1103/PhysRevLett.127.110505.

[9] Yuchen Wang, Zixuan Hu, Barry C. Sanders, and Sabre Kais. Qudits and high-dimensional quantum computing. *Frontiers in Physics*, 8:479, August 2020. DOI: 10.3389/fphy.2020.589504.

[10] Fern H. E. Watson, Hussain Anwar, and Dan E. Browne. Fast fault-tolerant decoder for qubit and qudit surface codes. *Physical Review A*, 92(3):032309, September 2015. DOI: 10.1103/PhysRevA.92.032309.

[11] Earl T. Campbell, Hussain Anwar, and Dan E. Browne. Magic-State Distillation in All Prime Dimensions Using Quantum Reed-Muller Codes. *Physical Review X*, 2(4):041021, December 2012. DOI: 10.1103/PhysRevX.2.041021.

[12] Earl T. Campbell. Enhanced Fault-Tolerant Quantum Computing in *d*-Level Systems. *Physical Review Letters*, 113(23):230501, December 2014. DOI: 10.1103/PhysRevLett.113.230501.

[13] D. Gross, S. T. Flammia, and J. Eisert. Most quantum states are too entangled to be useful as computational resources. *Physical Review Letters*, 102(19):190501, May 2009. DOI: 10.1103/physrevlett.102.190501.

[14] Robert Raussendorf, Daniel E Browne, and Hans J Briegel. Measurement-based quantum computation on cluster states. *Physical review A*, 68(2):022312, 2003. DOI: 10.1103/PhysRevA.68.022312.

[15] D. Bruß and C. Macchiavello. Multipartite entanglement in quantum algorithms. *Physical Review A*, 83:052313, May 2011. DOI: 10.1103/PhysRevA.83.052313.

[16] M. Hein, J. Eisert, and H. J. Briegel. Multiparty entanglement in graph states. *Physical Review A*, 69(6):062311, June 2004. DOI: 10.1103/PhysRevA.69.062311.

[17] Zahra Raissi, Adam Teixidó, Christian Gogolin, and Antonio Acín. Constructions of k-uniform and absolutely maximally entangled states beyond maximum distance codes. *Phys. Rev. Research*, 2: 033411, Sep 2020. DOI: 10.1103/PhysRevResearch.2.033411.

[18] M Rossi, M Huber, D Bruß, and C Macchiavello. Quantum hypergraph states. *New Journal of Physics*, 15(11):113022, nov 2013. DOI: 10.1088/1367-2630/15/11/113022.

[19] Mariami Gachechiladze, Costantino Budroni, and Otfried Gühne. Extreme violation of local realism in quantum hypergraph states. *Physical Review Letters*, 116:070401, February 2016. DOI: 10.1103/PhysRevLett.116.070401.

[20] J. Miller and A. Miyake. Hierarchy of universal entanglement in 2D measurement-based quantum computation. *npj Quantum Information*, 2:16036, November 2016. DOI: 10.1038/npjqi.2016.36.

[21] Mariami Gachechiladze, Otfried Gühne, and Akimasa Miyake. Changing the circuit-depth complexity of measurement-based quantum computation with hypergraph states. *Phys. Rev. A*, 99:052304, May 2019. DOI: 10.1103/PhysRevA.99.052304.

[22] Yuki Takeuchi, Tomoyuki Morimae, and Masahito Hayashi. Quantum computational universality of hypergraph states with pauli-x and z basis measurements. *Scientific Reports*, 9(1):13585, Sep 2019. ISSN 2045-2322. DOI: 10.1038/s41598-019-49968-3.

[23] Ri Qu, Juan Wang, Zong-shang Li, and Yan-ru Bao. Encoding hypergraphs into quantum states. *Physical Review A*, 87:022311, February 2013. DOI: 10.1103/PhysRevA.87.022311.

[24] Supriyo Dutta. A boolean functions theoretic approach to quantum hypergraph states and entanglement. November 2018. DOI: 10.48550/arXiv.1811.00308.

[25] David Deutsch and Richard Jozsa. Rapid solution of problems by quantum computation. *Proceedings of the Royal Society of London. Series A: Mathematical and Physical Sciences*, 439(1907):553–558, 1992. DOI: 10.1098/rspa.1992.0167.

[26] Lov K. Grover. A fast quantum mechanical algorithm for database search. In *Proceedings of the Twenty-Eighth Annual ACM Symposium on Theory of Computing*, STOC '96, page 212–219, New York, NY, USA, 1996. Association for Computing Machinery. ISBN 0897917855. DOI: 10.1145/237814.237866.

[27] Anthony Martin, Thiago Guerreiro, Alexey Tiranov, Sébastien Designolle, Florian Fröwis, Nicolas Brunner, Marcus Huber, and Nicolas Gisin. Quantifying photonic high-dimensional entanglement. *Physical Review Letters*, 118:110501, March 2017. DOI: 10.1103/PhysRevLett.118.110501.

[28] Sebastian Ecker, Frédéric Bouchard, Lukas Bulla, Florian Brandt, Oskar Kohout, Fabian Steinlechner, Robert Fickler, Mehul Malik, Yelena Guryanova, Rupert Ursin, and Marcus Huber. Overcoming noise in entanglement distribution. *Physical Review X*, 9(4):041042, Nov 2019. ISSN 2160-3308. DOI: 10.1103/physrevx.9.041042.

[29] Benjamin P. Lanyon, Marco Barbieri, Marcelo P. Almeida, Thomas Jennewein, Timothy C. Ralph, Kevin J. Resch, Geoff J. Pryde, Jeremy L. O'Brien, Alexei Gilchrist, and Andrew G. White. Simplifying quantum logic using higher-dimensional Hilbert spaces. *Nature Physics*, 5:134–140, February 2009. DOI: 10.1038/nphys1150.

[30] Luke E. Heyfron and Earl Campbell. A quantum compiler for qudits of prime dimension greater than 3. *arXiv:1902.05634 [quant-ph]*, February 2019. DOI: 10.48550/arXiv.1902.05634.

[31] Wojciek Tadej and Karol Zyczkowski. A concise guide to complex Hadamard matrices. *Open Systems & Information Dynamics*, 13:133–177, 2006. DOI: 10.1007/s11080-006-8220-2.

[32] D. H. Zhang, H. Fan, and D. L. Zhou. Stabilizer dimension of graph states. *Physical Review A*, 79 (4):042318, April 2009. DOI: 10.1103/PhysRevA.79.042318.

[33] David W. Lyons, Daniel J. Upchurch, Scott N. Walck, and Chase D. Yetter. Local unitary symmetries of hypergraph states. *Journal of Physics A: Mathematical and Theoretical*, 48(9):095301, February 2015. DOI: 10.1088/1751-8113/48/9/095301.

[34] David Singmaster. On polynomial functions (mod m). *Journal of Number Theory*, 6(5):345–352, October 1974. ISSN 0022-314X. DOI: 10.1016/0022-314X(74)90031-6.

[35] Svetlana N. Selezneva. On the number of functions of k-valued logic which are polynomials modulo composite k. *Discrete Mathematics and Applications*, 27(1):7–14, January 2017. ISSN 0924-9265, 1569-3929. DOI: 10.1515/dma-2017-0002.

[36] O. Gühne, M. Cuquet, F. E. S. Steinhoff, T. Moroder, M. Rossi, D. Bruß, B. Kraus, and C. Macchiavello. Entanglement and nonclassical properties of hypergraph states. *Journal of Physics A: Mathematical and Theoretical*, 47(33):335303, 2014. DOI: 10.1088/1751-8113/47/33/335303.

[37] Shiang Yong Looi, Li Yu, Vlad Gheorghiu, and Robert B Griffiths. Quantum-error-correcting codes using qudit graph states. *Physical Review A*, 78(4):042303, 2008. DOI: 10.1103/PhysRevA.78.042303.

[38] Adrian Keet, Ben Fortescue, Damian Markham, and Barry C Sanders. Quantum secret sharing with qudit graph states. *Physical Review A*, 82(6):062315, 2010. DOI: 10.1103/PhysRevA.82.062315.
[39] Marc Hein, Jens Eisert, and Hans J Briegel. Multiparty entanglement in graph states. *Physical Review A*, 69(6):062311, 2004. DOI: 10.1103/PhysRevA.69.062311.
[40] Michael A. Nielsen and Isaac L. Chuang. *Quantum Computation and Quantum Information: 10th Anniversary Edition*. Cambridge University Press, New York, NY, USA, tenth edition, 2011. ISBN 1-107-00217-6 978-1-107-00217-3.
[41] C. Eltschka and J. Siewert. Quantifying entanglement resources. *Journal of Physics A: Mathematical and Theoretical*, 47:424005, 2014. DOI: 10.1088/1751-8113/47/42/424005.
[42] Eric Chitambar, Debbie Leung, Laura Mančinska, Maris Ozols, and Andreas Winter. Everything you always wanted to know about locc (but were afraid to ask). *Communications in Mathematical Physics*, 328(1):303–326, Mar 2014. ISSN 1432-0916. DOI: 10.1007/s00220-014-1953-9.
[43] D. Gross and M. Van den Nest. The lu-lc conjecture, diagonal local operations and quadratic forms over gf(2). *Quantum Inf. Comput. 8, 263 (2008)*, 2007. DOI: 10.48550/arXiv.0707.4000.
[44] Zhengfeng Ji, Jianxin Chen, Zhaohui Wei, and Mingsheng Ying. The lu-lc conjecture is false. *Quantum Inf. Comput. 10, 97 (2010)*, 2008. DOI: 10.48550/arXiv.0709.1266.
[45] Maarten Van den Nest, Jeroen Dehaene, and Bart De Moor. Local unitary versus local clifford equivalence of stabilizer states. *Physical Review A*, 71(6):062323, Jun 2005. ISSN 1094-1622. DOI: 10.1103/physreva.71.062323.
[46] Dardo Goyeneche and Karol Życzkowski. Genuinely multipartite entangled states and orthogonal arrays. *Physical Review A*, 90(2):022316, Aug 2014. ISSN 1094-1622. DOI: 10.1103/physreva.90.022316.
[47] Dardo Goyeneche, Daniel Alsina, José I. Latorre, Arnau Riera, and Karol Życzkowski. Absolutely maximally entangled states, combinatorial designs, and multiunitary matrices. *Phys. Rev. A*, 92: 032316, Sep 2015. DOI: 10.1103/PhysRevA.92.032316.
[48] Dardo Goyeneche, Zahra Raissi, Sara Di Martino, and Karol Życzkowski. Entanglement and quantum combinatorial designs. *Phys. Rev. A*, 97:062326, Jun 2018. DOI: 10.1103/PhysRevA.97.062326.
[49] Felix Huber, Christopher Eltschka, Jens Siewert, and Otfried Gühne. Bounds on absolutely maximally entangled states from shadow inequalities, and the quantum MacWilliams identity. *Journal of Physics A: Mathematical and Theoretical*, 51(17):175301, mar 2018. DOI: 10.1088/1751-8121/aaade5.
[50] A. J. Scott. Multipartite entanglement, quantum-error-correcting codes, and entangling power of quantum evolutions. *Physical Review A*, 69(5):052330, May 2004. ISSN 1094-1622. DOI: 10.1103/physreva.69.052330.
[51] Felix Huber, Otfried Gühne, and Jens Siewert. Absolutely maximally entangled states of seven qubits do not exist. *Phys. Rev. Lett.*, 118:200502, May 2017. DOI: 10.1103/PhysRevLett.118.200502.
[52] Wojciek Tadej. Permutation equivalence classes of Kronecker Products of unitary Fourier matrices. *Linear Algebra and Its Applications*, 418:719–736, 2006. DOI: 10.1016/j.laa.2006.03.004.
[53] P. H. J. Lampio, P. Östergård, and F. Szöllősi. Orderly generation of butson hadamard matrices. *Math. Comp.*, 89:313–331, 2020. DOI: 10.1090/mcom/3453.
[54] Uffe Haagerup. Orthogonal maximal abelian *-subalgebras of the $n \times n$ matrices and cyclic n-roots. *Operator Algebras and Quantum Field Theory (Rome)*, pages 296 – 322, 1996. URL `http://citeseerx.ist.psu.edu/viewdoc/summary?doi=10.1.1.35.8457`.
[55] Terence Tao. Fuglede's conjecture is false in 5 and higher dimensions. *Math. Res. Letters*, 11:251–258, 2004. DOI: 10.4310/MRL.2004.v11.n2.a8.
[56] David W. Lyons and Scott N. Walck. Minimum orbit dimension for local unitary action on n-qubit pure states. *Journal of Mathematical Physics*, 46:102106, 2005. DOI: 10.1063/1.2048327.
[57] Ferenc Szöllősi. Complex hadamard matrices of order 6: a four-parameter family. *Journal of the London Mathematical Society*, 85(3):616–632, Mar 2012. ISSN 0024-6107. DOI: 10.1112/jlms/jdr052.

A Polynomial Representability and Normal Form

We can make use of a normal form defined below to simply generate unique polynomials representing all polynomial functions. We will use the form given in [35] since it favours "local" terms over "non-local" ones . First let us introduce the *composite degree*, a quantity which is used to restrict both the degree of the monomials as well as the values of the coefficients of the unique polynomial representative we construct here. The composite degree $c_{p,m}$ of a single variable monomial x^e in a prime power ring $d = p^m$ is defined as the greatest number $t \in \{0, \ldots, m-1\}$ such that the factorial $e!$ is divisible by p^t. For

multivariate monomials, $\mathbf{x}^{\mathbf{e}}$ with $x_i, e_i \in \mathbb{Z}_d$ we have $c_{p,m}(\mathbf{x}^{\mathbf{e}}) = \min(m, \sum_{i=1}^{n} c_{p,m}(x_i^{e_i}))$. Now following Theorem 1 in [35] we find:

Remark 4. *For $d = p^m$ with p a prime and $m > 0$ any polynomial function $p(x_1, \ldots, x_n)$ is in one-to-one correspondence with the polynomials of the form*

$$p(x_1, \ldots, x_n) = \sum_{\mathbf{e}} c_{\mathbf{e}} \mathbf{x}^{\mathbf{e}}$$

with $c_{p,m}(\mathbf{x}^{\mathbf{e}}) < m$, $c_{\mathbf{e}} \in \mathbb{Z}_d^n$, $c_{\mathbf{e}} < p^{m - c_{p,m}(\mathbf{x}^{\mathbf{e}})}$

Let us give an example for $d = p^m = 2^2$ and $n = 2$: The first step is to identify the monomials which have a composite degree smaller than m: Note that for a single variable monomials

$$c_{p,m}(x^e) = \begin{cases} 0 & \text{if } e \in \{0, \ldots, p-1\} = \{0, 1\} \\ 1 & \text{if } e \in \{p, \ldots, 2p-1\} = \{2, 3\} \end{cases}$$

From this we can immediately see that all monomials of the form $x^i y^j$ with: (i) $i, j \leq 1$, (ii) $i \leq 1$ and $2 \leq j \leq 3$, (iii) $j \leq 1$ and $2 \leq i \leq 3$ appear in the polynomial we are constructing. All others i.e. $2 \leq i, j$ do not appear. Thus we find that any polynomial function over $\mathbb{Z}_4$ can be represented as:

$$\begin{aligned} f(x, y) = {} & c_{00} + c_{10}x + c_{01}y + c_{11}xy \\ & + c_{20}x^2 + c_{30}x^3 + c_{02}y^2 + c_{03}y^3 + c_{21}x^2y + c_{31}x^3y + c_{12}xy^2 + c_{13}xy^3 \end{aligned}$$

where the c_{ij} are restricted by the composite degree of the corresponding monomials, i.e. the coefficients in the first row are smaller than $2^{2-0} = 4$ and the coefficients in the second row are smaller than $2^{2-1} = 2$.

Finally, let us take a look at the case of arbitrary composite dimension, i.e., $d = p_1^{m_1} \ldots p_r^{m_r}$: First, it is straightforward to use the method above to find a unique polynomial representative for each prime factor $p_i^{m_i}$. Now, each monomial of these polynomials will be found in the polynomial for the composite degree. If the same monomial appears in multiple polynomials for different $p_i^{m_i}$ its coefficients in the composite degree are found by the Chinese remainder theorem. In other words let $c_i \in \mathbb{Z}_{p_i^{m_i}}$ be the coefficients of an arbitrary fixed monomial in each of the polynomials in prime factor $p_i^{m_i}$. Then the corresponding coefficient $c \in \mathbb{Z}_d$ for the composite d is the unique solution to the system of congruences $c \equiv c_i \mod (p_i^{m_i})$.

B Stabilizers: Proofs of the main Propositions

Proof (of Proposition 1). Let $|\psi\rangle = \sum_{\mathbf{x}} c_{\mathbf{x}} |\mathbf{x}\rangle$ be any pure n-qudit state (we do not assume that $|\psi\rangle$ is a finite-function-encoding state, but we soon show that this must be the case), and assume that $S_{f,\kappa_i} |\psi\rangle = |\psi\rangle$ for all i. Then we have

$$X_{\kappa_i} Z_{f \circ \kappa_i - f} |\psi\rangle = \sum_{\mathbf{x}} \omega^{f(\kappa_i(\mathbf{x})) - f(\mathbf{x})} c_{\mathbf{x}} |\kappa_i(\mathbf{x})\rangle = \sum_{\mathbf{x}} \omega^{f(\mathbf{x}) - f(\kappa_i^{-1}(\mathbf{x}))} c_{\kappa_i^{-1}(\mathbf{x})} |\mathbf{x}\rangle . \tag{25}$$

It follows that

$$c_{\mathbf{x}} = \omega^{f(\mathbf{x}) - f(\kappa_i^{-1}(\mathbf{x}))} c_{\kappa_i^{-1}(\mathbf{x})}$$

for all i and for all $\mathbf{x}$. Because for each i κ_i is a d-cycle, letting x_i vary, forces that coefficients

$$c_{x_1, x_2, \ldots, x_i, \ldots, x_n}, \qquad \text{and} \quad c_{x_1, x_2, \ldots, \kappa_i(x_i), \ldots, x_n}$$

have the same norm, and also differ by a factor that is a d-th root of unity, for all x_i. Now allowing $\mathbf{x}$ to vary, we get that all the state vector coefficients $c_{\mathbf{x}}$ have the same norm and any two differ by a factor of a d-th root of unity. Thus we can always associate a finite function to the phases of the coefficients, and thereby establish that $|\psi\rangle$ is a FFE state.

Let us then denote the state as $|g\rangle$, calling g the function encoded in its phase. With this notation Eq. (25) reads

$$X_{\kappa_i} Z_{f \circ \kappa_i - f} |g\rangle = \sum_{\mathbf{x}} \omega^{f(\mathbf{x}) - f(\kappa_i^{-1}(\mathbf{x})) + g(\kappa_i^{-1}(\mathbf{x}))} |\mathbf{x}\rangle \tag{26}$$

and we have

$$f(\mathbf{x}) - f(\kappa_i^{-1}(\mathbf{x})) + g(\kappa_i^{-1}(\mathbf{x})) = g(\mathbf{x})$$

for all i and for all $\mathbf{x}$. If we set $d(\mathbf{x}) = f(\mathbf{x}) - g(\mathbf{x})$, the above expression becomes

$$d(\mathbf{x}) = d(\kappa_i^{-1}(\mathbf{x}))$$

for all i and for all $\mathbf{x}$. Once again, by varying i, then by varying $\mathbf{x}$, we conclude that d is constant. This establishes that $|g\rangle$ is in fact equal to $|f\rangle$ (up to a global phase), and the proof of the proposition is complete. ∎

Before we prove Proposition 2 let us state the following two remarks.

Remark 5. *Two permutation cycles $\sigma = (i_1 i_2 \dots i_k)$ and $\kappa = (i'_1 i'_2 \dots i'_k)$ of the same size k are called* conjugate *and one can write $\sigma = \pi^{-1}\kappa\pi$, where $\pi(i'_j) = i_j$ for $1 \leq j \leq k$. In particular, any d-cycle κ can be written as $\pi^{-1}\kappa^+\pi$, where κ^+ is a permutation mapping x to $x + 1 \mod d$ and simultaneously $\pi^{-1}\kappa^+\pi$ is a d cycle for any permutation π.*

Remark 6. *Note also that, for a given κ, the choice of π in Remark 5 is not unique, since each κ_i can be decomposed into $\pi_i^{-1}\kappa^+\pi_i$ in exactly d different ways. This follows from the fact that vectors $(i_1 \dots i_d)$ and $(i_d i_1 \dots i_{d-1})$ represent the same d-cycle.*

Now we are finally ready to prove Proposition 2:

Proof (of Proposition 2). For the first direction, we assume that the function f can be decomposed as

$$f = f' \circ \pi_1 \circ \dots \circ \pi_n,$$

for some polynomial f' of degree at most 1 in each variable. Then, let us consider the stabilizer $X_{\kappa_1} Z_{f\circ\kappa_1 - f}$ where κ_1 is some d-cycle, which, by remark 5 can be written as $\kappa_1 = \pi_1^{-1}\kappa^+\pi_1$. Given that f' is of degree 1 in x_1, we can write $f \circ \kappa_1$ as

$$f \circ \kappa_1 = f'(\pi_1(\kappa_1(x_1)), \pi_2(x_2), \dots, \pi_n(x_n)) = h_1(x_2, \dots, x_n) + \pi_1(\kappa_1(x_1)) g_1(x_2, \dots, x_n),$$

where for simplicity of notation we have incorporated all the other permutations $\pi_2, \dots, \pi_n$ into the functions h_1 and g_1. Now using remark 5 we consider the d-cycle $\kappa_1 = \pi_1^{-1}\kappa^+\pi_1$ and we have

$$f \circ \kappa_1 = h_1(x_2, \dots, x_n) + (\kappa^+\pi_1(x_1)) g_1(x_2, \dots, x_n),$$

where $h_1(x_2, \dots, x_n)$ and $g_1(x_2, \dots, x_n)$ are functions linear in all variables. In the next step we will use the fact that for every d the permutation $\kappa^+(x)$ can be written as a polynomial $x + 1 \mod d$, therefore the equation can be modified to

$$f \circ \kappa_1 = h_1(x_2, \dots, x_n) + (\pi_1(x_1) + 1) g_1(x_2, \dots, x_n),$$

This, in turn, implies that

$$f \circ \kappa_1 - f = g_1(x_2, \dots, x_n),$$

and from Lemma 1 if follows that $X_{\kappa_1} Z_{f\circ\kappa_1 - f} = Z_{f\circ\kappa_1 - f} X_{\kappa_1}$. Repeating the same reasoning for all variables x_i shows that we can find a set of internally commuting stabilizers $\{X_{\kappa_i} Z_{f\circ\kappa_i - f}\}_{i=1}^n$ where all the κ_i are d-cycles and thus by Proposition 1 they completely specify the state $|f\rangle$.

For the other direction, let us consider a set of stabilizers $\{X_{\kappa_i} Z_{f\circ\kappa_i - f}\}_{i=1}^n$ where all the κ_i are d-cycles. We first note that from Lemma 1 it also follows that $X_{\kappa_i} Z_{f\circ\kappa_i - f} = Z_{f\circ\kappa_i - f} X_{\kappa_i}$ only if the function $f(x_1, \dots, \kappa_i(x_i), \dots, x_n) - f(x_1, \dots, x_n)$ does not depend on the variable x_i. In other words, taking $i = 1$, we have

$$f(\kappa_1(x_1), x_2, \dots, x_n) - f(x_1, \dots, x_n) = g_1(x_2, \dots, x_n). \tag{27}$$

From Remark 5 and the polynomial representation of κ^+ we also know that for every d-cycle κ_1 we can find some permutation π_1 such that

$$\kappa_1(x_1) = \pi_1^{-1}(\pi_1(x) + 1).$$

Thus, Eq. (27) simplifies to

$$f'(y_1+1,x_2,\ldots,x_n)-f'(y_1,x_2,\ldots,x_n)=g_1(x_2,\ldots,x_n),$$

where we called $f'=f\circ\pi_1^{-1}$ and $y_1=\pi(x_1)$. It is easy to see that the above difference equation in y_1 has solution

$$f'(y_1,x_2,\ldots,x_n)=h_1(x_2,\ldots,x_n)+y_1g_1(x_2,\ldots,x_n),$$

where h_1 is a function independent of x_1. Hence, if Eq. (27) holds (for $i=1$), then the function f can be written as

$$f(x_1,\ldots,x_n)=h_1(x_2,\ldots,x_n)+\pi(x_1)g_1(x_2,\ldots,x_n).$$

for some $g_1(x_2,\ldots,x_n)$. Repeating the reasoning for all variables x_i proves the Proposition. ∎

C FFE states with continuous unitary stabilizers

Besides the complete characterization of (discrete) stabilizer groups associated to general FFE states, following past works on hypergraph states, we can also ask for which FFE states continuous families of stabilizers exist. In fact, classes of graph states and hypergraph states that have continuous local unitary stabilizers are known [32, 33]. In the following we generalize the results of Ref. [32, 33] to the FFE scenario.

Lemma 4. *Let $|f\rangle$ be a n-partite FFE state associated to a function $f(\mathbf{x})$ such that*

$$f(\sigma(a),\sigma^{-1}(b),x_3,\ldots,x_n)=f(\sigma(b),\sigma^{-1}(a),x_3,\ldots,x_n),\tag{28}$$

for all $a,b\in\mathbb{Z}_d$ and for some permutation σ, and let A be the operator such that $X_\sigma=\exp(i2\pi A/d)$. The operator $S_{f,\sigma_1,\sigma_2^{-1}}(t)=[\exp(itA)\otimes\exp(-itA)]\,Z_{f\circ\sigma_1\circ\sigma_2^{-1}-f}$ stabilizes $|f\rangle$ for all values of t.

Proof. First, we observe that $S_{f,\sigma_1,\sigma_2^{-1}}(t)$ is a stabilizer for $t=2\pi/d$. In fact, it is just the product of two operators as in Eq. (7), namely

$$S_{f,\sigma_1,\sigma_2^{-1}}(2\pi/d)=X_{\sigma_1}X_{\sigma_2^{-1}}Z_{f\circ\sigma_1\circ\sigma_2^{-1}-f}=X_{\sigma_1}Z_{f\circ\sigma_1-f}X_{\sigma_2^{-1}}Z_{f\circ\sigma_2^{-1}-f},\tag{29}$$

due to the commutation relation (6c) and the fact that $Z_{f\circ\sigma_1\circ\sigma_2^{-1}-f\circ\sigma_2^{-1}}Z_{f\circ\sigma_2^{-1}-f}=Z_{f\circ\sigma_1\circ\sigma_2^{-1}-f}$. Then, for different values of $t\in\mathbb{R}$ we have that a sufficient condition for $S_{f,\sigma_1,\sigma_2}(t)\,|f\rangle=|f\rangle$ is that (cf. Sec. 3 of [56])

$$(A\otimes\mathbb{1}-\mathbb{1}\otimes A)Z_{f\circ\sigma_1\circ\sigma_2^{-1}-f}\,|f\rangle=(A\otimes\mathbb{1}-\mathbb{1}\otimes A)\left|f\circ\sigma_1\circ\sigma_2^{-1}\right\rangle=0.\tag{30}$$

This holds true from the assumption that $f(\sigma(a),\sigma^{-1}(b),x_3,\ldots,x_n)=f(\sigma(b),\sigma^{-1}(a),x_3,\ldots,x_n)$ for all $a,b\in\mathbb{Z}_d$, since in that case the state is invariant under exchange of the first two parties. ∎

A particular example of function that fits in the above proposition and gives rise to a continuous family of stabilizers is $f(\mathbf{x})=(x_1+x_2)g(x_3,\ldots,x_n)$, with the corresponding permutation given by $\sigma=\kappa^+$ (or $\sigma=\kappa^-$). Note, how this function satisfies $f(\kappa^+(x_1),\kappa^-(x_2),x_3,\ldots,x_n)=f(\kappa^-(x_1),\kappa^+(x_2),x_3,\ldots,x_n)=f(\mathbf{x})$, which is in turn invariant under exchanging $x_1\leftrightarrow x_2$.

D Simple known results on Hadamard matrices $H(d,d)$ for $d=4$ and $d=6$

In $d=4$, all Hadamard matrices of type $H(4,4)$ belong to a single continuous 1-parameter family [31]:

$$H_4(q)=\begin{pmatrix}1 & 1 & 1 & 1\\ 1 & ie^{iq} & -1 & -ie^{iq}\\ 1 & -1 & 1 & -1\\ 1 & -ie^{iq} & -1 & ie^{iq}\end{pmatrix},$$

where q is any real number. This family can be also expressed as

$$H_4(q)=F_4\circ_H\mathrm{EXP}(iqh_4(x,y)),\tag{31}$$

with $h_4(x,y) = x^2y + xy^2 + 3xy \mod 4$, as in our language of finite functions, where EXP is the elementwise exponential. Here the operation $\circ_H$ denotes the Hadamard product of two matrices, i.e., the elementwise multiplication.

For $d = 6$ the theory of Hadamard matrices becomes already extremely complicated and not all $BH(6,6)$ matrices are known. For example, analogously to the $d = 4$ a continous family with two real parameter (a, b) is known:

$$H_6(a,b) = \begin{pmatrix} 1 & 1 & 1 & 1 & 1 & 1 \\ 1 & \omega_6 e^{ia} & \omega_6^2 e^{ib} & \omega_6^3 & \omega_6^4 e^{ia} & \omega_6^5 e^{ib} \\ 1 & \omega_6^2 & \omega_6^4 & 1 & \omega_6^2 & \omega_6^4 \\ 1 & \omega_6^3 e^{ia} & e^{ib} & \omega_6^3 & e^{ia} & \omega_6^3 e^{ib} \\ 1 & \omega_6^4 & \omega_6^2 & 1 & \omega_6^4 & \omega_6^2 \\ 1 & \omega_6^5 e^{ia} & \omega_6^4 e^{ib} & \omega_6^3 & \omega_6^2 e^{ia} & \omega_6 e^{ib} \end{pmatrix}.$$

This family includes F_6 and $F_3 \otimes F_2$. These two matrices are however, contrary to the analogous $d = 4$ case, LFP equivalent [52]. Again, this family can be expressed as a Hadamard product with F_6, namely

$$H_6(a,b) = F_6 \circ_H \mathrm{EXP}(i(ag_6(x,y) + bh_6(x,y))), \tag{32}$$

where $g_6(x,y)$ and $h_6(x,y)$ are, in our language, finite functions from $\mathbb{Z}_6^2$ to $\mathbb{Z}_6$. Recently, a non-affine 4-parameter family has been found [57] and it has been conjectured that the full set of complex Hadamard matrices in $d = 6$ consists of such a 4-parameter family plus the isolated matrix S_6 found by Tao in [55].

It is also curious to observe that the functions corresponding to the matrices $F_3 \otimes F_2$ and S_6, namely

$$f_{3,2} = \begin{pmatrix} 0 & 0 & 0 & 0 & 0 & 0 \\ 0 & 3 & 0 & 3 & 0 & 3 \\ 0 & 0 & 2 & 2 & 2 & 2 \\ 0 & 3 & 2 & 5 & 4 & 1 \\ 0 & 0 & 4 & 4 & 2 & 2 \\ 0 & 3 & 4 & 1 & 2 & 5 \end{pmatrix}, \qquad \text{and} \qquad s_6 = \begin{pmatrix} 0 & 0 & 0 & 0 & 0 & 0 \\ 0 & 0 & 2 & 2 & 4 & 4 \\ 0 & 2 & 0 & 4 & 4 & 2 \\ 0 & 2 & 4 & 0 & 2 & 4 \\ 0 & 4 & 4 & 2 & 0 & 2 \\ 0 & 4 & 2 & 4 & 2 & 0 \end{pmatrix}, \tag{33}$$

are not polynomials. To conclude this section we remark that a set of invariants $\{I_{a,b,c,d}(f)\}$ for equivalence classes of Hadamard matrices has been defined [31, 54], the elements of which in our context can be put in the form

$$I_{a,b,c,d}(f) = f(a,b) - f(c,b) + f(c,d) - f(a,d) \quad \text{for} \quad (a,b,c,d) \in \mathbb{Z}_d^4. \tag{34}$$

Note that each of the elements of the set is invariant under local Z-type operations since each index appears both with a plus and a minus sign. X-type operations, instead, can exchange elements between each other. However, the whole set remains invariant also under those transformations.

E Details on LU and LFP classification of states as in Lemma 2

Here let us prove the statement in Lemma 3 and then make some further observations regarding the more general LU and LFP classification of states as in Lemma 2. Let us first introduce a notation for the single particle reduced density matrix of a bipartite FFE state:

$$\rho_f := \mathrm{tr}_2(|f\rangle\langle f|) = \frac{1}{d^2}\sum_{a=0}^{d-1} |f(\cdot,a)\rangle\langle f(\cdot,a)|, \tag{35}$$

where $|f(\cdot,a)\rangle$ is the (single particle) FFE state corresponding to $f(\cdot,a) = f(x,a)$ as a (single variable) function of x. For states as in Lemma 2 we have:

$$\rho_f = \frac{1}{d^2}\sum_{a=0}^{d-1}\sum_{x,y=0}^{d-1} \omega^{g_B(a)(g_A(x)-g_A(y))} |x\rangle\langle y|, \tag{36}$$

which will be useful for the following observations.

Proof (of lemma 3). Let us consider a function $f_r(x,y) = g_A(x)g_B(y)$ such that g_B has d distinct outputs. Using LFP operations (i.e., permutations of the inputs) we can always transform this function

into $g_B(y) = y$. Furthermore, we can also permute the inputs of g_A such that the distinct r outputs are precisely the first (i.e. $g_A(0) \neq g_A(1) \neq \ldots \neq g_A(r-1)$). Then, substituting $g_B(y) = y$ in Eq. (36) we can see that the single particle reduced density matrix has elements which are either equal to $1/d$ or to zero due to the fact that $\sum_{i=0}^{d-1} \omega^i = 0$. In particular, nonzero elements (l, k) appear wherever $g_A(k) = g_A(l)$ and are symmetrical. Thus overall, the matrix has elements $1/d$ along the whole diagonal and has some off-diagonal elements equal to $1/d$ appearing symmetrically. Hence, we can, e.g., subtract some rows from each other so to reduce the matrix to the form

$$\rho_f = \tfrac{1}{d} \begin{pmatrix} \mathbb{1}_r & \star \\ \mathbf{0} & \mathbf{0} \end{pmatrix},$$

where we indicated as $\mathbf{0}$ a matrix with all elements equal to 0 and as $\star$ some leftover elements. This concludes the proof that indeed ρ_f has rank r, which is by definition equal to the Schmidt rank of $|f_r\rangle$.

For the second part of the proof, let us assume that the r divides d and that the outputs appear exactly d/r times each. Then, we permute the rows of T_f such that they repeat themselves exactly with cyclicity d/r and we have

$$\rho_f = \tfrac{1}{d} \mathbb{1}_r \otimes J_{d/r},$$

where $\mathbb{1}_r$ is the identity in dimension r and $J_{d/r}$ is the $(\frac{d}{r})$-dimensional matrix with every coefficient equal to 1. Thus, we have that its eigenvalues are all equal to $1/r$. ∎

In what follows we state and prove a Lemma that supports Proposition 5.

Lemma 5. *Let p be a prime, let m be a nonnegative integer, and let k be an integer in the range $0 < k \leq p^{m-1}$. We have $\binom{p^{m-1}}{k} p^k \equiv 0 \mod p^m$.*

Proof. Kummer's Theorem says the following. Let p be a prime, and let $\nu(x)$ denote the highest power of p that divides an integer x. Given integers a, b we have that $\nu(\binom{a}{b})$ is the number of carries in the addition modulo p of b with $b - a$.

Let $a = p^{m-1}$ and let $b = k$. Then expansion of b in powers of p is

$$b = b_0 p^0 + b_1 p^1 + \cdots + b_{m-1} p^{m-1}.$$

Further, let s be the smallest index such that $b_s \neq 0$. If $s = m-1$, then $b = a$ and we have $\binom{p^{m-1}}{p^{m-1}} p^{p^{m-1}} \equiv 0 \mod p^m$, so the Lemma holds. If $s < m - 1$, we have

$$a - b = (p - b_s)p^s + ((p-1) - b_{s+1})p^{s+1} + ((p-1) - b_{s+2})p^{s+2} + \cdots + ((p-1) - b_{m-2})p^{m-2}.$$

When adding b and $a - b$ modulo p, there is a carry when adding in positions $s, s+1, \ldots, m-2$, so that there are $m - s - 1$ carries total. Applying Kummer's Theorem, we have $\nu\left(\binom{a}{b}\right) = m - s - 1$. We also have $b = k \geq p^s$, so $k > s$. It follows that

$$\nu\left(\binom{a}{b} p^k\right) = m - s - 1 + k = m + (k - s - 1) \geq m.$$

Thus the Lemma holds in this case, and this concludes the proof. ∎

E.1 Exemplary LU classification of states as in Lemma 3

Now, as an instructive example, let us try to make a classification of FFE states from the construction in Lemma 3 for functions $g_A(x)$ with only two distinct outputs, which is essentially the simplest case. Notice that when $g_A(x)$ is a constant function the FFE state belongs to the separable class. In this case we have $\rho_f = J_d/d$ and there is only a single nonzero eigenvalue equal to 1. Thus, let us consider the case in which $g_A(x)$ has two distinct outputs. In order to classify the corresponding FFE states into LU classes, we can calculate the characteristic polynomial $\chi(\rho_f)$ of ρ_f, which is of the form

$$\begin{aligned} \chi(\rho_f)(x) &= x^d + c_1 x^{d-1} + c_2 x^{d-2}, \quad \text{with} \\ c_1 &= -\operatorname{tr}(\rho_f) = -1, \\ c_2 &= -\tfrac{1}{2}\left(\operatorname{tr}(\rho_f^2) - \operatorname{tr}(\rho_f)^2\right). \end{aligned} \tag{37}$$

To calculate the coefficients above we have also to specify, for each output, how many inputs it corresponds to. For example, let us assume that the first output only corresponds to one input and the other one to $d-1$ inputs. In this case, we have that

$$\rho_f = \tfrac{1}{d}\begin{pmatrix} 1 & \mathbf{0} \\ \mathbf{0}^T & J_{d-1} \end{pmatrix},$$

with $\mathbf{0} = (0, 0, \ldots, 0)$. Thus, in this case the full matrix ρ_f has the eigenvalue 0 with multiplicity $(d-2)$ and one eigenvalue $1/d$, which is the top left diagonal element. Then, due to the fact that the total trace of the matrix is 1, we deduce that the only remaining nonzero eigenvalue must be $1-1/d$. Thus, the corresponding class of FFE states has Schmidt vector given by

$$\lambda = (1/\sqrt{d}, \sqrt{1-1/d}, 0, \ldots, 0). \tag{38}$$

As explained above, in more general cases, when the two distinct outputs correspond to different numbers of inputs, we essentially just need to calculate $\mathrm{tr}(\rho_f^2)$. From Eq. (36) we then obtain

$$\begin{aligned} \mathrm{tr}(\rho_f^2) &= \tfrac{1}{d^4}\sum_{ab}\sum_{xy}\omega^{(a-b)(g_A(x)-g_A(y))} = \tfrac{2d-1}{d^2} + \tfrac{1}{d^4}\sum_{a\neq b}\sum_{x\neq y}\omega^{(a-b)(g_A(x)-g_A(y))} \\ &= \tfrac{2d-1}{d^2} + \tfrac{d-1}{d^3}(N_1^2 - N_1 + (d-N_1)^2 - (d-N_1)), \end{aligned} \tag{39}$$

where we called N_1 the number of times output o_1 appears.

To conclude, let us briefly consider the even more general construction of Lemma 2, still for the case in which $g_A(x)$ has just two distinct outputs and g_B has an arbitrary number of outputs. In this case the Schmidt rank of the corresponding FFE state is still 2, and thus, to make the LU classification we have still to calculate just $\mathrm{tr}(\rho_f^2)$. However, this time we have

$$\mathrm{tr}(\rho_f^2) = \tfrac{1}{d^4}\sum_{ab}\sum_{xy}\omega^{(g_A(x)-g_A(y))(g_B(a)-g_B(b))}, \tag{40}$$

and we see that this time the LU class depends also, besides the number of times they appear, on the concrete values of all the outputs of the functions g_A and g_B.

E.2 Exemplary classes constructed as in Lemma 2 for prime dimension

In prime dimension d, we can use that $x^{d-1} = 1$ for all $x > 0$. Thus, the function $g_A(x) = kx^{d-1} = k$ has only two distinct outputs, namely 0 and k, the latter appearing $d-1$ times. Then, we can make the following combinations, which have associated rank-2 FFE states for every $1 \leq k \leq d-1$:

$$\begin{aligned} f_{k,d-1} &= kx^{d-1}y, \\ g_{k,d-1} &= kxy^{d-1}, \\ h_{k,d-1} &= kx^{d-1}y^{d-1}. \end{aligned} \tag{41}$$

One can see that all the $|f_{k,d-1}\rangle$ and $|g_{k,d-1}\rangle$ belong to the same LU class, for which the two nonzero Schmidt eigenvalues are given by $\lambda_1 = 1/\sqrt{d}$, and $\lambda_2 = \sqrt{1-\lambda_1^2}$ (cf. Eq. (38)). However, from the invariant (18) we see that $|f_{k,d-1}\rangle$ and $|g_{k,d-1}\rangle$ belong to different LFP classes. In fact, we have that $I_1(f_{k,d-1})$ has nonzero elements, while $I_1(g_{k,d-1}) = \{0, \ldots, 0\}$.

On the other hand, the $|h_{k,d-1}\rangle$ belong to different LU classes for $1 \leq k \leq (d+1)/2$, while for the remaining k the corresponding states are obtained via complex conjugation from the previous ones. The LU classes are determined by calculating the characteristic polynomial of ρ_h, which is of the form given in Eq. (37) with $c_2 = 2\frac{(d-1)^2}{d^4}\cos(2\pi k/d)$. Thus, we see that there is a different class for each $1 \leq k \leq (d+1)/2$ and there is a symmetry under exchanging k with $-k$. On the other hand, for each k they belong to a different LFP class, as it can be easily witnessed by the invariant (17) which gives $S(h_{k,d-1}) = k$.

F Brute-force algorithms for LFP and bipartite LU classification

As mentioned in the main text, we can derive a simple brute-force algorithm that finds all LFP classes of FFE states of a given number of parties n and dimension d. Let us first describe it briefly and then

show it in the practical example of the bipartite 3×3 case. This algorithm makes use of what we called the "dephased" normal form under LFP, given by Eq. (15). Thus, it starts by considering a generic state in the dephased form, and its (initially empty) LFP class. Then, essentially, by scanning all elementary local finite-function-encoding Pauli operations, it fills all of its LFP class. Then it moves on to another (dephased) FFE state and repeats the procedure, until all possible dephased matrices have been scanned and thus all possible LFP classes have been filled.

Explicitly, it goes as follows:

Algorithm 1: Brute force LFP classification of d^n-dimensional FFE states

Create an empty list of classes Cl;
for *all dephased coefficient tensor* $T_f \in \mathbb{C}^{d^n}$ **do**
  if $T_f \notin Cl$ **then**
    Create an empty list TMP;
    for *all elementary permutation* X_π **do**
      Apply the permutation $T_f \longleftarrow X_\pi T_f X_\pi^\dagger$;
      Transform it back to dephased form $T_f' \longleftarrow Z_{\text{dephf}} T_f Z_{\text{dephf}}^\dagger$ where $Z_{\text{dephf}} = \bigotimes_{k=1}^n Z_{-f(x_k=0)}$;
      Append TMP with T_f';
    Append CL with TMP

After we scan every possible dephased matrix for the given number of parties and dimension and repeat the above procedure we are left as the output with the full list of dephased FFE states for the number of parties and dimension considered, separated into the full list of LFP classes.

Let us now see how this algorith works in practice in the particular example of all 3×3 FFE states. Let us start considering the function image

$$f = \begin{pmatrix} 0 & 0 & 0 \\ 0 & 0 & 0 \\ 0 & 0 & 0 \end{pmatrix} \longrightarrow T_f = \begin{pmatrix} 1 & 1 & 1 \\ 1 & 1 & 1 \\ 1 & 1 & 1 \end{pmatrix}$$

and apply the following list of passages:

1. Check if it belongs already to some LFP class.
2. If not, store it to the next class and proceed further.
   (a) Swap two components of the coefficient tensor, e.g.,
   $$(T_f)_{1,i_2,\ldots,i_n} \longleftrightarrow (T_f)_{2,i_2,\ldots,i_n}, \tag{42}$$
   which amounts to apply a local X_{π_1} to the FFE state. In this case, our initial tensor is left invariant under this operation.
   (b) Then, bring the tensor back to the dephased form, by subtracting the functions $f(0, i_2, \ldots, i_n)$, $f(i_1, 0, \ldots, i_n)$ etc. (which amounts to apply local Z operators of the form $Z_{-f(i_1=0)}$, $Z_{-f(i_2=0)}$, etc.). Again, in this case the tensor is already in dephased form.
   (c) Check if the tensor is already in some LFP class. Yes, in this case it is already stored. So, stop here and repeat from step 2a with a different swap.

We see that our initial matrix is completely invariant under permutations of rows and columns. Thus it is the only member of its class, which is that of product states. In fact, this corresponds to the FFE state $|+\rangle^{\otimes 2}$.

Afterwards, we can consider for example the matrix (remember that we have to change only its core)

$$f = \begin{pmatrix} 0 & 0 & 0 \\ 0 & 1 & 0 \\ 0 & 0 & 0 \end{pmatrix} \longrightarrow T_f = \begin{pmatrix} 1 & 1 & 1 \\ 1 & \omega_3 & 1 \\ 1 & 1 & 1 \end{pmatrix},$$

and apply again the passages 1 and 2 above. This time, permutations of the matrix rows and columns give a nontrivial result. Let us then swap columns 1 and 3. We get (for simplicity working only with the function image matrix)

$$\begin{pmatrix} 0 & 0 & 0 \\ 0 & 1 & 0 \\ 0 & 0 & 0 \end{pmatrix} \overset{\text{cols } 2\leftrightarrow 3}{\longrightarrow} \begin{pmatrix} 0 & 0 & 0 \\ 0 & 0 & 1 \\ 0 & 0 & 0 \end{pmatrix},$$

which is already in dephased form as well. Then we do

(d) Store the resulting core state into the same LFP class.

Then repeat from step 2a with a different swap. We can now permute, for example, the rows 1 and 2 and columns 2 and 3, obtaining

$$\begin{pmatrix} 0 & 0 & 0 \\ 0 & 1 & 0 \\ 0 & 0 & 0 \end{pmatrix} \overset{\substack{\text{cols } 2\leftrightarrow 3 \\ \text{rows } 1\leftrightarrow 2}}{\longrightarrow} \begin{pmatrix} 0 & 0 & 1 \\ 0 & 0 & 0 \\ 0 & 0 & 0 \end{pmatrix},$$

which is now not in normal form. Thus, for bringing it back to normal form (step 2b) we subtract 1 to all the elements of the third column, getting to (remember that we take numbers modulo 3)

$$\begin{pmatrix} 0 & 0 & 1 \\ 0 & 0 & 0 \\ 0 & 0 & 0 \end{pmatrix} \overset{+2 \text{ col } 3}{\longrightarrow} \begin{pmatrix} 0 & 0 & 0 \\ 0 & 0 & 2 \\ 0 & 0 & 2 \end{pmatrix},$$

which is a different dephased matrix belonging to the same LFP class. Thus, we store it to the same class and repeat with a different swap (step 2d).

Let us for example swap the columns 1 and 2 and rows 1 and 2, obtaining

$$\begin{pmatrix} 0 & 0 & 0 \\ 0 & 1 & 0 \\ 0 & 0 & 0 \end{pmatrix} \overset{\substack{\text{cols } 1\leftrightarrow 2 \\ \text{rows } 1\leftrightarrow 2}}{\longrightarrow} \begin{pmatrix} 1 & 0 & 0 \\ 0 & 0 & 0 \\ 0 & 0 & 0 \end{pmatrix},$$

which, again, can be brought back to dephased form by adding 2 to the first column and then subtracting 2 from the second and third rows.

$$\begin{pmatrix} 1 & 0 & 0 \\ 0 & 0 & 0 \\ 0 & 0 & 0 \end{pmatrix} \overset{+2 \text{ col } 1}{\longrightarrow} \begin{pmatrix} 0 & 0 & 0 \\ 2 & 0 & 0 \\ 2 & 0 & 0 \end{pmatrix},$$

This way we get to

$$\begin{pmatrix} 0 & 0 & 0 \\ 2 & 0 & 0 \\ 2 & 0 & 0 \end{pmatrix} \overset{+1 \text{ rows } 2,3}{\longrightarrow} \begin{pmatrix} 0 & 0 & 0 \\ 0 & 1 & 1 \\ 0 & 1 & 1 \end{pmatrix},$$

which is yet another dephased matrix belonging to the same LFP class. Proceeding further this way we will at some point find all possible matrices belonging to that class (which is listed as Class 2 in Sec. G), exhausting also all possible permutations of the initially chosen state. We can then pick another initial state which is not in the same class and repeat the same procedure, until we exhaust all possible dephased matrices. This way it is possible to do by hand the full LFP classification in $d = 3$, which results in the classes listed in Sec. G below. However, already the bipartite $d = 5$ case and the tripartite $d = 3$ case are too hard to be handled with regular computational power.

A brute force algorithm can be also given for finding all the LU classes in the bipartite case. The idea is based on the observation that each LU class in a bipartite $d \times d$ system is associated to a specific vector $\mathbf{t}_f = (\mathrm{tr}(\rho_f^2), \ldots, \mathrm{tr}(\rho_f^d))$, where $\mathrm{tr}(\rho_f) = 1$ has been omitted. I.e., all matrices T_f in the same LU class will have the same values of the vector $\mathbf{t}_f$. This comes from the fact that all matrices T_f in the same LU class will have the same vector of singular values $\lambda(T_f)$, which, in turn, is related to the coefficients of the characteristic polynomial of ρ_f, and those coefficients are given by linear combinations of the elements of $\mathbf{t}_f$.

Then, a brute force algorithm to find all the LU classes works by: (1) scanning all possible dephased coefficient matrices T_f; (2) calculating for each of them the value of the vector t_f (3) store and count the

different t_f and the associated T_f.

Algorithm 2: Brute force LU classification of d^2-dimensional FFE states

Create an empty list of classes Cl;
Create an empty list of traces vectors cl;
for *all dephased coefficient matrices* $T_f \in \mathbb{C}^{d^2}$ **do**
  Calculate $\rho_f \longleftarrow T_f^\dagger T_f$;
  for k *from* 2 *to* d **do**
    Create and calculate the components $t_f(k) \longleftarrow \mathrm{tr}(\rho_f^k)$;
  if $t_f \notin cl$ **then**
    Assign t_f to $cl(end+1, end+1) \longleftarrow t_f$;
    Assign T_f to the LU class $Cl(end+1, end+1) \longleftarrow T_f$;
  else
    Find the i for which $t_f \in cl(i)$;
    Assign T_f to the LU class $Cl(i, end+1) \longleftarrow T_f$;

Note that also the performance of this algorithm scales very unfavorably with d, since all possible dephased $d \times d$ FFE states must be scanned. Still, in the $d = 3$ it is easy to make the classification analytically and in the $d = 4$ case in a short time with a regular pc.

Let us then illustrate how the algorithm works in the $d = 3$ case. Let us consider a generic 3×3 dephased FFE state

$$T_f = \tfrac{1}{3}\begin{pmatrix} 1 & 1 & 1 \\ 1 & \omega_3^a & \omega_3^b \\ 1 & \omega_3^c & \omega_3^d \end{pmatrix}. \tag{43}$$

Let us now take the single particle reduced density matrix ρ_f and calculate the traces of its 2-nd and 3-rd power. We obtain

$$\begin{aligned}
\mathrm{tr}(\rho_f^2) &= \frac{5}{9} + \frac{4}{81}\Big(R\omega_3(a) + R\omega_3(b) + R\omega_3(c) + R\omega_3(d) + R\omega_3(a-b) + R\omega_3(a-c) \\
&\quad + R\omega_3(b-d) + R\omega_3(c-d) + R\omega_3(a-b-c+d) \Big), \\
\mathrm{tr}(\rho_f^3) &= \frac{29}{81} + \frac{16}{243}\Big(R\omega_3(a) + R\omega_3(b) + R\omega_3(c) + R\omega_3(d) + +R\omega_3(a-b) + R\omega_3(a-c) \\
&\quad + R\omega_3(b-d) + R\omega_3(c-d) + R\omega_3(a-b-c+d) \Big) \\
&\quad + \frac{2}{243}\Big(R\omega_3(a-d) + R\omega_3(b-c) + R\omega_3(a-b-c) + R\omega_3(a-b+d) + R\omega_3(a-c+d) \\
&\qquad + R\omega_3(b+c-d) \Big),
\end{aligned} \tag{44}$$

where we used the shortened notation $R\omega_3(x) := \cos(2\pi x/3)$.

Now, let us count how many different possible vectors t_f there are in $d = 3$. We see from Eq. (44) that, since the function $R\omega_3$ is even in x, those expressions have several symmetries with respect to exchanging the numbers (a, b, c, d). For example, the exchanges $a \leftrightarrow d$ leaves both expression invariant, as well as $b \leftrightarrow c$. The latter corresponds to just taking the transpose of T_f, while the former is connected with the complex conjugation of T_f. Thus, we can consider just the cases in which $a \geq d$ and $b \geq c$, which are just 36 out of the total 81. Also, the permutations $(a \leftrightarrow b, c \leftrightarrow d)$ and $(a \leftrightarrow c, b \leftrightarrow d)$ leave both expressions invariant. Note that these are just LFP operations on the T_f matrix (i.e., swaps of two rows or columns). Due to these symmetries, we see that it is sufficient to scan just 21 cases, of which only 6 give different values of $\mathbf{t}_f$. Thus, we see that in total we have 6 different LU classes in $d = 3$.

This example also suggests that in general more clever algorithms can be found by identifying from the beginning what symmetries there have to be imposed on the matrix coefficients based, e.g., on LFP operations, transpositions and complex conjugations among other LU operations. However, while the $d = 4$ case is still easy to handle, and results in 127 different LU classes, larger dimensions become already intractable with regular computational power, even if symmetries are taken into account.

G LFP and LU classes of bipartite qutrits

In this appendix we list all the LFP equivalence classes of a bipartite qutrit FFE states. We added a comprehensive list of matrices to an online repository.

Table 3: The full classification of the equivalences of bipartite FFE/TEH states under LU and LFP operations in dimension 3. The horizontal lines indicate different LFP classes while the singular values identify different LU classes.

Schmidt Rank	Singular Values	Polynomial
1	(1.0, 0.0, 0.0)	$f(x,y) = 0$
2	(0.90506, 0.42527, 0.0)	$f(x,y) = x^2y^2 + x^2y + xy^2 + xy$ $f(x,y) = x^2y^2 + 2\,x^2y + xy^2 + 2\,xy$ $f(x,y) = x^2y^2 + x^2y + 2\,xy^2 + 2\,xy$ $f(x,y) = x^2y^2 + 2\,x^2y + 2\,xy^2 + xy$ $f(x,y) = x^2y^2 + xy^2$ $f(x,y) = x^2y^2 + x^2y$ $f(x,y) = x^2y^2 + 2\,x^2y$ $f(x,y) = x^2y^2 + 2\,xy^2$ $f(x,y) = x^2y^2$
2	(0.90506, 0.42527, 0.0)	$f(x,y) = 2\,x^2y^2 + 2\,x^2y + 2\,xy^2 + 2\,xy$ $f(x,y) = 2\,x^2y^2 + x^2y + 2\,xy^2 + xy$ $f(x,y) = 2\,x^2y^2 + 2\,x^2y + xy^2 + xy$ $f(x,y) = 2\,x^2y^2 + x^2y + xy^2 + 2\,xy$ $f(x,y) = 2\,x^2y^2 + 2\,xy^2$ $f(x,y) = 2\,x^2y^2 + 2\,x^2y$ $f(x,y) = 2\,x^2y^2 + x^2y$ $f(x,y) = 2\,x^2y^2 + xy^2$ $f(x,y) = 2\,x^2y^2$
2	(0.8165, 0.57735, 0.0)	$f(x,y) = 2\,xy^2$ $f(x,y) = xy^2$ $f(x,y) = xy^2 + xy$ $f(x,y) = 2\,xy^2 + 2\,xy$ $f(x,y) = xy^2 + 2\,xy$ $f(x,y) = 2\,xy^2 + xy$
2	(0.8165, 0.57735, 0.0)	$f(x,y) = 2\,x^2y$ $f(x,y) = x^2y$ $f(x,y) = 2\,x^2y + xy$ $f(x,y) = x^2y + 2\,xy$ $f(x,y) = 2\,x^2y + 2\,xy$ $f(x,y) = x^2y + xy$
3	(0.77814, 0.57735, 0.24732)	$f(x,y) = 2\,x^2y^2 + 2\,xy$ $f(x,y) = 2\,x^2y^2 + xy$ $f(x,y) = 2\,x^2y^2 + 2\,x^2y + 2\,xy$ $f(x,y) = 2\,x^2y^2 + x^2y + xy$ $f(x,y) = 2\,x^2y^2 + x^2y + 2\,xy$ $f(x,y) = 2\,x^2y^2 + 2\,x^2y + xy$ $f(x,y) = 2\,x^2y^2 + 2\,xy^2 + 2\,xy$ $f(x,y) = 2\,x^2y^2 + xy^2 + xy$ $f(x,y) = 2\,x^2y^2 + 2\,xy^2 + xy$ $f(x,y) = 2\,x^2y^2 + xy^2 + 2\,xy$ $f(x,y) = 2\,x^2y^2 + x^2y + xy^2 + xy$ $f(x,y) = 2\,x^2y^2 + 2\,x^2y + xy^2 + 2\,xy$ $f(x,y) = 2\,x^2y^2 + x^2y + 2\,xy^2 + 2\,xy$ $f(x,y) = 2\,x^2y^2 + 2\,x^2y + 2\,xy^2 + xy$ $f(x,y) = 2\,x^2y^2 + 2\,x^2y + xy^2$ $f(x,y) = 2\,x^2y^2 + x^2y + 2\,xy^2$ $f(x,y) = 2\,x^2y^2 + 2\,x^2y + 2\,xy^2$ $f(x,y) = 2\,x^2y^2 + x^2y + xy^2$

Schmidt Rank	Singular Values	Polynomial
3	(0.77814, 0.57735, 0.24732)	$f(x,y) = x^2y^2 + xy$ $f(x,y) = x^2y^2 + 2\,xy$ $f(x,y) = x^2y^2 + x^2y + xy$ $f(x,y) = x^2y^2 + 2\,x^2y + 2\,xy$ $f(x,y) = x^2y^2 + 2\,x^2y + xy$ $f(x,y) = x^2y^2 + x^2y + 2\,xy$ $f(x,y) = x^2y^2 + xy^2 + xy$ $f(x,y) = x^2y^2 + 2\,xy^2 + 2\,xy$ $f(x,y) = x^2y^2 + xy^2 + 2\,xy$ $f(x,y) = x^2y^2 + 2\,xy^2 + xy$ $f(x,y) = x^2y^2 + 2\,x^2y + 2\,xy^2 + 2\,xy$ $f(x,y) = x^2y^2 + x^2y + 2\,xy^2 + xy$ $f(x,y) = x^2y^2 + 2\,x^2y + xy^2 + xy$ $f(x,y) = x^2y^2 + x^2y + xy^2 + 2\,xy$ $f(x,y) = x^2y^2 + x^2y + 2\,xy^2$ $f(x,y) = x^2y^2 + 2\,x^2y + xy^2$ $f(x,y) = x^2y^2 + x^2y + xy^2$ $f(x,y) = x^2y^2 + 2\,x^2y + 2\,xy^2$
3	(0.84403, 0.4491, 0.29313)	$f(x,y) = 2\,x^2y + 2\,xy^2$ $f(x,y) = x^2y + xy^2$ $f(x,y) = x^2y + 2\,xy^2$ $f(x,y) = 2\,x^2y + xy^2$ $f(x,y) = x^2y + xy^2 + 2\,xy$ $f(x,y) = 2\,x^2y + xy^2 + xy$ $f(x,y) = x^2y + 2\,xy^2 + xy$ $f(x,y) = 2\,x^2y + 2\,xy^2 + 2\,xy$ $f(x,y) = 2\,x^2y + 2\,xy^2 + xy$ $f(x,y) = x^2y + 2\,xy^2 + 2\,xy$ $f(x,y) = 2\,x^2y + xy^2 + 2\,xy$ $f(x,y) = x^2y + xy^2 + xy$
3	(0.57735, 0.57735, 0.57735)	$f(x,y) = 2\,xy$ $f(x,y) = xy$

H LFP and LU classes of bipartite ququarts

In this appendix we list all the LFP and LU equivalence classes of a bipartite qutquart *TEH* states, i.e., only states which correspond to polynomial functions. We added a comprehensive list of the matrices to an online repository.

Table 4: The full classification of the equivalences of bipartite *TEH* states under LU and LFP operations in dimension 4. The horizontal lines indicate different LFP classes while the singular values identify different LU classes.

Schmidt Rank	Singular Values	Polynomial
1	(1.0, 0.0, 0.0, 0.0)	$f(x,y) = 0$
2	(0.92388, 0.38268, 0.0, 0.0)	$f(x,y) = x^2y + xy^2 + xy$ $f(x,y) = x^2y + xy^2 + 3\,xy$
2	(0.86603, 0.5, 0.0, 0.0)	$f(x,y) = xy^3 + xy^2$ $f(x,y) = xy^3 + xy$ $f(x,y) = xy^3 + xy^2 + 2\,xy$ $f(x,y) = xy^3 + 3\,xy$
2	(0.86603, 0.5, 0.0, 0.0)	$f(x,y) = x^3y + x^2y$ $f(x,y) = x^3y + xy$ $f(x,y) = x^3y + x^2y + 2\,xy$ $f(x,y) = x^3y + 3\,xy$

Schmidt Rank	Singular Values	Polynomial
2	(0.86603, 0.5, 0.0, 0.0)	$f(x,y) = xy^3 + x^2y + xy^2$ $f(x,y) = xy^3 + x^2y + xy$ $f(x,y) = xy^3 + x^2y + xy^2 + 2\,xy$ $f(x,y) = xy^3 + x^2y + 3\,xy$
2	(0.86603, 0.5, 0.0, 0.0)	$f(x,y) = x^3y + x^2y + xy^2$ $f(x,y) = x^3y + xy^2 + xy$ $f(x,y) = x^3y + x^2y + xy^2 + 2\,xy$ $f(x,y) = x^3y + xy^2 + 3\,xy$
2	(0.70711, 0.70711, 0.0, 0.0)	$f(x,y) = x^2y + xy$ $f(x,y) = xy^2 + xy$ $f(x,y) = 2\,xy$ $f(x,y) = x^2y + 3\,xy$ $f(x,y) = xy^2 + 3\,xy$
2	(0.70711, 0.70711, 0.0, 0.0)	$f(x,y) = xy^2$ $f(x,y) = xy^2 + 2\,xy$
2	(0.70711, 0.70711, 0.0, 0.0)	$f(x,y) = x^2y$ $f(x,y) = x^2y + 2\,xy$
3	(0.80902, 0.5, 0.30902, 0.0)	$f(x,y) = x^3y + xy^3$ $f(x,y) = x^3y + xy^3 + x^2y + xy^2$ $f(x,y) = x^3y + xy^3 + x^2y + xy$ $f(x,y) = x^3y + xy^3 + xy^2 + xy$ $f(x,y) = x^3y + xy^3 + 2\,xy$ $f(x,y) = x^3y + xy^3 + x^2y + xy^2 + 2\,xy$ $f(x,y) = x^3y + xy^3 + x^2y + 3\,xy$ $f(x,y) = x^3y + xy^3 + xy^2 + 3\,xy$
3	(0.80902, 0.5, 0.30902, 0.0)	$f(x,y) = x^3y + xy^3 + x^2y$ $f(x,y) = x^3y + xy^3 + xy^2$ $f(x,y) = x^3y + xy^3 + xy$ $f(x,y) = x^3y + xy^3 + x^2y + xy^2 + xy$ $f(x,y) = x^3y + xy^3 + x^2y + 2\,xy$ $f(x,y) = x^3y + xy^3 + xy^2 + 2\,xy$ $f(x,y) = x^3y + xy^3 + 3\,xy$ $f(x,y) = x^3y + xy^3 + x^2y + xy^2 + 3\,xy$
3	(0.70711, 0.5, 0.5, 0.0)	$f(x,y) = xy^3 + x^2y$ $f(x,y) = xy^3 + x^2y + xy^2 + xy$ $f(x,y) = xy^3 + x^2y + 2\,xy$ $f(x,y) = xy^3 + x^2y + xy^2 + 3\,xy$
3	(0.70711, 0.5, 0.5, 0.0)	$f(x,y) = xy^3$ $f(x,y) = xy^3 + xy^2 + xy$ $f(x,y) = xy^3 + 2\,xy$ $f(x,y) = xy^3 + xy^2 + 3\,xy$
3	(0.70711, 0.5, 0.5, 0.0)	$f(x,y) = x^3y + xy^2$ $f(x,y) = x^3y + x^2y + xy^2 + xy$ $f(x,y) = x^3y + xy^2 + 2\,xy$ $f(x,y) = x^3y + x^2y + xy^2 + 3\,xy$
3	(0.70711, 0.5, 0.5, 0.0)	$f(x,y) = x^3y$ $f(x,y) = x^3y + x^2y + xy$ $f(x,y) = x^3y + 2\,xy$ $f(x,y) = x^3y + x^2y + 3\,xy$
4	(0.5, 0.5, 0.5, 0.5)	$f(x,y) = x^2y + xy^2$ $f(x,y) = x^2y + xy^2 + 2\,xy$
4	(0.5, 0.5, 0.5, 0.5)	$f(x,y) = xy$ $f(x,y) = 3\,xy$

I LGP and LU classes of bipartite qusext

In this appendix we list all the LFP equivalence classes of a bipartite qusext *TEH* states, i.e., states that correspond to polynomial functions. We added a comprehensive list of matrices to an online repository.

Table 5: The full classification of the equivalences of bipartite *TEH* states und LU and LFP operations in dimension 6. The horizontal lines indicate different LFP classes while the singular values identify different LU classes.

Schmidt Rank	Singular Values	Polynomial
1	(1.0, 0.0, 0.0, 0.0, 0.0, 0.0)	$f(x,y) = 0$
2	(0.70711, 0.70711, 0.0, 0.0, 0.0, 0.0)	$f(x,y) = 3\,xy$
2	(0.90506, 0.42527, 0.0, 0.0, 0.0, 0.0)	$f(x,y) = 2\,x^2y^2$ $f(x,y) = 2\,x^2y^2 + 2\,xy^2$ $f(x,y) = 2\,x^2y^2 + xy^2 + 3\,xy$
2	(0.90506, 0.42527, 0.0, 0.0, 0.0, 0.0)	$f(x,y) = x^2y^2 + x^2y$ $f(x,y) = x^2y^2 + x^2y + xy^2 + xy$ $f(x,y) = x^2y^2 + 2\,x^2y + 2\,xy^2 + xy$ $f(x,y) = x^2y^2 + 2\,x^2y + xy^2 + 2\,xy$ $f(x,y) = x^2y^2 + x^2y + 2\,xy^2 + 2\,xy$ $f(x,y) = x^2y^2 + 2\,x^2y + 3\,xy$
2	(0.90506, 0.42527, 0.0, 0.0, 0.0, 0.0)	$f(x,y) = 2\,x^2y^2 + 2\,x^2y$ $f(x,y) = 2\,x^2y^2 + 2\,x^2y + xy^2 + xy$ $f(x,y) = 2\,x^2y^2 + x^2y + 2\,xy^2 + xy$ $f(x,y) = 2\,x^2y^2 + x^2y + xy^2 + 2\,xy$ $f(x,y) = 2\,x^2y^2 + 2\,x^2y + 2\,xy^2 + 2\,xy$ $f(x,y) = 2\,x^2y^2 + x^2y + 3\,xy$
2	(0.90506, 0.42527, 0.0, 0.0, 0.0, 0.0)	$f(x,y) = x^2y^2 + xy^2$ $f(x,y) = x^2y^2 + 3\,xy$ $f(x,y) = x^2y^2 + 2\,xy^2 + 3\,xy$
2	(0.8165, 0.57735, 0.0, 0.0, 0.0, 0.0)	$f(x,y) = 2\,x^2y$ $f(x,y) = x^2y + xy$ $f(x,y) = 2\,x^2y + 2\,xy$ $f(x,y) = x^2y + 3\,xy$ $f(x,y) = 2\,x^2y + 4\,xy$ $f(x,y) = x^2y + 5\,xy$
2	(0.8165, 0.57735, 0.0, 0.0, 0.0, 0.0)	$f(x,y) = 2\,xy^2$ $f(x,y) = xy^2 + 3\,xy$
2	(0.8165, 0.57735, 0.0, 0.0, 0.0, 0.0)	$f(x,y) = xy^2 + xy$ $f(x,y) = 2\,xy^2 + 2\,xy$ $f(x,y) = 2\,xy^2 + 4\,xy$ $f(x,y) = xy^2 + 5\,xy$
3	(0.84403, 0.4491, 0.29313, 0.0, 0.0, 0.0)	$f(x,y) = x^2y + xy^2$ $f(x,y) = 2\,x^2y + 2\,xy^2$ $f(x,y) = 2\,x^2y + xy^2 + xy$ $f(x,y) = x^2y + 2\,xy^2 + xy$ $f(x,y) = x^2y + xy^2 + 2\,xy$ $f(x,y) = 2\,x^2y + 2\,xy^2 + 2\,xy$ $f(x,y) = 2\,x^2y + xy^2 + 3\,xy$ $f(x,y) = x^2y + 2\,xy^2 + 3\,xy$ $f(x,y) = x^2y + xy^2 + 4\,xy$ $f(x,y) = 2\,x^2y + 2\,xy^2 + 4\,xy$ $f(x,y) = 2\,x^2y + xy^2 + 5\,xy$ $f(x,y) = x^2y + 2\,xy^2 + 5\,xy$

Schmidt Rank	Singular Values	Polynomial
3	(0.77814, 0.57735, 0.24732, 0.0, 0.0, 0.0)	$f(x,y) = 2\,x^2y^2 + x^2y + xy^2$ $f(x,y) = 2\,x^2y^2 + 2\,x^2y + 2\,xy^2$ $f(x,y) = 2\,x^2y^2 + x^2y + xy$ $f(x,y) = 2\,x^2y^2 + 2\,x^2y + 2\,xy$ $f(x,y) = 2\,x^2y^2 + 2\,x^2y + xy^2 + 3\,xy$ $f(x,y) = 2\,x^2y^2 + x^2y + 2\,xy^2 + 3\,xy$ $f(x,y) = 2\,x^2y^2 + 2\,x^2y + 4\,xy$ $f(x,y) = 2\,x^2y^2 + x^2y + xy^2 + 4\,xy$ $f(x,y) = 2\,x^2y^2 + 2\,x^2y + 2\,xy^2 + 4\,xy$ $f(x,y) = 2\,x^2y^2 + x^2y + 5\,xy$ $f(x,y) = 2\,x^2y^2 + 2\,x^2y + xy^2 + 5\,xy$ $f(x,y) = 2\,x^2y^2 + x^2y + 2\,xy^2 + 5\,xy$
3	(0.77814, 0.57735, 0.24732, 0.0, 0.0, 0.0)	$f(x,y) = x^2y^2 + 2\,x^2y + xy^2$ $f(x,y) = x^2y^2 + x^2y + 2\,xy^2$ $f(x,y) = x^2y^2 + 2\,x^2y + xy$ $f(x,y) = x^2y^2 + x^2y + 2\,xy$ $f(x,y) = x^2y^2 + x^2y + xy^2 + 3\,xy$ $f(x,y) = x^2y^2 + 2\,x^2y + 2\,xy^2 + 3\,xy$ $f(x,y) = x^2y^2 + x^2y + 4\,xy$ $f(x,y) = x^2y^2 + 2\,x^2y + xy^2 + 4\,xy$ $f(x,y) = x^2y^2 + x^2y + 2\,xy^2 + 4\,xy$ $f(x,y) = x^2y^2 + 2\,x^2y + 5\,xy$ $f(x,y) = x^2y^2 + x^2y + xy^2 + 5\,xy$ $f(x,y) = x^2y^2 + 2\,x^2y + 2\,xy^2 + 5\,xy$
3	(0.77814, 0.57735, 0.24732, 0.0, 0.0, 0.0)	$f(x,y) = x^2y^2 + xy$ $f(x,y) = x^2y^2 + 2\,xy^2 + xy$ $f(x,y) = x^2y^2 + xy^2 + 2\,xy$ $f(x,y) = x^2y^2 + xy^2 + 4\,xy$ $f(x,y) = x^2y^2 + 5\,xy$ $f(x,y) = x^2y^2 + 2\,xy^2 + 5\,xy$
3	(0.77814, 0.57735, 0.24732, 0.0, 0.0, 0.0)	$f(x,y) = 2\,x^2y^2 + xy^2 + xy$ $f(x,y) = 2\,x^2y^2 + 2\,xy$ $f(x,y) = 2\,x^2y^2 + 2\,xy^2 + 2\,xy$ $f(x,y) = 2\,x^2y^2 + 4\,xy$ $f(x,y) = 2\,x^2y^2 + 2\,xy^2 + 4\,xy$ $f(x,y) = 2\,x^2y^2 + xy^2 + 5\,xy$
3	(0.57735, 0.57735, 0.57735, 0.0, 0.0, 0.0)	$f(x,y) = 2\,xy$ $f(x,y) = 4\,xy$
4	(0.63998, 0.63998, 0.30071, 0.30071, 0.0, 0.0)	$f(x,y) = x^2y^2$ $f(x,y) = x^2y^2 + 2\,xy^2$ $f(x,y) = x^2y^2 + xy^2 + 3\,xy$
4	(0.63998, 0.63998, 0.30071, 0.30071, 0.0, 0.0)	$f(x,y) = 2\,x^2y^2 + x^2y$ $f(x,y) = 2\,x^2y^2 + 2\,x^2y + 3\,xy$ $f(x,y) = 2\,x^2y^2 + 2\,x^2y + xy^2 + 4\,xy$ $f(x,y) = 2\,x^2y^2 + x^2y + 2\,xy^2 + 4\,xy$ $f(x,y) = 2\,x^2y^2 + x^2y + xy^2 + 5\,xy$ $f(x,y) = 2\,x^2y^2 + 2\,x^2y + 2\,xy^2 + 5\,xy$
4	(0.63998, 0.63998, 0.30071, 0.30071, 0.0, 0.0)	$f(x,y) = x^2y^2 + 2\,x^2y$ $f(x,y) = x^2y^2 + x^2y + 3\,xy$ $f(x,y) = x^2y^2 + x^2y + xy^2 + 4\,xy$ $f(x,y) = x^2y^2 + 2\,x^2y + 2\,xy^2 + 4\,xy$ $f(x,y) = x^2y^2 + 2\,x^2y + xy^2 + 5\,xy$ $f(x,y) = x^2y^2 + x^2y + 2\,xy^2 + 5\,xy$
4	(0.63998, 0.63998, 0.30071, 0.30071, 0.0, 0.0)	$f(x,y) = 2\,x^2y^2 + xy^2$ $f(x,y) = 2\,x^2y^2 + 3\,xy$ $f(x,y) = 2\,x^2y^2 + 2\,xy^2 + 3\,xy$

Schmidt Rank	Singular Values	Polynomial
4	(0.57735, 0.57735, 0.40825, 0.40825, 0.0, 0.0)	$f(x,y) = x^2y$ $f(x,y) = 2\,x^2y + xy$ $f(x,y) = x^2y + 2\,xy$ $f(x,y) = 2\,x^2y + 3\,xy$ $f(x,y) = x^2y + 4\,xy$ $f(x,y) = 2\,x^2y + 5\,xy$
4	(0.57735, 0.57735, 0.40825, 0.40825, 0.0, 0.0)	$f(x,y) = xy^2$ $f(x,y) = 2\,xy^2 + 3\,xy$
4	(0.57735, 0.57735, 0.40825, 0.40825, 0.0, 0.0)	$f(x,y) = 2\,xy^2 + xy$ $f(x,y) = xy^2 + 2\,xy$ $f(x,y) = xy^2 + 4\,xy$ $f(x,y) = 2\,xy^2 + 5\,xy$
6	(0.55023, 0.55023, 0.40825, 0.40825, 0.17488, 0.17488)	$f(x,y) = x^2y^2 + x^2y + xy^2$ $f(x,y) = x^2y^2 + 2\,x^2y + 2\,xy^2$ $f(x,y) = x^2y^2 + x^2y + xy$ $f(x,y) = x^2y^2 + 2\,x^2y + xy^2 + xy$ $f(x,y) = x^2y^2 + x^2y + 2\,xy^2 + xy$ $f(x,y) = x^2y^2 + 2\,x^2y + 2\,xy$ $f(x,y) = x^2y^2 + x^2y + xy^2 + 2\,xy$ $f(x,y) = x^2y^2 + 2\,x^2y + 2\,xy^2 + 2\,xy$ $f(x,y) = x^2y^2 + 2\,x^2y + xy^2 + 3\,xy$ $f(x,y) = x^2y^2 + x^2y + 2\,xy^2 + 3\,xy$ $f(x,y) = x^2y^2 + 2\,x^2y + 4\,xy$ $f(x,y) = x^2y^2 + x^2y + 5\,xy$
6	(0.55023, 0.55023, 0.40825, 0.40825, 0.17488, 0.17488)	$f(x,y) = 2\,x^2y^2 + 2\,x^2y + xy^2$ $f(x,y) = 2\,x^2y^2 + x^2y + 2\,xy^2$ $f(x,y) = 2\,x^2y^2 + 2\,x^2y + xy$ $f(x,y) = 2\,x^2y^2 + x^2y + xy^2 + xy$ $f(x,y) = 2\,x^2y^2 + 2\,x^2y + 2\,xy^2 + xy$ $f(x,y) = 2\,x^2y^2 + x^2y + 2\,xy$ $f(x,y) = 2\,x^2y^2 + 2\,x^2y + xy^2 + 2\,xy$ $f(x,y) = 2\,x^2y^2 + x^2y + 2\,xy^2 + 2\,xy$ $f(x,y) = 2\,x^2y^2 + x^2y + xy^2 + 3\,xy$ $f(x,y) = 2\,x^2y^2 + 2\,x^2y + 2\,xy^2 + 3\,xy$ $f(x,y) = 2\,x^2y^2 + x^2y + 4\,xy$ $f(x,y) = 2\,x^2y^2 + 2\,x^2y + 5\,xy$
6	(0.55023, 0.55023, 0.40825, 0.40825, 0.17488, 0.17488)	$f(x,y) = 2\,x^2y^2 + xy$ $f(x,y) = 2\,x^2y^2 + 2\,xy^2 + xy$ $f(x,y) = 2\,x^2y^2 + xy^2 + 2\,xy$ $f(x,y) = 2\,x^2y^2 + xy^2 + 4\,xy$ $f(x,y) = 2\,x^2y^2 + 5\,xy$ $f(x,y) = 2\,x^2y^2 + 2\,xy^2 + 5\,xy$
6	(0.55023, 0.55023, 0.40825, 0.40825, 0.17488, 0.17488)	$f(x,y) = x^2y^2 + xy^2 + xy$ $f(x,y) = x^2y^2 + 2\,xy$ $f(x,y) = x^2y^2 + 2\,xy^2 + 2\,xy$ $f(x,y) = x^2y^2 + 4\,xy$ $f(x,y) = x^2y^2 + 2\,xy^2 + 4\,xy$ $f(x,y) = x^2y^2 + xy^2 + 5\,xy$

Schmidt Rank	Singular Values	Polynomial
6	(0.59682, 0.59682, 0.31756, 0.31756, 0.20727, 0.20727)	$f(x,y) = 2\,x^2y + xy^2$ $f(x,y) = x^2y + 2\,xy^2$ $f(x,y) = x^2y + xy^2 + xy$ $f(x,y) = 2\,x^2y + 2\,xy^2 + xy$ $f(x,y) = 2\,x^2y + xy^2 + 2\,xy$ $f(x,y) = x^2y + 2\,xy^2 + 2\,xy$ $f(x,y) = x^2y + xy^2 + 3\,xy$ $f(x,y) = 2\,x^2y + 2\,xy^2 + 3\,xy$ $f(x,y) = 2\,x^2y + xy^2 + 4\,xy$ $f(x,y) = x^2y + 2\,xy^2 + 4\,xy$ $f(x,y) = x^2y + xy^2 + 5\,xy$ $f(x,y) = 2\,x^2y + 2\,xy^2 + 5\,xy$
6	(0.40825, 0.40825, 0.40825, 0.40825, 0.40825, 0.40825)	$f(x,y) = xy$ $f(x,y) = 5\,xy$

5 On the role of entanglement in qudit-based circuit compression

5.1 Summary

The circuit model of quantum computation provides a framework in which quantum algorithms are represented as sequences of unitary operations arranged into circuits. These operations are restricted to a finite set of one- and two-partite gates that approximate arbitrary unitaries to any desired precision. Although the existence of such decompositions is well established, optimal constructions are generally unknown, motivating strategies to reduce circuit complexity within this model.

In this work, we address this challenge by proposing a two-stage procedure to systematically reduce the *non-local* cost of a circuit. Our method applies whenever a low-dimensional implementation is known and provides a constructive route to derive high-dimensional circuits that can subsequently be optimized.

We begin from a given low-dimensional circuit and group multiple subsystems into higher-dimensional ones, mapping parts of the original circuit into local operations on the grouped system. In a second step, we optimize the remaining non-local operations using entangling gates available in the higher-dimensional setting. Thus, from a known qubit circuit we obtain a functionally equivalent qudit circuit whose non-local content can be further simplified by exploiting native qudit interactions.

The reduction we target is measured in the *non-local gate count*, which we adopt as the relevant cost in the NISQ regime, where coherence, two-body fidelity, and connectivity constraints typically make non-local operations the dominant bottleneck. This choice does not imply improvements under *other* complexity measures (e.g., T-gate count in fault-tolerant settings); rather, it focuses on the operational cost that is limiting in near-term architectures.

We model the grouping step as a graph-partitioning problem: each qubit is a node, with an edge between two nodes whenever at least one non-local gate acts between them, weighted by the number of such gates. The goal is to find a partition that minimizes the weight of edges crossing between parts, subject to local-dimension constraints on each group. This reduces the first stage to a (minimum) k-cut instance and makes the method platform independent at this stage.

In the second stage, we exploit the richer entangling structure available in high-dimensional systems. Once subsets of qubits have been grouped into qudits, gates acting between these subsystems are adapted accordingly. Rather than using embedded constructions that restrict the dynamics to a tensor product of qubit subspaces, we replace them with *genuine* two-qudit unitaries acting on the full Hilbert space. Such native qudit operations can exhibit different entangling behavior and may yield more efficient implementations.

The first stage—grouping qubits into qudits—relies only on the connectivity structure of the original circuit and is therefore purely *combinatorial*. By contrast, the second stage depends on the specific gate set and entanglement structure available on the target platform, so its benefits are inherently platform dependent.

We quantify performance by a *compression ratio* C_d, defined as the ratio of the number of entangling gates in the compressed (qudit) circuit to that in the original (qubit) circuit, and we derive *upper* and *lower* bounds for C_d that reflect the two-stage structure. The upper (worst-case) bound corresponds to the scenario where grouping alone reduces non-local interactions (with no further optimization), while the lower (best-case) bound corresponds to the case where native two-qudit gates realize the full inter-part entangling action with a single operation across each cut. We show that these bounds can be *saturated*, demonstrating optimal compression under our metric. The degree of achievable compression is tied to the available gate set and the commutativity/entangling power of the native two-qudit interactions.

We evaluate our method on circuits including multi-controlled phase gates and cluster-state preparations, and find substantial reductions in non-local gate count. These gains translate into shallower circuits and potentially higher-fidelity implementations in the NISQ setting. We also discuss feasibility on platforms with native high-dimensional control, such as photonics and trapped ions, where qudit-native gates can preserve or improve fidelity while reducing the number of entangling operations.

In conclusion, tailoring circuit representations to reflect the native structure and constraints of quantum hardware—both local dimension and gate availability—reduces non-local cost in a way that is practically relevant for near-term devices. While our reductions target *operational* cost rather than asymptotic complexity, they provide a direct and experimentally meaningful advantage when high-dimensional resources are available.

Viewed through the lens of this thesis, the circuit results preserve the conceptual core of the circuit model—computation as local composition on a tensor-product register—while allowing the *form* of the primitive library to change with dimension. This alignment of form with hardware is precisely the kind of dimension-aware generalization that yields concrete operational gains without claiming an asymptotic advantage.

5.2 Own Contribution

Xiaoqin Gao was the first author of the paper and was closely involved in all aspects of the project, with a particular focus on the photonic implementation. At the time, she was a visiting PhD student in Marcus Huber's group. Nicolai Friis, a postdoctoral researcher in Marcus Huber's group during the writing of the paper, contributed throughout and was involved in all parts of the project. Martin Ringbauer, Assistant Professor at the University of Innsbruck during the creation of the paper, was involved in the reception of the core idea and provided expert input on the discussion of trapped-ion implementations, drawing on his experience with experimental trapped-ion systems. Marcus Huber, last author of the paper, contributed to all conceptual and technical aspects. He provided the examples demonstrating the saturation of the theoretical bounds and was instrumental in shaping the core idea of the work. As second author, I contributed to the theoretical foundation of the paper. My main responsibilities were the proof of the lower and upper bounds of the compression ratio and the construction of detailed examples, in particular concerning CNOT decompositions.

On the role of entanglement in qudit-based circuit compression

Xiaoqin Gao[1,2], Paul Appel[2], Nicolai Friis[3,2], Martin Ringbauer[4], and Marcus Huber[3,2]

[1]Department of Physics, University of Ottawa, Advanced Research Complex, 25 Templeton Street, K1N 6N5, Ottawa, ON, Canada

[2]Institute for Quantum Optics and Quantum Information – IQOQI Vienna, Austrian Academy of Sciences, Boltzmanngasse 3, 1090 Vienna, Austria

[3]Atominstitut, Technische Universität Wien, Stadionallee 2, 1020 Vienna, Austria

[4]Universität Innsbruck, Institut für Experimentalphysik, Technikerstrasse 25, 6020 Innsbruck, Austria

Gate-based universal quantum computation is formulated in terms of two types of operations: local single-qubit gates, which are typically easily implementable, and two-qubit entangling gates, whose faithful implementation remains one of the major experimental challenges since it requires controlled interactions between individual systems. To make the most of quantum hardware it is crucial to process information in the most efficient way. One promising avenue is to use higher-dimensional systems, qudits, as the fundamental units of quantum information, in order to replace a fraction of the qubit-entangling gates with qudit-local gates. Here, we show how the complexity of multi-qubit circuits can be lowered significantly by employing qudit encodings, which we quantify by considering exemplary circuits with exactly known (multi-qubit) gate complexity. We discuss general principles for circuit compression, derive upper and lower bounds on the achievable advantage, and highlight the key role played by entanglement and the available gate set. Explicit experimental schemes for photonic as well as for trapped-ion implementations are provided and demonstrate a significant expected gain in circuit performance for both platforms.

Quantum computation is a disruptive technology that has irrevocably changed the way that computation is envisioned. It holds the potential for addressing a wide range of computational challenges [1], from factoring [2] and database search [3], to applications in quantum machine learning [4, 5]. Yet, current noisy intermediate-scale quantum (NISQ) devices [6] are still far from addressing these applications at a practically relevant scale and early demonstrations of quantum advantages remain confined to algorithms that do not yet have clearly identifiable broad applications [7, 8]. The primary obstacle for today's quantum computers, which now feature 10s to 100s of qubits [9–16] remains noise and decoherence, which limits the number of entangling operations and therefore the achievable circuit depth. Hence, for current as well as future quantum computers, efficiency at the circuit level will be key to getting the most out of these devices.

Fortunately, there is a lot of unused potential in current quantum devices, which tend to use only a small fraction of the available Hilbert space. Indeed, control over the inherently high-dimensional Hilbert space has been demonstrated in all major quantum technology platforms [17–20], motivating the exploitation of a new paradigm of quantum computing based on d-dimensional *qudits*, rather than qubits. Compared to their two-level counterpart, qudit architectures offer much richer coherence [21] and entanglement structures [22], which can be exploited for efficient quantum information processing [23–26] and improved quantum error correction [27, 28]. Since entangling operations tend to be the bottleneck in current quantum devices, the efficiency of a quantum computation, or the complexity of a quantum circuit, is traditionally measured by counting the number of entangling operations [29]. While this is an incomplete picture, it serves as a good hardware-agnostic approximation, because the optimal circuit for a given quantum operation is elusive and highly dependent on the available gate set.

Here, we investigate *qudit circuit compression*, as a way to simplify a given qubit circuit by rephrasing it as a qudit circuit. We achieve this in two steps:

First, the qubits are partitioned into groups of equal size such that the number of gates within the groups is maximized. Each group is then interpreted as a qudit, turning entangling gates into local gates and thus reducing the overall entangling gate count by a combinatorial factor for which we find lower and upper bounds using a graph-based approach. Second, by considering an extended gate set including not only qubit-entangling gates, but also genuine qudit-entangling gates, the number of entangling gates in the resulting qudit circuit can be further reduced, even saturating the combinatorial lower bound. To showcase these two effects, we study the compression of exemplary qubit circuits under different gate sets. We illustrate this gate compression with experimental details for two contemporary quantum technologies using qudits: photonic qudits encoded in orbital angular momentum and trapped ions with multiple addressable levels, showing that, already today, qubit circuits can be more efficiently compiled on qudit architectures. Aside from algorithmic improvements, reducing the number of quantum information carriers tends to make the system experimentally easier to control, leading to improved performance. We provide general design principles, as well as upper and lower bounds for the possible reduction in the number of gates, exemplified with explicit constructions for photonic systems and trapped ions.

Circuit compression. Quantum circuits are built from a sequence of gate operations. At the lowest level of abstraction, circuit compression is hence concerned with compiling an N-qubit unitary to an M-qudit architecture ($M < N$), which we call *gate compression*, see Fig. 1. The task is to encode the qubit circuit into the qudit architecture in such a way that the maximal number of entangling gates in the qubit circuit manifests as local gates in the resulting qudit circuit. Importantly, the remaining entangling gates retain their qubit-entangling structure, in terms of maximally generated entanglement entropy, when embedded in the qudit Hilbert space. Consequently, this procedure always reduces the amount of entanglement needed (irrespective of the available gate set for qudits), by compressing non-local gates into local ones. Consider the example of a four-qubit circuit, where qubits 1 and 2 are encoded in one qudit, and qubits 3 and 4 in another. Now all non-local gates between the original qubits 1 and 2 as well as between qubits 3 and 4 are local in the respective qudits. The non-local gates between qubits that are now encoded in different qudits remain non-local and maintain their tensor-product structure, which is why we call them embedded qubit gates.

Importantly, while embedded qubit gates still create two-level entanglement (i.e., equivalent to a two-qubit gate in terms of entanglement entropy), they are not necessarily easily implementable in a qudit architecture. To see this, consider the example of a CNOT gate $U_{\mathrm{CNOT}}^{(c,t)}$ applied to qubits 2 (control) and 3 (target) in the above example of a four-qubit register, taking the form $\mathbb{1}^{(1)} \otimes U_{\mathrm{CNOT}}^{(2,3)} \otimes \mathbb{1}^{(4)}$. When qubits 1 and 2 are encoded in the first qudit, and 3 and 4 in the second, the resulting embedded version of the original gate would have to be a subspace-agnostic operation (i.e., applying the same operation on both subspaces pertaining to the encoded qubits 1 and 4). Already for a single-qudit example with the canonical encoding $|0\rangle = |00\rangle, |1\rangle = |01\rangle, |2\rangle = |10\rangle, |3\rangle = |11\rangle$, we see that performing an operation of the form $\mathbb{1} \otimes U$, which acts on the second encoded qubit only requires the application of the same U to the subspaces $\{|0\rangle, |1\rangle\}$ and $\{|2\rangle, |3\rangle\}$ in order to realize the original tensor-product structure. While embedded qubit entangling gates still only create two-level entanglement, they are hence often not available natively. On the other hand, the qudit encoding enables new kinds of two-level entangling operations, which do not admit a tensor-product structure in the corresponding qubit circuit. Such gates provide new powerful tools for circuit compression, as discussed below, while also emphasizing the importance of the available gate set for qudit architectures. This again highlights the importance of considering the available gate set, rather than just qudit dimension, for efficient circuit compression.

While finding the ideal embedding of qubits into qudits is difficult, we can use weighted graphs to find a simplified representation of the circuit which in turn allows for powerful tools of graph theory to be employed. A weighted graph $G = (V, E)$ is a pair of a set of vertices $V = \{v_1, \ldots, v_n\}$ and a set of edges $E = \{e_1, \ldots, e_k\}$, where each edge $e_i = ((v_l, v_m), w_i)$ is a pair of vertices together with a weight w_i. To encode the non-local properties of the quantum circuit into the graph, we associate each vertex with a qubit and draw an edge whenever a non-local gate is present between two qubits. The weight of each edge is determined by counting the number of non-local gates between the respective qubits. This graph representation simplifies the circuit by ignoring the gate order, but it works for both qubits and

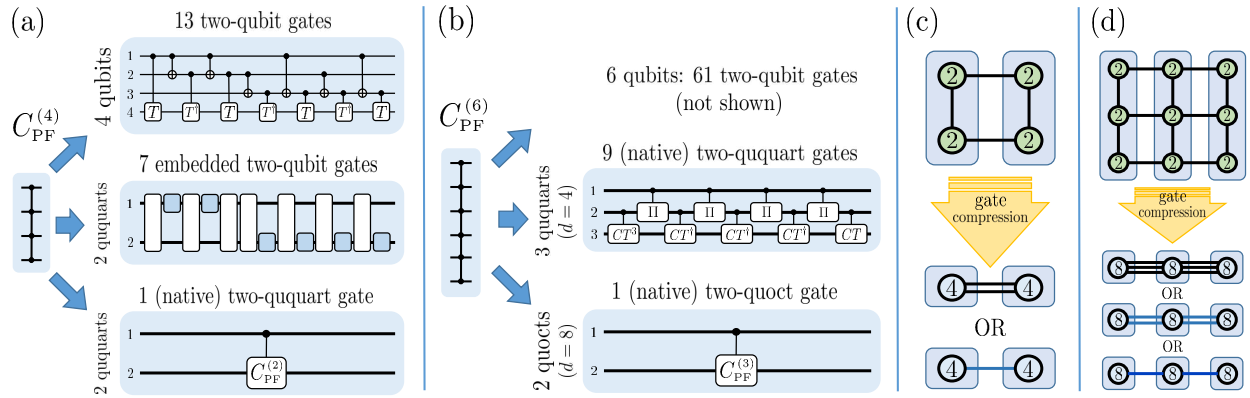

Figure 1: **Gate compression**. (a) & (b) Compression of quantum circuits of N-qubit controlled phase-flip (CPF) gates $C_{\mathrm{PF}}^{(N)}$. (a) The best known [30] decomposition of a 4-qubit CPF gate $C_{\mathrm{PF}}^{(4)}$ in terms of two-qubit gates requires 13 entangling gates, i.e., 6 CNOTs and 7 controlled T (or $T^\dagger$) gates (CT) with $T = \mathrm{diag}\{1, \exp(i\pi/4)\}$. By compressing the circuit to two qudits of dimension 4, two quarts, only 7 entangling gates are required in terms of embedded two-qubit gates, while 6 previously non-local gates become local. However, the same operation $C_{\mathrm{PF}}^{(4)}$ could also be realized by a single controlled-$C_{\mathrm{PF}}^{(2)}$ =CZ= $\mathrm{diag}\{1, 1, 1, -1\}$ gate on two ququarts, carried out if ququart 1 is in the state $|d-1\rangle = |3\rangle$ corresponding to the two-qubit state $|11\rangle$. (b) Similarly, the most efficient decomposition of $C_{\mathrm{PF}}^{(6)}$ for 6 qubits requires 61 two-qubit gates [30], whereas the compression to 3 ququarts ($d = 4$) requires (at most) 9 (native) two-ququart gates, including adjoints and powers of controlled CT gates as well as controlled Π gates, where $\Pi = \sum_{n=0}^{3} |(n-1)_{\mathrm{mod}(3)}\rangle\langle n|$ is a permutation. Further compressing to two quocts ($d = 8$), as little as 1 controlled-$C_{\mathrm{PF}}^{(3)}$ gate, conditioned on the quoct computational-basis state $|d-1\rangle = |7\rangle$ may be required. In both (a) and (b) the final decomposition of the N-qubit CPF gate into a single controlled-$C_{\mathrm{PF}}^{(N/2)}$ gate requires a non-factorizable two-level entangling gate. (c) & (d) Illustration of the effect of gate compression for the creation of a (quadratic) 2D cluster state consisting of four (c) and nine qubits (d), respectively. Cluster states are a particular type of graph state that can be schematically represented by vertices (here shown as circles carrying the local subsystem dimension d as labels, 2 for qubits, 4 for ququarts, etc.) connected by lines representing entangling gates (controlled-Z gates for qubits). By grouping (blue boxes) the qubits into pairs (c) or triples (d) the subsystem dimension becomes $d = 4$ (ququart) and $d = 8$ (quoct), respectively, but the number of non-local entangling gates can be reduced (c) from 4 two-qubit gates to either 2 embedded two-qubit gates or even 1 single-qudit gate, and (d) from 12 two-qubit gates to 6 embedded two-qubit gates, 4 two-qudit gates, or 2 two-quoct gates, as is explained below.

qudits. Using this graph representation, one can employ graph-partition algorithms [31, 32] to divide the graph into subgraphs (partitions) in a way that maximizes the number of non-local gates within each partition. Specifically, we try to find a minimal k-cut, which involves identifying a set of edges E' that, when removed, partitions the graph into k parts while minimizing the sum of weights in E'. Note that this paradigm can cover a wide range of optimization goals, including unequal-size partitions or different cost functions. In particular, we highlight the importance of considering the structure of the original circuit, as well as the available forms of qudit entanglement in the target hardware to achieve optimal encoding of qubits into qudits.

Gate set optimization. After we have reduced the *width* of the circuit, we can further improve upon the circuit *depth* by considering the extended gate set we can access for qudits. Recall that the embedded gates, resulting from circuit compression, still generate two-level entanglement and retain their original tensor-product structure. While such gates can be constructed from a universal set of qudit gates, there is much more untapped potential in the qudit Hilbert space, including gates that do not respect the tensor-product structure of the original qubit Hilbert space. By expanding the gate set, a significant reduction in circuit depth can thus be achieved, as illustrated in Fig. 1. However, the choice of gates for the expansion strongly depends on the chosen hardware platform.

Upper and lower bounds. Using the above principles, we can derive upper and lower bounds on the *compression ratio* C_d, which we define as the ratio of the number of entangling gates in the compressed circuit to the number of gates in the original circuit. To compute these bounds, we denote the weights of the original qubit graph by $\vec{\omega}$ and the weights of the qudit graph after compression by $\vec{\tilde{\omega}}$. The latter is obtained by dropping all components of the original vector that correspond to non-local gates between qubits that are

encoded in the same qudit, and which thus become local, and then assigning all edges between qubits that are encoded in different qudits to the respective qudits in the new graph (and adding the corresponding weights). The upper (worst-case) bound is then obtained by comparing the sum of weights (i.e., the 1-norm of $\vec{\omega}$) before and after compression, representing the scenario where no further gate optimization is possible. The lower bound, on the other hand, represents the scenario where gate optimization is able to fully exploit native qudit gates to realize the full qudit-entangling operation with a single gate operation. This bound is hence determined by the number of non-zero weights in $\vec{\tilde{\omega}}$. By normalizing these bounds using the number of gates in the initial circuit, $\|\vec{w}\|_1$, we can establish the compression-ratio bounds

$$\frac{\|\vec{\tilde{w}}\|_0}{\|\vec{w}\|_1} \leq C_d \leq \frac{\|\vec{\tilde{w}}\|_1}{\|\vec{w}\|_1}, \tag{1}$$

where, $\|\cdot\|_0$ and $\|\cdot\|_1$ refer to the l_0 (quasi-)norm and the l_1 norm, respectively. The span between the lower and upper bounds indicates potential improvements based on an appropriate gate set. In the following, we will provide examples saturating both the lower and the upper bound.

Controlled phase gates. As a key example, we will now study N-qubit controlled phase-flip gates $C_{\mathrm{PF}}^{(N)}$ (i.e., phase gates with a π phase shift). These gates are central elements in quantum computing, for example, as a key part of Grover's search algorithm [3]. It can be written as follows,

$$C_{\mathrm{PF}}^{(N)} = \mathbb{1}^{\otimes N} + |1\rangle\langle 1|^{\otimes(N-1)} \otimes (Z - \mathbb{1}), \tag{2}$$

where $\mathbb{1}$ is the identity operator and Z denotes the single-qubit Pauli-z gate. Due to its central role, the decomposition of $C_{\mathrm{PF}}^{(N)}$ is often used as a benchmark for comparing circuit decompositions and gate sets. Importantly, provably optimal decompositions into two-qubit gates and local operations are known for 3 to 8 qubits [30]. As we noted above, the optimality of a quantum circuit depends on the metric used. However, even when the metric is fixed, finding an efficient way to realize the circuit is highly non-trivial. For example, for a four-qubit controlled phase flip $C_{\mathrm{PF}}^{(4)}$, the most efficient decomposition known, believed to be optimal, requires 13 two-qubit gates [30], as shown in Fig. 1 (a). The same circuit can be realized in a qudit system by embedding two qubits each into two ququarts. There are 3 ways to achieve such a partition, and the best choice turns 6 entangling gates into local gates, leaving 7 embedded two-qubit gates between the two ququarts. If we consider also ququart gates in our gate set, this can further reduce the non-local gate count to just a single gate between the two ququarts, which turn out to generate only two-level entanglement, as shown in Fig. 1 (a). In case $N > 4$, we can cut N qubits into k equal parts by using a $2^{N/k}$-dimensional qudit in each part and achieve similar improvements. For the six-qubit controlled phase-flip gate ($C_{\mathrm{PF}}^{(6)}$), for example, 61 two-qubit gates are needed in the best known (again, believed to be optimal) decomposition [30]. Encoding the same circuit into 3 ququarts reduces the requirement to 9 two-ququart gates, including four two-ququart controlled-shift gates and five two-ququart controlled phase gates [33], see Fig. 1 (b). Going further by encoding the gate into two qudits of dimension $d = 8$ (quocts), the gate can again be realized with a single two-level entangling qudit gate.

Graph states and the saturation of graph partitioning bounds.– Graph states are another highly relevant example. For a set of edges $E = \{e\}$, they can always be created by applying controlled-Z gates across all edges on computational-superposition product states, i.e., $|G\rangle := \prod_{e\in E} CZ_e |+\rangle^{\otimes n}$ with $|+\rangle = (|0\rangle + |1\rangle)/\sqrt{2}$. As all CZ_e commute, it directly follows that, with an unrestricted entangling power of the gate set, the lower bound $\|\vec{\tilde{w}}\|_0$ can be saturated. If the gate set is restricted to two-level entangling gates, however, the fact that a high amount of entanglement may be generated if multiple edges cut across a bipartition directly implies that the upper bound needs to be observed with $\|\vec{\tilde{w}}\|_1$ embedded qubit gates.

Consider, for example, a 4-qubit quadratic 2D cluster state as illustrated in Fig. 1 (c). Due to the symmetry of the state the partition is irrelevant and we can thus combine the first and second qubit as well as the third and fourth qubit to a qudit each without loss of generality. This reduces the number of non-local gates from 4 to 2, which saturates the upper bound $\|\vec{\tilde{w}}\|_1$. Now, we can use gate optimization to reduce the number to 1 by combining the two non-local gates between the qudits to a single genuine qudit gate, saturating the lower bound $\|\vec{\tilde{w}}\|_0$. This example demonstrates that the commutativity of the entangling gates across compressed partitions as well as the maximum amount of entanglement generated across these partitions are crucial parameters that determine how well a qubit circuit can be compressed when compiled on a qudit architecture and which gate set would be required for the qudits.

Photonic implementation.– Photonic systems are excellent candidates for gate compression. Current developments enable increased control over higher-dimensional degrees of freedom by manipulating a photon's polarization, spatial profile, temporal profile, or frequency, either separately or simultaneously. This enables the encoding of multiple bits into a single photon, as is routinely done in entanglement-based quantum communication [34–36]. Local unitary operations are easily done within a certain degree of freedom, such as spatial manipulation through multi-plane light conversion [37], frequency manipulation [38, 39], or between different degrees of freedom, for example, using polarizing beam splitters to couple path and polarization. For instance, high-dimensional Pauli X- and Z-gates, which are parts of higher-dimensional universal gate sets, have recently been implemented in a number of ways [37, 40–43]. While local gates can often be performed with near-unit efficiency and fidelity, entangling gates remain the Achilles heel of photonic information processing, as entangling two photons can be achieved probabilistically at best, leading to an exponential decrease in success probability with the number of entangling gates.

The latter aspect is where high-dimensional encodings can become particularly useful, as more information can be processed at higher fidelity and with potentially much higher success probability. Recent developments already show promising results [44, 45], including the implementations of high-dimensional multi-partite quantum gates [46] and of the SUM gate (a high-dimensional controlled-X gate) in the time and frequency degrees of freedom of photons [47]. Here, we propose a scheme for a photonic two-qudit entangling gate that grows only logarithmically in complexity with dimension and achieves a constant success probability of $1/4$ that is independent of the qudit dimension, see Appendix A for details.

Trapped-ion implementation.– Trapped ions are among the leading platforms for quantum information processing [48], where the electronic energy levels of each ion naturally provide a high-dimensional Hilbert space. Recently it was shown that such a system can be operated as a universal qudit quantum processor up to dimension 7 [19]. The qudit-gate set used in this demonstrations consisted of arbitrary local gates and two-qubit CNOT gates embedded in a qudit Hilbert space. Compared to a standard qubit CNOT, the embedded version exhibits error rates larger by roughly a factor of 2, independent of the Hilbert-space dimension. Beyond this basic gate set, it has been shown that both dominant gate mechanisms in this platform, the Mølmer-Sørensen gates [49] and light-shift gates [50], can be generalized to achieve genuine qudit entanglement. A first experimental realization of the latter demonstrated the generation of genuine qudit entanglement in a scalable fashion and with highly competitive error rates [50].

Compiling the example of Fig. 1 (a) and using state-of-the-art error rates for trapped-ion quantum processors of about 0.01 per qubit CNOT gate [48], a rough estimate suggests that the implementation of the four-qubit $C_{\mathrm{PF}}^{(4)}$ gate could achieve an error rate on the order of 0.12 with the standard two-level decomposition using 13 two-qubit entangling gates. Curiously, while it is known on the one hand that enlarging the Hilbert space locally (i.e., encoding 4 qubits into 4 qudits) can reduce the required number of gates quadratically [23], this gain is offset almost exactly in the 4-qubit case by the factor of 2 increased error rates incurred in the experimental implementation [19]. On the other hand, when two qubits each are encoded in a qudit of dimension 5 (4 computational levels and 1 auxiliary level), the required number of two-level entangling gates drops to 1 (albeit with a rotation angle equivalent to 4 qubit gates), achieving an estimated error rate of 0.04, see Appendix B for the circuit. Curiously, this is an example where it is optimal to use a two-level entangling gate in the qudit circuit, which is not an embedded qubit gate.

Conclusion.– We have explored two ways in which higher-dimensional architectures are universally beneficial to quantum computing. First, using gate compression, we can cut down on the amount of entanglement needed for a specific N-qubit circuit, and second, by exploiting the added capabilities of qudit systems in the form of richer gate sets, we can further reduce the number of non-local gates required to generate that entanglement. This highlights the key role played by entanglement and the available gate set in efficient qudit QIP. As every higher-dimensional gate can be achieved by any universal gate set applied a number of times, the advantage from larger gate sets is constant in the number of qubits. Similarly, even the most efficient partitioning of the qubit circuit leads to only a constant advantage. Such constant improvements, however, can make the difference between feasibility and failure.

Another important aspect is the potential breakdown of conventional wisdom regarding easily implementable local gates versus hard non-local gates. Once qudit dimensions get sufficiently large, the performance gap between local and non-local gates might change. Moreover, gate performance typically degrades somewhat with system size, providing another motivation for reducing the number of quantum-information carriers and making more efficient use of available resources. Finally, we emphasize that a case-by-case evaluation of the actual tradeoffs is critical to finding the optimal dimensionality for a given problem and hardware platform.

Our examples provide a promising first step, showing that qudit encodings can lead to a significant reduction in gate count. Hence, this approach can greatly increase the utility of current and future quantum hardware, using only degrees of freedom that are already present in today's quantum technology. Indeed, various quantum-computing platforms have demonstrated qudit control with ever-increasing performance. Both gate compression and gate-set optimization will be central tools for making the most of the next generation of high-dimensional quantum processors, harnessing the full potential of physical quantum information carriers.

Acknowledgments.– We are indebted to Mateus Araújo for discussion and input during early stages of this work, and we thank him for his Krapfen. We acknowledge financial support from the Austrian Science Fund (FWF) through the START project Y879-N27, the stand-alone project P 31339-N27, and the stand-alone project P 36478-N funded by the European Union – NextGenerationEU, as well as by the Austrian Federal Ministry of Education, Science and Research via the Austrian Research Promotion Agency (FFG) through the flagship project FO999897481 funded by the European Union – NextGenerationEU. This project has received funding from the European Union's Horizon 2020 research and innovation programme under the Marie Skłodowska-Curie grant agreement No 840450. X.G. acknowledges the support of Joint Centre for Extreme Photonics (JCEP). M.H. acknowledges funding from the European Research Council (Consolidator grant 'Cocoquest' 101043705). M.R. acknowledges funding from the European Research Council (Starting Grant 'QUDITS' 101039522) and the European Union under the Horizon Europe Programme – Grant Agreement 101080086 – NeQST. Views and opinions expressed are however those of the author(s) only and do not necessarily reflect those of the European Union or the European Research Council. Neither the European Union nor the granting authority can be held responsible for them.

References

[1] Arkady K. Fedorov, Nicolas Gisin, Serguei M. Beloussov, and Alexander I. Lvovsky, *Quantum computing at the quantum advantage threshold: a down-to-business review,* arXiv:2203.17181 [quant-ph] (2022).

[2] Peter W. Shor, *Algorithms for quantum computation: Discrete logarithms and factoring,* in *Proceedings 35th Annual Symposium on Foundations of Computer Science* (IEEE, 1994) pp. 124–134.

[3] Lov K. Grover, *A fast quantum mechanical algorithm for database search,* in *Proceedings of the Twenty-eighth Annual ACM Symposium on Theory of Computing* (ACM, New York, NY, USA, 1996) pp. 212–219, arXiv:quant-ph/9605043.

[4] Vedran Dunjko and Hans J. Briegel, *Machine learning & artificial intelligence in the quantum domain: a review of recent progress,* Rep. Prog. Phys. **81**, 074001 (2018), arXiv:1709.02779.

[5] Iris Cong, Soonwon Choi, and Mikhail D. Lukin, *Quantum convolutional neural networks,* Nat. Phys. **15**, 1273 (2019), arXiv:1810.03787.

[6] John Preskill, *Quantum Computing in the NISQ era and beyond,* Quantum **2**, 79 (2018), arXiv:1801.00862.

[7] Frank Arute *et al.*, *Quantum supremacy using a programmable superconducting processor,* Nature **574**, 505 (2019), arXiv:1910.11333.

[8] Qingling Zhu *et al.*, *Quantum computational advantage via 60-qubit 24-cycle random circuit sampling,* arXiv:2109.03494 [quant-ph] (2021).

[9] Hannes Bernien, Sylvain Schwartz, Alexander Keesling, Harry Levine, Ahmed Omran, Hannes Pichler, Soonwon Choi, Alexander S. Zibrov, Manuel Endres, Markus Greiner, Vladan Vuletić, and Mikhail D. Lukin, *Probing many-body dynamics on a 51-atom quantum simulator,* Nature **551**, 579 (2017), arXiv:1707.04344.

[10] Jiehang Zhang, Guido Pagano, Paul W. Hess, Antonis Kyprianidis, Patrick Becker, Harvey Kaplan, Alexey V. Gorshkov, Zhexuan Gong,

and Christopher Monroe, *Observation of a many-body dynamical phase transition with a 53-qubit quantum simulator,* Nature **551**, 601 (2017), arXiv:1708.01044.

[11] Johannes S. Otterbach *et al.*, *Unsupervised machine learning on a hybrid quantum computer,* arXiv:1712.05771 [quant-ph] (2017).

[12] Xi-Lin Wang, Yi-Han Luo, He-Liang Huang, Ming-Cheng Chen, Zu-En Su, Chang Liu, Chao Chen, Wei Li, Yu-Qiang Fang, Xiao Jiang, Jun Zhang, Li Li, Nai-Le Liu, Chao-Yang Lu, and Jian-Wei Pan, *18-Qubit Entanglement with Six Photons' Three Degrees of Freedom,* Phys. Rev. Lett. **120**, 260502 (2018), arXiv:1801.04043.

[13] Nicolai Friis, Oliver Marty, Christine Maier, Cornelius Hempel, Milan Holzäpfel, Petar Jurcevic, Martin B. Plenio, Marcus Huber, Christian Roos, Rainer Blatt, and Ben Lanyon, *Observation of Entangled States of a Fully Controlled 20-Qubit System,* Phys. Rev. X **8**, 021012 (2018), arXiv:1711.11092.

[14] Conor E. Bradley, Joe Randall, Mohamed H. Abobeih, Remon C. Berrevoets, Maarten J. Degen, Michiel A. Bakker, Matthew L. Markham, Daniel J. Twitchen, and Tim Hugo Taminiau, *A Ten-Qubit Solid-State Spin Register with Quantum Memory up to One Minute,* Phys. Rev. X **9**, 031045 (2019), arXiv:1905.02094.

[15] Ivan Pogorelov, Thomas Feldker, Christian D. Marciniak, Georg Jacob, Verena Podlesnic, Michael Meth, Vlad Negnevitsky, Martin Stadler, Kirill Lakhmanskiy, Rainer Blatt, Philipp Schindler, and Thomas Monz, *Compact ion-trap quantum computing demonstrator,* PRX Quantum **2**, 020343 (2021), arXiv:2101.11390.

[16] Gary J. Mooney, Gregory A. L. White, Charles D. Hill, and Lloyd C. L. Hollenberg, *Whole-Device Entanglement in a 65-Qubit Superconducting Quantum Computer,* Adv. Quantum Technol. **4**, 2100061 (2021), arXiv:2102.11521.

[17] Jianwei Wang, Stefano Paesani, Yunhong Ding, Raffaele Santagati, Paul Skrzypczyk, Alexia Salavrakos, Jordi Tura, Remigiusz Augusiak, Laura Mančinska, Davide Bacco, Damien Bonneau, Joshua W. Silverstone, Qihuang Gong, Antonio Acín, Karsten Rottwitt, Leif K. Oxenløwe, Jeremy L. O'Brien, Anthony Laing, and Mark G. Thompson, *Multidimensional quantum entanglement with large-scale integrated optics,* Science **360**, 285 (2018), arXiv:1803.04449.

[18] Alexis Morvan, Vinay V. Ramasesh, Machiel S. Blok, John Mark Kreikebaum, Kevin P. O'Brien, Larry Chen, Bradley K. Mitchell, Ravi K. Naik, David I. Santiago, and Irfan Siddiqi, *Qutrit Randomized Benchmarking,* Phys. Rev. Lett. **126**, 210504 (2021), arXiv:2008.09134.

[19] Martin Ringbauer, Michael Meth, Lukas Postler, Roman Stricker, Rainer Blatt, Philipp Schindler, and Thomas Monz, *A universal qudit quantum processor with trapped ions,* Nat. Phys. **18**, 1053 (2022), arXiv:2109.06903.

[20] Yulin Chi, Jieshan Huang, Zhanchuan Zhang, Jun Mao, Zinan Zhou, Xiaojiong Chen, Chonghao Zhai, Jueming Bao, Tianxiang Dai, Huihong Yuan, Ming Zhang, Daoxin Dai, Bo Tang, Yan Yang, Zhihua Li, Yunhong Ding, Leif K. Oxenløwe, Mark G. Thompson, Jeremy L. O'Brien, Yan Li, Qihuang Gong, and Jianwei Wang, *A programmable qudit-based quantum processor,* Nat. Commun. **13**, 1166 (2022), arXiv:1803.04449.

[21] Martin Ringbauer, Thomas R. Bromley, Marco Cianciaruso, Ludovico Lami, W. Y. Sarah Lau, Gerardo Adesso, Andrew G. White, Alessandro Fedrizzi, and Marco Piani, *Certification and Quantification of Multilevel Quantum Coherence,* Phys. Rev. X **8**, 041007 (2018), arXiv:1707.05282.

[22] Tristan Kraft, Christina Ritz, Nicolas Brunner, Marcus Huber, and Otfried Gühne, *Characterizing Genuine Multilevel Entanglement,* Phys. Rev. Lett. **120**, 060502 (2018), arXiv:1707.01050.

[23] Benjamin P. Lanyon, Marco Barbieri, Marcelo P. Almeida, Thomas Jennewein, Timothy C. Ralph, Kevin J. Resch, Geoff J. Pryde, Jeremy L. O'Brien, Alexei Gilchrist, and Andrew G. White, *Simplifying quantum logic using higher-dimensional Hilbert spaces,* Nat. Phys. **5**, 134 (2009), arXiv:0804.0272.

[24] Anastasiia S. Nikolaeva, Evgeniy O. Kiktenko, and Arkady K. Fedorov, *Efficient realization of quantum algorithms with qudits,* arXiv:2111.04384 [quant-ph] (2021).

[25] Evgeniy O. Kiktenko, Anastasiia S. Nikolaeva, Peng Xu, Georgy V. Shlyapnikov, and Arkady K. Fedorov, *Scalable quantum comput-*

ing with qudits on a graph, Phys. Rev. A **101**, 022304 (2020), arXiv:1909.08973.

[26] Yuchen Wang, Zixuan Hu, Barry C. Sanders, and Sabre Kais, *Qudits and High-Dimensional Quantum Computing,* Front. Phys. **8**, 479 (2020), arXiv:2008.00959.

[27] Fern H. E. Watson, Earl T. Campbell, Hussain Anwar, and Dan E. Browne, *Qudit color codes and gauge color codes in all spatial dimensions,* Phys. Rev. A **92**, 022312 (2015), arXiv:1503.08800.

[28] Earl T. Campbell, *Enhanced Fault-Tolerant Quantum Computing in d-Level Systems,* Phys. Rev. Lett. **113**, 230501 (2014), arXiv:1406.3055.

[29] Jonas Haferkamp, Philippe Faist, Naga B. T. Kothakonda, Jens Eisert, and Nicole Yunger Halpern, *Linear growth of quantum circuit complexity,* Nat. Phys. **18**, 5 (2022), arXiv:2106.05305.

[30] Adriano Barenco, Charles H. Bennett, Richard Cleve, David P. DiVincenzo, Norman Margolus, Peter Shor, Tycho Sleator, John A. Smolin, and Harald Weinfurter, *Elementary gates for quantum computation,* Phys. Rev. A **52**, 3457 (1995), arXiv:quant-ph/9503016.

[31] Goldschmidt Olivier and Dorit S. Hochbaum, *A Polynomial Algorithm for the K-Cut Problem for Fixed k,* Math. Oper. Res. **19**, 24 (1994).

[32] Aydin Buluç, Henning Meyerhenke, Ilya Safro, Peter Sanders, and Christian Schulz, *Recent Advances in Graph Partitioning,* in *Algorithm Engineering. Lecture Notes in Computer Science vol 9220*, edited by L. Kliemann and P. Sanders (Springer, Cham, 2016) Chap. 4, pp. 117–158, arXiv:1311.3144.

[33] Gavin K. Brennen, Stephen S. Bullock, and Dianne P. O'Leary, *Efficient circuits for exact-universal computation with qudits,* Quantum Inf. Comput. **6**, 436 (2006), arXiv:quant-ph/0509161.

[34] Alicia Sit, Frédéric Bouchard, Robert Fickler, Jérémie Gagnon-Bischoff, Hugo Larocque, Khabat Heshami, Dominique Elser, Christian Peuntinger, Kevin Günthner, Bettina Heim, Christoph Marquardt, Gerd Leuchs, Robert W. Boyd, and Ebrahim Karimi, *High-dimensional intracity quantum cryptography with structured photons,* Optica **4**, 1006 (2017), arXiv:1612.05195.

[35] Lukas Achatz, Lukas Bulla, Evelyn A. Ortega, Michael Bartokos, Sebastian Ecker, Martin Bohmann, Rupert Ursin, and Marcus Huber, *Simultaneous transmission of hyper-entanglement in three degrees of freedom through a multicore fiber,* npj Quantum Inf. **9**, 45 (2023), arXiv:2208.10777.

[36] Natalia Herrera Valencia, Vatshal Srivastav, Matej Pivoluska, Marcus Huber, Nicolai Friis, Will McCutcheon, and Mehul Malik, *High-Dimensional Pixel Entanglement: Efficient Generation and Certification,* Quantum **4**, 376 (2020), arXiv:2004.04994.

[37] Florian Brandt, Markus Hiekkamäki, Frédéric Bouchard, Marcus Huber, and Robert Fickler, *High-dimensional quantum gates using full-field spatial modes of photons,* Optica **7**, 98 (2020), arXiv:1907.13002.

[38] Michael Kues, Christian Reimer, Piotr Roztocki, Luis Romero Cortés, Stefania Sciara, Benjamin Wetzel, Yanbing Zhang, Alfonso Cino, Sai T. Chu, Brent E. Little, *et al.*, *On-chip generation of high-dimensional entangled quantum states and their coherent control,* Nature **546**, 622 (2017).

[39] Meritxell Cabrejo Ponce, André Luiz Marques Muniz, Marcus Huber, and Fabian Steinlechner, *High-Dimensional Entanglement for Quantum Communication in the Frequency Domain,* Laser Photonics Rev. , 2201010 (2023), arXiv:2206.00969.

[40] Ali Asadian, Paul Erker, Marcus Huber, and Claude Klöckl, *Heisenberg-Weyl observables: Bloch vectors in phase space,* Phys. Rev. A **94**, 010301(R) (2016), arXiv:1512.05640.

[41] Amin Babazadeh, Manuel Erhard, Feiran Wang, Mehul Malik, Rahman Nouroozi, Mario Krenn, and Anton Zeilinger, *High-Dimensional Single-Photon Quantum Gates: Concepts and Experiments,* Phys. Rev. Lett. **119**, 180510 (2017), arXiv:1702.07299.

[42] Xi-Lin Wang, Xin-Dong Cai, Zu-En Su, Ming-Cheng Chen, Dian Wu, Li Li, Nai-Le Liu, Chao-Yang Lu, and Jian-Wei Pan, *Quantum teleportation of multiple degrees of freedom of a single photon,* Nature **518**, 516 (2015), arXiv:1409.7769.

[43] Xiaoqin Gao, Mario Krenn, Jaroslav Kysela, and Anton Zeilinger, *Arbitrary d-dimensional Pauli X gates of a flying qudit,* Phys. Rev. A **99**, 023825 (2019), arXiv:1811.01814.

[44] Ashok Muthukrishnan and Carlos R. Stroud Jr.,

Multivalued logic gates for quantum computation, Phys. Rev. A **62**, 052309 (2000), arXiv:quant-ph/0002033.

[45] Manuel Erhard, Robert Fickler, Mario Krenn, and Anton Zeilinger, *Twisted photons: new quantum perspectives in high dimensions,* Light Sci. Appl. **7**, 17146 (2018), arXiv:1708.06101.

[46] Xiaoqin Gao, Manuel Erhard, Anton Zeilinger, and Mario Krenn, *Computer-Inspired Concept for High-Dimensional Multipartite Quantum Gates,* Phys. Rev. Lett. **125**, 050501 (2020), arXiv:1910.05677.

[47] Poolad Imany, Jose A. Jaramillo-Villegas, Mohammed S. Alshaykh, Joseph M. Lukens, Ogaga D. Odele, Alexandria J. Moore, Daniel E. Leaird, Minghao Qi, and Andrew M. Weiner, *High-dimensional optical quantum logic in large operational spaces,* npj Quantum Inf. **5**, 1 (2019), arXiv:1805.04410.

[48] Alejandro Bermudez, Xiaosi Xu, Ramil Nigmatullin, Joe O'Gorman, Vlad Negnevitsky, Philipp Schindler, Thomas Monz, Ulrich G. Poschinger, Cornelius Hempel, Jonathan P. Home, Ferdinand Schmidt-Kaler, Michael J. Biercuk, Rainer Blatt, Simon C. Benjamin, and Markus Müller, *Assessing the Progress of Trapped-Ion Processors Towards Fault-Tolerant Quantum Computation,* Phys. Rev. X **7**, 041061 (2017), arXiv:1705.02771.

[49] Pei Jiang Low, Brendan M. White, Andrew A. Cox, Matthew L. Day, and Crystal Senko, *Practical trapped-ion protocols for universal qudit-based quantum computing,* Phys. Rev. Research **2**, 033128 (2020), arXiv:1907.08569.

[50] Pavel Hrmo, Benjamin Wilhelm, Lukas Gerster, Martin W. van Mourik, Marcus Huber, Rainer Blatt, Philipp Schindler, Thomas Monz, and Martin Ringbauer, *Native qudit entanglement in a trapped ion quantum processor,* Nat. Commun. **14**, 2242 (2023), arXiv:2206.04104.

[51] Noelia González, Gabriel Molina-Terriza, and Juan P. Torres, *How a Dove prism transforms the orbital angular momentum of a light beam,* Opt. Express **14**, 9093 (2006).

A Photonic Implementation with the orbital angular momentum

To implement quantum circuits with high-dimensional quantum gates, we propose a general experimental scheme for two-qudit CPF gates in the orbital angular momentum (OAM) of two photons. The scheme succeeds with a probability of $\frac{1}{4}$, irrespective of the encoding dimension, but requires an auxiliary two-qubit Bell state. Hence, this scheme does not overcome some of the fundamental limitations that all photonic computing suffers from but carries the potential to increase the number of gates that can be realized with a given set of resources, as well as exploring gates in one of the many potential degrees of freedom that can be harnessed in single-photons.

In order to implement an efficient photonic circuit for $C_{\mathrm{PF}}^{(N)}$ in the OAM degree-of-freedom via a qudit encoding, high-dimensional quantum gates with high success probability are required. These include single-qudit gates, which have been well developed for the OAM of a single photon, i.e., Pauli X- [37, 41, 43] and Z-gates [42], and non-local two-qudit quantum gates, which include two-qudit quantum controlled-phase gates or two-qudit quantum controlled-cyclic (permutation) gates. All of these non-local quantum gates are conditioned on the highest state $|d-1\rangle$ of the control qudit with computational basis $\{|m\rangle\}_{m=0,1,\ldots,d-1}$.

Here we are interested in performing two-qudit gates in the subspace spanned by the OAM modes $\{|m\rangle\}_{m=0,1,\ldots,d_1-1}$ and $\{|m\rangle\}_{m=0,1,\ldots,d_2-1}$ of two photons, where d_1 and d_2 are any (integer) dimensions. The main idea of our proposal for a potential experimental implementation is shown in Fig. 2 (a).

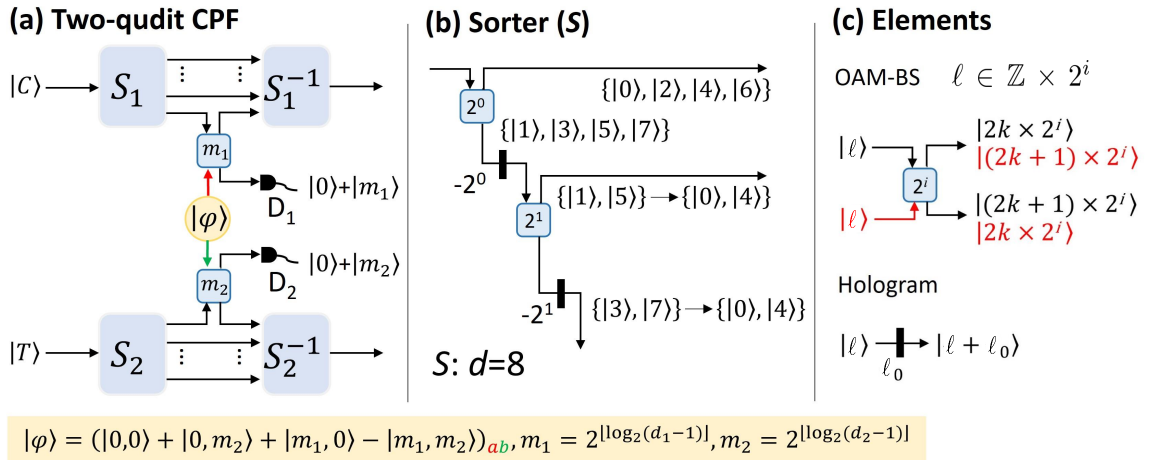

Figure 2: **Experimental scheme for realizing a two-qudit CPF gate in the OAM degree-of-freedom of two photons**. **(a)** The setup has three main parts representing the two subsystems in question, control (upper part) and target (lower part), as well as an auxiliary state $|\varphi\rangle$ in a two-qubit subspace spanned by two OAM modes ($|0\rangle$ and $|m_1\rangle$, as well as $|0\rangle$ and $|m_2\rangle$, respectively) each of two additional photons, here shown for arbitrary local dimension d. The control and target parts each consist of single-photon input states $|C\rangle$ and $|T\rangle$ that are fed into OAM sorters S_1 and S_2, respectively, which split pairs of the different OAM modes into orthogonal spatial modes. There are $\lfloor \log_2(d_{1/2}-1) \rfloor + 1$ outputs from the sorter $S_{1/2}$. For each of these parts, the paths corresponding to the pair of OAM modes $|d_{1/2}-1-2^{\lfloor \log_2(d_{1/2}-1)\rfloor}\rangle$ and $|d_{1/2}-1\rangle$, respectively, are each combined with one of the photons of $|\varphi\rangle$ (normalization not shown) on additional OAM beam splitters (OAM-BS) $m_1 = 2^{\lfloor \log_2(d_1-1)\rfloor}$ and $m_2 = 2^{\lfloor \log_2(d_2-1)\rfloor}$ respectively. One of the output paths of each OAM-BS is then projected onto an equally weighted superposition of $|0\rangle$ and $|m_{1/2}\rangle$, while the remaining output paths of the OAM-BSs are fed back into a final inverse OAM-sorter operation $S_{1/2}^{-1}$ that recombines the different paths into a single path. **(b)** Example for OAM sorter S in dimension eight ($d=8$) realized by a combination of two OAM-BSs [labeled by $2^i=1$ and $2^i=2$ with $i=0$ and $i=1$, respectively, as shown in **(c)**] and two holograms [for $\ell_0=-1$ and $\ell_0=-2$ as shown in **(c)**]. The first OAM-BS ($2^i=1$, $i\in\mathbb{Z}^{0+}$) separates the modes $|0\rangle$, $|2\rangle$, $|4\rangle$, and $|6\rangle$ from $|1\rangle$, $|3\rangle$, $|5\rangle$, and $|7\rangle$. The first hologram ($\ell_0=-1$) shifts the latter modes to $|0\rangle$, $|2\rangle$, $|4\rangle$, and $|6\rangle$, before the second OAM-BS ($2^i=2$) separates $|0\rangle$ and $|4\rangle$ (formerly $|1\rangle$ and $|5\rangle$) from $|2\rangle$ and $|6\rangle$ (formerly $|3\rangle$ and $|7\rangle$). The second hologram ($\ell_0=-2$) then maps $|2\rangle$ and $|6\rangle$ to $|0\rangle$ and $|4\rangle$, originally corresponding to $|d-1-2^{\lfloor \log_2(d-1)\rfloor}\rangle = |3\rangle$ and $|d-1\rangle = |7\rangle$. **(c)** Two basic elements: OAM beam splitters (OAM-BSs) and holograms. The label i determines the sorting property of the OAM-BS. Holograms shift the azimuthal quantum number of the OAM modes fixed amount. For details about the structure of OAM-BS see Fig. 3 (b).

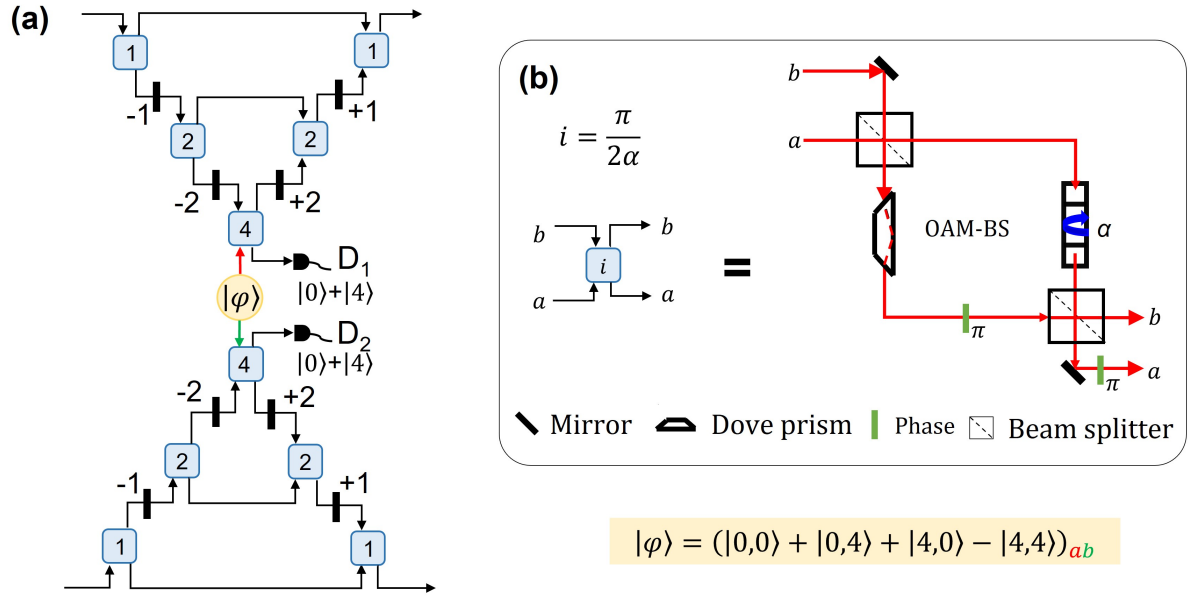

Figure 3: **Experimental scheme for two-qudit controlled phase flip in the OAM of two photons with eight dimensions**. (a) Experimental setup. 10 OAM-BSs (blue boxes) together with holograms (thick, black, vertical lines) are used in the setup. A two-qubit Bell state is necessary for facilitating the interaction between the two photons. (b) Structure of the OAM-BS. The OAM-BS works for sorting OAM modes, the sorting property is determined by i, which is related to the rotation angle α of the Dove prism.

The operation S splits modes from one path into multiple paths, while S^{-1} does the opposite, regrouping all modes into a single path. First, the input photon goes through S, which sends the highest mode $|d-1\rangle$ to its own path together with the mode $|d-1-2^{\lfloor \log_2(d-1) \rfloor}\rangle$ by using $\lfloor \log_2(d-1) \rfloor$ OAM-BSs and $\lfloor \log_2(d-1) \rfloor$ holograms. Subsequently, $|d-1\rangle$ and $|d-1-2^{\lfloor \log_2(d-1) \rfloor}\rangle$ are combined with a photon from the Bell state $|\varphi\rangle$ in an OAM-BS. Finally, the operation S^{-1} recombines all modes into one single path. The gate works if two single-photon detectors click at the same time with probability of 1/4 (due to the auxiliary Bell state, normalization not shown). As an example, we show the operation S for dimensions $d = 8$ in Fig. 2 (b). The highest mode $|7\rangle$ and mode $|3\rangle$ are split into their own paths and enter into an OAM-BS together with another photon (red) from the auxiliary state. Afterward, all modes are routed into one single path via S^{-1}. The operation S consists of multiple OAM-BSs and holograms, as shown in Fig. 2 (c). An OAM-BS is an interferometer containing two Dove prisms [51], see Fig. 3. The operations S and S^{-1} features a high symmetry: S^{-1} is a mirror reflection of S, with an inversion of the hologram values.

There are two basic elements in the setup: holograms and OAM beam splitters, each of which has a finite (below 1) fidelity, meaning an advantage can only materialise in high dimensions if one needs at most a logarithmic number of these elements for a specific gate. And indeed, the number $N(d_{1/2})$ of OAM-BSs scales logarithmically with d_1 and d_2:

$$N(d_{1/2}) = 2 \times (\lfloor \log_2(d_1 - 1) \rfloor + \lfloor \log_2(d_2 - 1) \rfloor) + 2, \tag{3}$$

where $N(d_{1/2})$ is an upper bound obtained by studying a simple setup. For certain circuits, we know the actual number can still be lower. In the case of two eight-dimensional qudits, the complete $C_{\mathrm{PF}}^{(6)}$ can be achieved with 10 OAM-BSs, as shown in Fig. 3.

Remarkably, the probability of success is 1/4, irrespective of the dimension. Therefore, the efficiency of the circuit increases significantly when using higher-dimensional gates. It is also interesting to implement such gates in other degrees of freedom of photons, such as path.

B Trapped ion implementation

In Fig. 4, we provide a circuit for the implementation of a four-qubit CPF gate $C_{\mathrm{PF}}^{(4)}$ using either four qubits, or 2 qudits.

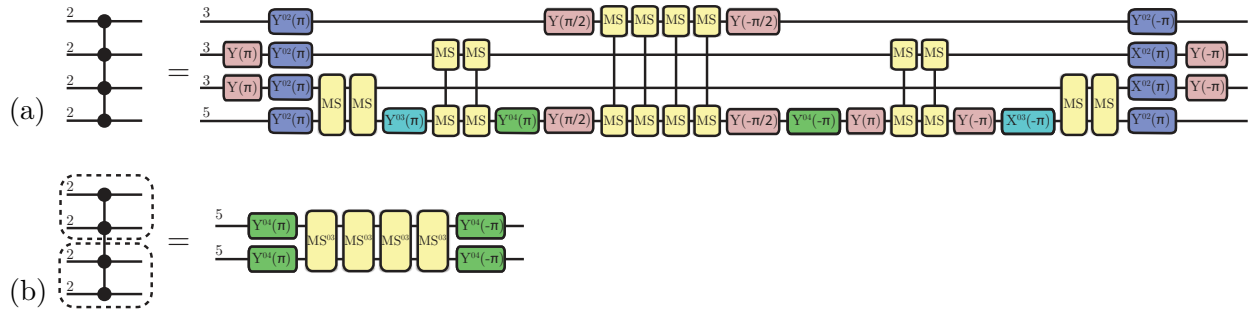

Figure 4: **Trapped-ion circuits for implementing a four-qubit CPF gate** $C_{\mathrm{PF}}^{(4)}$. Implementations are shown for (a) 4 qubits with auxiliary level, or (b) two qudits that encode 2 qubits each. In both cases only two-level entangling operations are used, where each yellow gate corresponds to a Mølmer-Sørensen (MS) gate with rotation angle $\pi/2$, which is maximally entangling for qubits. The local rotations are X or Y rotations with acting on the subspace indicated in the superscript (and color coding), where operations without superscript act on the 01-subspace of the original qubits. Note that, while using auxiliary levels enables a reduction to only 5 non-local gates, those gates require larger rotation angles and thus come with an increased experimental cost per gate. Even taking this into account the qudit-assisted circuit is expected to perform slightly better than a pure qubit circuit. In case (b) each ion occupies a 5-dimensional Hilbert space and encodes two qubits. Exploiting again the auxiliary level, only a single non-local gate is required.

6 Conclusion

Quantum information theory developed naturally around the qubit—the simplest quantum system and a direct analogue of the classical bit. The bit is a canonical abstraction in classical computation: minimal, universal, and mathematically sufficient to represent any logic. Yet this analogy has limits. Classical information theory belongs to pure mathematics, while quantum information theory is a theory in physics. As such, it must ultimately reflect how information is represented and manipulated in the physical world.

When we look to nature, we find that the systems used to store and process quantum information—photonic modes, trapped ions, superconducting circuits—are rarely restricted to two levels. They are inherently multilevel. This observation motivates the study of high-dimensional quantum information theory, where qudits, rather than qubits, are treated as the natural units of the theory. The qubit remains an elegant abstraction, but from the standpoint of physics, the restriction to two levels is a matter of convenience, not of principle.

The results presented here form part of this broader effort to build a systematic framework for high-dimensional quantum information theory. We examine how core concepts generalize when local dimension increases: monogamy and entropy make hidden dimension-dependence explicit without losing conceptual meaning; finite-function encoding identifies structural invariants by extending phase encodings beyond the graphical regime; and circuit compression shows that aligning formal structure with multilevel hardware yields practical reductions in nonlocal cost even without asymptotic speedups.

Viewed this way, the qudit is not a mere higher-dimensional qubit but the natural unit of a physical theory of information—one that recognizes dimension as an intrinsic feature of the systems it seeks to describe.

Acknowledgements

First and foremost, I would like to thank my family — my father, my mother, and my sister — for all the love, support, and patience I have received throughout these years. None of this would have been possible without you.

To Bärchen — thank you for *bearing* with me through all the long nights, last-minute deadlines, and the endless stream of half-coherent thoughts. Your patience and love kept me grounded and pushed me over the line. Without you I wouldn't have made it.

My deepest gratitude goes to Marcus Huber, for his patience, guidance, and for showing me the beautiful side of science — the sense of community, freedom, and camaraderie that make it such a rewarding pursuit. Wherever Marcus is, he creates a space that brings people together and inspires collaboration.

I am deeply thankful to Claude Klöckl, Giuseppe Vitagliano, Matej Pivoluska, and Nicolai Friis. Claude was one of the first people I met, even before starting my PhD, and his openness made joining the group feel easy. Working closely with Giuseppe and Matej has been one of the most rewarding parts of this journey — their positivity, humor, and friendship made even the hard days enjoyable. Nico's structure and thoughtful advice were always an anchor whenever I needed an open ear.

I would also like to thank my fellow PhD students for all the discussions, coffee breaks, and our PhD meetings where we managed to talk about everything and nothing. You made everyday life in the group lighter and more enjoyable. I especially want to thank Mirdit, meeting you has given me a good friend.

To all my coauthors, collaborators, and colleagues — thank you for the discussions, ideas, and laughter along the way. The legendary conferences in Benasque, and all the moments shared there, are memories I'll always cherish.

References

[1] C. H. Bennett and S. J. Wiesner. "Communication via One- and Two-Particle Operators on Einstein-Podolsky-Rosen States". In: *Physical Review Letters* 69.20 (Nov. 16, 1992), pp. 2881–2884. DOI: 10.1103/PhysRevLett.69.2881.

[2] C. H. Bennett, G. Brassard, C. Crépeau, R. Jozsa, A. Peres, and W. K. Wootters. "Teleporting an Unknown Quantum State via Dual Classical and Einstein-Podolsky-Rosen Channels". In: *Physical Review Letters* 70.13 (Mar. 29, 1993), pp. 1895–1899. DOI: 10.1103/PhysRevLett.70.1895.

[3] P. Shor. "Algorithms for Quantum Computation: Discrete Logarithms and Factoring". In: *Proceedings 35th Annual Symposium on Foundations of Computer Science*. 35th Annual Symposium on Foundations of Computer Science. Santa Fe, NM, USA: IEEE Comput. Soc. Press, 1994, pp. 124–134. DOI: 10.1109/SFCS.1994.365700.

[4] L. K. Grover. “A Fast Quantum Mechanical Algorithm for Database Search”. In: *Proceedings of the Twenty-Eighth Annual ACM Symposium on Theory of Computing - STOC ’96*. The Twenty-Eighth Annual ACM Symposium. Philadelphia, Pennsylvania, United States: ACM Press, 1996, pp. 212–219. DOI: 10.1145/237814.237866.

[5] C. H. Bennett and G. Brassard. “Quantum Cryptography: Public Key Distribution and Coin Tossing”. In: *Theoretical Computer Science* 560 (Dec. 2014), pp. 7–11. DOI: 10.1016/j.tcs.2014.05.025.

[6] P. W. Shor and J. Preskill. “Simple Proof of Security of the BB84 Quantum Key Distribution Protocol”. In: *Physical Review Letters* 85.2 (July 10, 2000), pp. 441–444. DOI: 10.1103/PhysRevLett.85.441.

[7] M. Kues, C. Reimer, P. Roztocki, L. R. Cortés, S. Sciara, B. Wetzel, Y. Zhang, A. Cino, S. T. Chu, B. E. Little, D. J. Moss, L. Caspani, J. Azaña, and R. Morandotti. “On-Chip Generation of High-Dimensional Entangled Quantum States and Their Coherent Control”. In: *Nature* 546.7660 (June 2017), pp. 622–626. DOI: 10.1038/nature22986.

[8] J. Wang, S. Paesani, Y. Ding, R. Santagati, P. Skrzypczyk, A. Salavrakos, J. Tura, R. Augusiak, L. Mančinska, D. Bacco, D. Bonneau, J. W. Silverstone, Q. Gong, A. Acín, K. Rottwitt, L. K. Oxenløwe, J. L. O’Brien, A. Laing, and M. G. Thompson. “Multidimensional Quantum Entanglement with Large-Scale Integrated Optics”. In: *Science* 360.6386 (Apr. 20, 2018), pp. 285–291. DOI: 10.1126/science.aar7053.

[9] M. Ringbauer, M. Meth, L. Postler, R. Stricker, R. Blatt, P. Schindler, and T. Monz. “A Universal Qudit Quantum Processor with Trapped Ions”. In: *Nature Physics* 18.9 (Sept. 2022), pp. 1053–1057. DOI: 10.1038/s41567-022-01658-0.

[10] A. Morvan, V. V. Ramasesh, M. S. Blok, J. M. Kreikebaum, K. O’Brien, L. Chen, B. K. Mitchell, R. K. Naik, D. I. Santiago, and I. Siddiqi. “Qutrit Randomized Benchmarking”. In: *Physical Review Letters* 126.21 (May 27, 2021), p. 210504. DOI: 10.1103/PhysRevLett.126.210504.

[11] N. T. Islam, C. C. W. Lim, C. Cahall, J. Kim, and D. J. Gauthier. “Provably Secure and High-Rate Quantum Key Distribution with Time-Bin Qudits”. In: *Science advances* 3.11 (2017), e1701491. DOI: 10.1126/sciadv.1701491.

[12] M. Doda, M. Huber, G. Murta, M. Pivoluska, M. Plesch, and C. Vlachou. “Quantum Key Distribution Overcoming Extreme Noise: Simultaneous Subspace Coding Using High-Dimensional Entanglement”. In: *Physical Review Applied* 15.3 (Mar. 2021), p. 034003. DOI: 10.1103/PhysRevApplied.15.034003.

[13] D. Collins, N. Gisin, N. Linden, S. Massar, and S. Popescu. “Bell Inequalities for Arbitrarily High-Dimensional Systems”. In: *Physical Review Letters* 88.4 (Jan. 10, 2002), p. 040404. DOI: 10.1103/PhysRevLett.88.040404.

[14] A. C. Dada, J. Leach, G. S. Buller, M. J. Padgett, and E. Andersson. “Experimental High-Dimensional Two-Photon Entanglement and Violations of Generalized Bell Inequalities”. In: *Nature Physics* 7.9 (Sept. 2011), pp. 677–680. DOI: 10.1038/nphys1996.

[15] B. P. Lanyon, M. Barbieri, M. P. Almeida, T. Jennewein, T. C. Ralph, K. J. Resch, G. J. Pryde, J. L. O’Brien, A. Gilchrist, and A. G. White. “Simplifying Quantum Logic Using Higher-Dimensional Hilbert Spaces”. In: *Nature Physics* 5.2 (Feb. 2009), pp. 134–140. DOI: 10.1038/nphys1150.

[16] G. Brennen, S. Bullock, and D. O’Leary. “Efficient Circuits for Exact-Universal Computation with Qudits”. In: *Quantum Information and Computation* 6 (4&5 July 2006), pp. 436–454. DOI: 10.26421/QIC6.4-5-9.

[17] F. H. E. Watson, H. Anwar, and D. E. Browne. “Fast Fault-Tolerant Decoder for Qubit and Qudit Surface Codes”. In: *Physical Review A* 92.3 (Sept. 8, 2015), p. 032309. DOI: 10.1103/PhysRevA.92.032309.

[18] F. H. E. Watson, E. T. Campbell, H. Anwar, and D. E. Browne. “Qudit Colour Codes and Gauge Colour Codes in All Spatial Dimensions”. In: *Physical Review A* 92.2 (Aug. 7, 2015), p. 022312. DOI: 10.1103/PhysRevA.92.022312.

[19] E. T. Campbell. “Enhanced Fault-Tolerant Quantum Computing in d -Level Systems”. In: *Physical Review Letters* 113.23 (Dec. 3, 2014), p. 230501. DOI: 10.1103/PhysRevLett.113.230501.

[20] M. Ringbauer, T. R. Bromley, M. Cianciaruso, L. Lami, W. Y. S. Lau, G. Adesso, A. G. White, A. Fedrizzi, and M. Piani. “Certification and Quantification of Multilevel Quantum Coherence”. In: *Physical Review X* 8.4 (Oct. 10, 2018), p. 041007. DOI: 10.1103/PhysRevX.8.041007.

[21] T. Kraft, C. Ritz, N. Brunner, M. Huber, and O. Gühne. “Characterizing Genuine Multilevel Entanglement”. In: *Physical Review Letters* 120.6 (Feb. 8, 2018), p. 060502. DOI: 10.1103/PhysRevLett.120.060502.

[22] P. Appel, A. J. Heilman, E. W. Wertz, D. W. Lyons, M. Huber, M. Pivoluska, and G. Vitagliano. “Finite-Function-Encoding Quantum States”. In: *Quantum* 6 (May 9, 2022), p. 708. DOI: 10.22331/q-2022-05-09-708.

[23] P. Appel, M. Huber, and C. Klöckl. “Monogamy of Correlations and Entropy Inequalities in the Bloch Picture”. In: *Journal of Physics Communications* 4.2 (Feb. 1, 2020), p. 025009. DOI: 10.1088/2399-6528/ab6fb4.

[24] X. Gao, P. Appel, N. Friis, M. Ringbauer, and M. Huber. “On the Role of Entanglement in Qudit-Based Circuit Compression”. In: *Quantum* 7 (Oct. 16, 2023), p. 1141. DOI: 10.22331/q-2023-10-16-1141.

[25] D. Gottesman and H.-K. Lo. “From Quantum Cheating to Quantum Security”. In: *Physics Today* 53.11 (Nov. 1, 2000), pp. 22–27. DOI: 10.1063/1.1333282.

[26] E. P. Wigner. “The Unreasonable Effectiveness of Mathematics in the Natural Sciences. Richard Courant Lecture in Mathematical Sciences Delivered at New York University, May 11, 1959”. In: *Communications on Pure and Applied Mathematics* 13.1 (Feb. 1960), pp. 1–14. DOI: 10.1002/cpa.3160130102.

[27] M. Keyl. “Fundamentals of Quantum Information Theory”. In: *Physics Reports* 369.5 (Oct. 2002), pp. 431–548. DOI: 10.1016/S0370-1573(02)00266-1.

[28] M. A. Nielsen and I. L. Chuang. *Quantum Computation and Quantum Information: 10th Anniversary Edition*. 10th ed. New York, NY, USA: Cambridge University Press, 2011. DOI: 10.1017/CBO9780511976667.

[29] I. Bengtsson and K. Zyczkowski. *Geometry of Quantum States: An Introduction to Quantum Entanglement*. 1st ed. Cambridge University Press, May 11, 2006. DOI: 10.1017/CBO9780511535048.

[30] R. Horodecki, P. Horodecki, M. Horodecki, and K. Horodecki. “Quantum Entanglement”. In: *Reviews of Modern Physics* 81.2 (June 2009), pp. 865–942. DOI: 10.1103/RevModPhys.81.865.

[31] W. Dür, G. Vidal, and J. I. Cirac. “Three Qubits Can Be Entangled in Two Inequivalent Ways”. In: *Physical Review A* 62.6 (Nov. 14, 2000), p. 062314. DOI: 10.1103/PhysRevA.62.062314.

[32] N. Linden and S. Popescu. “On Multi-Particle Entanglement”. In: *Fortschritte der Physik* 46.4–5 (June 1998), pp. 567–578. DOI: 10.1002/(SICI)1521-3978(199806)46:4/5<567::AID-PROP567>3.0.CO;2-H.

[33] G. Kimura. “The Bloch Vector for N-level Systems”. In: *Physics Letters A* 314.5–6 (Aug. 2003), pp. 339–349. DOI: 10.1016/S0375-9601(03)00941-1.

[34] R. A. Bertlmann and P. Krammer. “Bloch Vectors for Qudits”. In: *Journal of Physics A: Mathematical and Theoretical* 41.23 (June 13, 2008), p. 235303. DOI: 10.1088/1751-8113/41/23/235303.

[35] J. I. De Vicente and M. Huber. “Multipartite Entanglement Detection from Correlation Tensors”. In: *Physical Review A* 84.6 (Dec. 6, 2011), p. 062306. DOI: 10.1103/PhysRevA.84.062306.

[36] F. T. Hioe and J. H. Eberly. “N -Level Coherence Vector and Higher Conservation Laws in Quantum Optics and Quantum Mechanics”. In: *Physical Review Letters* 47.12 (Sept. 21, 1981), pp. 838–841. DOI: 10.1103/PhysRevLett.47.838.

[37] H. Weyl. “Quantenmechanik und Gruppentheorie”. In: *Zeitschrift für Physik* 46.1–2 (Nov. 1927), pp. 1–46. DOI: 10.1007/BF02055756.

[38] G. Vidal. “Entanglement Monotones”. In: *Journal of Modern Optics* 47.2–3 (Feb. 2000), pp. 355–376. DOI: 10.1080/09500340008244048.

[39] W. K. Wootters. “Entanglement of Formation of an Arbitrary State of Two Qubits”. In: *Physical Review Letters* 80.10 (Mar. 9, 1998), pp. 2245–2248. DOI: 10.1103/PhysRevLett.80.2245.

[40] C. H. Bennett, D. P. DiVincenzo, J. A. Smolin, and W. K. Wootters. “Mixed-State Entanglement and Quantum Error Correction”. In: *Physical Review A* 54.5 (Nov. 1, 1996), pp. 3824–3851. DOI: 10.1103/PhysRevA.54.3824.

[41] G. Vidal and R. F. Werner. “Computable Measure of Entanglement”. In: *Physical Review A* 65.3 (Feb. 22, 2002), p. 032314. DOI: 10.1103/PhysRevA.65.032314.

[42] M. Christandl and A. Winter. ““Squashed Entanglement”: An Additive Entanglement Measure”. In: *Journal of Mathematical Physics* 45.3 (Mar. 1, 2004), pp. 829–840. DOI: 10.1063/1.1643788.

[43] B. Terhal. “Is Entanglement Monogamous?” In: *IBM Journal of Research and Development* 48.1 (2004). DOI: 10.1147/rd.481.0071.

[44] V. Coffman, J. Kundu, and W. K. Wootters. “Distributed Entanglement”. In: *Physical Review A* 61 (2000), p. 052306. DOI: 10.1103/PhysRevA.61.052306.

[45] T. J. Osborne and F. Verstraete. “General Monogamy Inequality for Bipartite Qubit Entanglement”. In: *Physical Review Letters* 96.22 (June 7, 2006), p. 220503. DOI: 10.1103/PhysRevLett.96.220503.

[46] M. Koashi and A. Winter. “Monogamy of Quantum Entanglement and Other Correlations”. In: *Physical Review A* 69.2 (Feb. 18, 2004), p. 022309. DOI: 10.1103/PhysRevA.69.022309.

[47] M. Gachechiladze, C. Budroni, and O. Gühne. “Extreme Violation of Local Realism in Quantum Hypergraph States”. In: *Physical Review Letters* 116.7 (Feb. 17, 2016), p. 070401. DOI: 10.1103/PhysRevLett.116.070401.

[48] O. Gühne, M. Cuquet, F. E. S. Steinhoff, T. Moroder, M. Rossi, D. Bruß, B. Kraus, and C. Macchiavello. “Entanglement and Nonclassical Properties of Hypergraph States”. In: *Journal of Physics A: Mathematical and Theoretical* 47.33 (Aug. 22, 2014), p. 335303. DOI: 10.1088/1751-8113/47/33/335303.

[49] Y. Takeuchi, T. Morimae, and M. Hayashi. “Quantum Computational Universality of Hypergraph States with Pauli-X and Z Basis Measurements”. In: *Scientific Reports* 9.1 (Sept. 19, 2019), p. 13585. DOI: 10.1038/s41598-019-49968-3.

[50] M. Rossi, M. Huber, D. Bruß, and C. Macchiavello. “Quantum Hypergraph States”. In: *New Journal of Physics* 15.11 (Nov. 11, 2013), p. 113022. DOI: 10.1088/1367-2630/15/11/113022.

[51] F. E. S. Steinhoff, C. Ritz, N. I. Miklin, and O. Gühne. “Qudit Hypergraph States”. In: *Physical Review A* 95.5 (May 22, 2017), p. 052340. DOI: 10.1103/PhysRevA.95.052340.

[52] D. Singmaster. “On Polynomial Functions (Mod m)”. In: *Journal of Number Theory* 6.5 (Oct. 1974), pp. 345–352. DOI: 10.1016/0022-314X(74)90031-6.

[53] S. N. Selezneva. “On the Number of Functions of k -Valued Logic Which Are Polynomials modulo Composite k”. In: *Discrete Mathematics and Applications* 27.1 (Feb. 1, 2017), pp. 7–14. DOI: 10.1515/dma-2017-0002.

[54] A. Barenco, C. H. Bennett, R. Cleve, D. P. DiVincenzo, N. Margolus, P. Shor, T. Sleator, J. A. Smolin, and H. Weinfurter. “Elementary Gates for Quantum Computation”. In: *Physical Review A* 52.5 (Nov. 1, 1995), pp. 3457–3467. DOI: 10.1103/PhysRevA.52.3457.

[55] M. J. Bremner, C. M. Dawson, J. L. Dodd, A. Gilchrist, A. W. Harrow, D. Mortimer, M. A. Nielsen, and T. J. Osborne. “Practical Scheme for Quantum Computation with Any Two-Qubit Entangling Gate”. In: *Physical Review Letters* 89.24 (Nov. 25, 2002), p. 247902. DOI: 10.1103/PhysRevLett.89.247902.

[56] “Universal Quantum Gates”. In: *Mathematics of Quantum Computation*. Ed. by R. K. Brylinski and G. Chen. 0th ed. Chapman and Hall/CRC, Feb. 14, 2002, pp. 117–134. DOI: 10.1201/9781420035377-5.

[57] A. Muthukrishnan and C. R. Stroud. “Multivalued Logic Gates for Quantum Computation”. In: *Physical Review A* 62.5 (Oct. 16, 2000), p. 052309. DOI: 10.1103/PhysRevA.62.052309.

[58] C. Dawson and M. Nielsen. “The Solovay-Kitaev Algorithm”. In: *Quantum Information and Computation* 6.1 (Jan. 2006), pp. 81–95. DOI: 10.26421/QIC6.1-6.

[59] M. Amy, D. Maslov, M. Mosca, and M. Roetteler. “A Meet-in-the-Middle Algorithm for Fast Synthesis of Depth-Optimal Quantum Circuits”. In: *IEEE Transactions on Computer-Aided Design of Integrated Circuits and Systems* 32.6 (June 2013), pp. 818–830. DOI: 10.1109/TCAD.2013.2244643.

[60] A. Sawicki and K. Karnas. “Criteria for Universality of Quantum Gates”. In: *Physical Review A* 95.6 (June 5, 2017), p. 062303. DOI: 10.1103/PhysRevA.95.062303.

[61] A. Sawicki, L. Mattioli, and Z. Zimborás. “Universality Verification for a Set of Quantum Gates”. In: *Physical Review A* 105.5 (May 12, 2022), p. 052602. DOI: 10.1103/PhysRevA.105.052602.

[62] C. Lancien, S. Di Martino, M. Huber, M. Piani, G. Adesso, and A. Winter. “Should Entanglement Measures Be Monogamous or Faithful?” In: *Physical Review Letters* 117.6 (Aug. 1, 2016), p. 060501. DOI: 10.1103/PhysRevLett.117.060501.